eman ta zabal zazu

Universidad del País Vasco
Euskal Herriko Unibertsitatea

Departamento de Neurociencias

Neurozientziak Saila

The role of purinergic receptor A1 in neurogenesis modulation from subventricular zone

Mónica Benito Muñoz

Leioa, June 2016

INTRODUCTION

AAV	Adeno-associated virus
Ache	Acetyl cholinesterase
AD	Alzhemier disease
aNSC	Activated neural stem cell
ADA	Adenosine deaminase
ADK	Adenosine kinase
ADP	Adenosine diphosphate
ADPβS	Adenosine-5′-O-(2-thiodiphosphate)
Ado	Adenosine
AMP	Adenosine monophosphate
AP	Alkaline phosphatases
AR	Adenosine receptor
ATP	Adenosine triphosphate
BBB	Blood brain barrier
BDNF	Brain-derived neurotrophic factor
bFGF	Fibroblast growth factor
bHLH	Basic helix-loop-helix
BMP	Bone morphogenetic protein
BrdU	5-bromo-2´-deoxyuridine
BfdA	Brefeldin A
2´,3´-BzATP	*2*'(*3*')-O-(4-Benzoylbenzoyl)adenosine-5'-triphosphate
Caff	Caffeine
cAMP	Cyclic adenosine monophosphate
CBDN	Calbindin
CCA	Common carotid artery
CNS	Central nervous system
CNT	Concentrative nucleoside transporter
CNTF	Ciliary neurotrophic factor

CR	Calretinin
CBF	Cerebral blood flow
CPA	N^6-Cyclopentyladenosine
CRYAB	Crystallin alpha B
CSF	Cerebrospinal fluid
CTP	Cytidine-5´-triphosphate
DAG	Dyacilglycerol
DAI	Days after ischemia
DARP	Dopamine-releasing protein
DCX	Doublecourtin
DIV	Days *in vitro*
Dlg4	Discs, large homolog 4 (Drosophila)
DM	Differentiation medium
DNA	Deoxyribonucleic acid
dNTP	Dinucleotidetriphosphate
DP	Dipyridamol
DPCPX	1, 3-dipropyl-8-cyclopentylxanthine
DTT	Dithiothreitol
ECA	External carotid artery
EGF	Epidermal growth factor
ELISA	Enzyme-linked immunosorbent assay
EMC	Extracellular matrix components
E-NPP	Ectonucleotide pyrophosphate/phosphodiesterase
ENT	Equilibrative nucleoside transporter
Epo	Erythropoietin
ET-1	Endothelin-1
FGF	Fibroblast growth factor
[^{18}F] FLT	3'-deoxy-3'-[^{18}F]-fluorothymidine

GABA	Gamma-amino butyric acid
GAPDH	Glyceraldehyde-3-phosphate dehydrogenase
GC	Granule cell
GDNF	Glial cell -derived neurotrophic factor
GFAP	Glial fibrillary acidic protein
GL	Glomerular layer
GPCR	G protein couple receptor
Gpi	Glucose-6-phosphate-isomerase
GrL	Granular layer
GSK3β	Glycogen synthase kinase 3 beta
GTP	Guanosine-5´-triphosphate
5-HT	5-hydroxytryptamine
HPRT1	Hypoxanthine phosphoribosyl-transferase 1
ICA	Internal carotid artery
IdU	5-Iodo-2´-deoxyuridine
IFN-γ	Interferon γ
IGF-I	Insulin-like growth factor I
IL	Interleukin
IMP	Inosine monophosphate
I.P.	Intraperitoneal
Ip5I	Diinosine pentaphosphate
$InsP_3$	Inositol triphosphate
JAK	Janus kinase
JGN	Juxtaglomerular neuron
LIF	Leukemia inhibitory factor
lncRNA	long non-coding ribonucleic acid
LV	Lateral ventricule
MAPK	Mitogen activated protein kinase

MCAO	Middle cerebral artery occlusion
MCA	Middle cerebral artery
MCP-1	Monocyte chemoattractant protein 1
α,β-meATP	*α,β*-methyleneadenosine 5′-triphosphate
2-MeSATP	2-(Methylthio)adenosine 5′-triphosphate
mRNA	Messenger ribonucleic acid
miRNA	Micro ribonucleic acid
MS	Multiple sclerosis
N	Neurosphere
NAD+	Nicotinamide adenine dinucleotide
NECA	5´-N-ethylcarboxamido-adenosine
NFM	Medium neurofilaments
NGF	Nerve growth factor
NINDS	National Institute of Neurological Disorders and Stroke
NMDA	N-methyl-D-aspartate
NO	Nitric oxide
NOS	Nitric oxide synthase
NSC	Neural stem cell
NT-3	Neurotrophin-3
NTP	Nucleoside triphosphate
NTPDase	Ectonucleoside triphosphate diphosphohydrolase
OB	Olfactory bulb
PBS	Phosphate-buffered saline
PD	Parkinson disease
PEDF	Pigment epithelium-derived factor
PET	Positron tomography emission
PFA	Paraformaldehyde
PGE2	Prostaglandin E2

PGC	Periglomerular cell
PKC	Protein kinase C
PPADS	Pyridoxal-phosphate-6-azophenyl-2',4'-disulfonate
PSA-NCAM	Polysialylated-neural cell adhesion molecule
Ptn	Pleiotrophin
qNSC	Quiescent neural stem cell
qRT-PCR	Quantitative real-time polymerase chain reaction
RMS	Rostral migratory stream
RNA	Ribonucleic acid
RNase	Ribonuclease
ROS	Reactive oxygen species
SCB	Scrambled plasmid
SCF	Stem cell factor
SGZ	Subgranular zone
SH3	Src-homology-3
Shh	Sonic hedgehog
sHsp	Small heat shock protein
shRNA	Short hairpin ribonucleic acid
siRNA	Small interfering ribonucleic acid
Syn	Synaptophysin
STAT3	Signal transducer and activator of transcription 3
SVZ	Subventricular zone
TGF-β	Transforming growth factor-β
TH	Tyrosine Hydroxylase
TNAP	Tissue nonspecific alkaline phosphatase
TNF-α	Tumor necrosis factor α
TNP-ATP	2',3'-*O*-(2,4,6-trinitrophenyl)adenosine-5'-triphosphate
TrkB	Tropomyosin receptor kinase B

TTC	2,3,5-Triphenyltetrazolium chloride
UDP	Uridine diphosphate
UDPβS	Uridine-5´-O-(2-thiodiphosphate)
UTP	Uridine triphosphate
VEGF	Vascular endothelial growth factor
VGLUT2	Vesicular glutamate transporter 2
VO	Vessel occlusion
VOI	Volume of interest

Introduction

1. ADULT NEUROGENESIS

The finding by Altman and Das (Altman & Das 1965) on the presence of new born neurons in the adult brain in 1960s demonstrated for the first time that active neurogenesis continues throughout life in the mammals brain. **Adult neurogenesis** is considered as a multistep process that includes cell proliferation, migration, differentiation, cell fate decision and functional integration into preexisting neuronal network. The adult progenitors are multipotent cells and can potentially differentiate only into neural phenotypes: neurons or glia (oligodendrocytes or astrocytes) (Kempermann et al. 2004; Zhao et al. 2008).

Generation of new neurons is largely restricted to specific neurogenic zones where cells are continuously produced: the subventricular zone (SVZ) of the lateral ventricules and the subgranular zone (SGZ) of dentate gyrus in the hippocampus (Fig. 1). While the latter gives rise to new glutamatergic granule cells that mature locally in the dentate gyrus (CA1 region), the former produces new cells that migrate through the rostral migratory stream (RMS) to reach the olfactory bulb (OB), where they differentiate mostly into GABAergic or dopaminergic local interneurons. Recently, it has been demonstrated that patterning specialization of progenitor cells in the SVZ regulates the differentiation of different cells in distinct regions of OB (Merkle et al. 2014; Fiorelli et al. 2015) (Fig. 2). Neurogenesis in the SGZ is much lower than in the SVZ and is especially involved in the mechanisms of memory and learning (Aimone et al. 2011). Actually, neurogenesis in the SVZ involves a higher number of cells and can be activated after neurodegeneration in the neighbor areas (e.g. striatum and cortex after brain ischemia) (Christie & Turnley 2012). Nevertheless, adult neurogenesis in mammals has been demonstrated also in peripheral nervous system. For example the carotid body elicits characteristics of neuroregeneration and cell proliferation and can produce new neuron-like cells from glia-like sustentacular cells (Pardal et al. 2007).

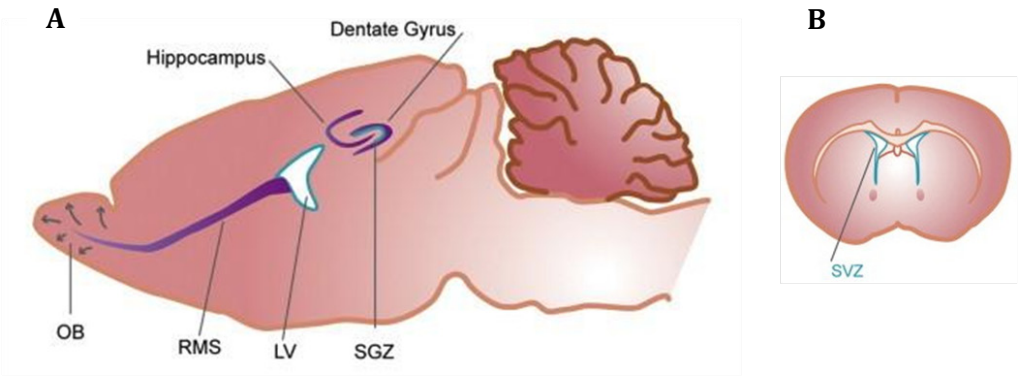

Figure 1. Neurogenic niches of the adult rodent brain. Sagittal (A) and coronal (B) section of the brain showing the two neurogenic niches: the subventricular zone (SVZ) that surrounds the lateral ventricle (LV) and the subgranular zone (SGZ) in the dentate gyrus of the hippocampus. Rostral migratory stream (RMS), olfactory bulb (OB). From (Vukovic et al. 2011).

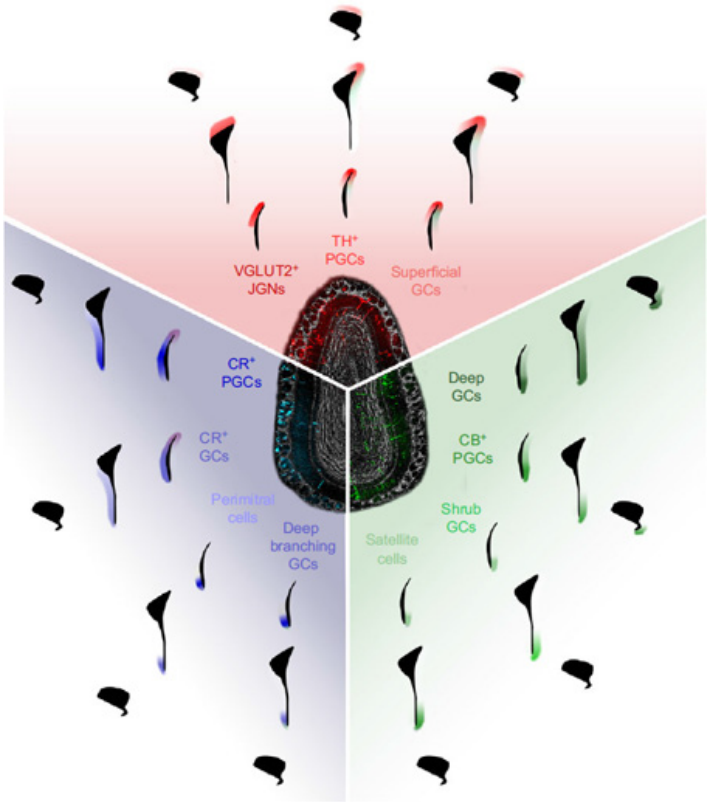

Figure 2. SVZ microdomains of origin of specific OB neuron subtypes. Neurons are colored according to their origin: red, green and blue define neurons that have originated from neural stem cells (NSCs) of the dorsal, ventral and medial microdomains of the SVZ, respectively. Granule cells (GCs), periglomerular cells (PGCs), juxtaglomerular neurons (JGNs), vesicular glutamate transporter 2 (VGLUT2), calretinin (CR), calbindin (CB), tyroxine hydroxylase (TH). Dorsal microdomains of the SVZ originate VGLUT2⁺ JGNs, TH⁺ PGCs and superficial GCs. Ventral microdomains originate deep GCs, CB⁺ PGCs, Shrub GCs and satellite cells. Medial microdomains originate deep branching GCs, perimitral cells, CR⁺ GCs and CR⁺ PGCs. From (Fiorelli et al. 2015).

2. THE SUBVENTRICULAR ZONE

The SVZ is located adjacent to the ependyma, the thin layer that lines the lateral ventricle, and exhibits a specific cellular structure and molecular milieu which constitutes an optimal niche for neural precursors.

-*Characteristics of subventricular zone cells.* As described previously, the main characteristic of adult progenitors is the multipotentiality. They can potentially differentiate only into neurons or glia (oligodendrocytes or astrocytes)(Kempermann et al. 2004; Zhao et al. 2008). The diversity of cell types and neuronal subtypes that can be spontaneously generated by adult NSCs is substantially limited compared to embryonic cells. This is probably largely due to a less permissive environment and lack of neurotrophic factors rather than a constitutive feature of the NSCs themselves (Parish & Thompson 2015).

Neural progenitor cells of SVZ can be visualized by incorporation of thymidine analogues such as e.g. 5-bromo-2´-deoxyuridine (BrdU). The adult neural progenitor cells are characterized by asymmetric division (Tajbakhsh et al. 2009). In this case a mother cell (B cell in Fig. 3) generates an identical daughter cell and another more specialized (C cell in Fig. 3), which can differentiate in neuroblast or glioblast. The times of duplication are different so self-renewal is slower than the duplication of the more specialized cells.

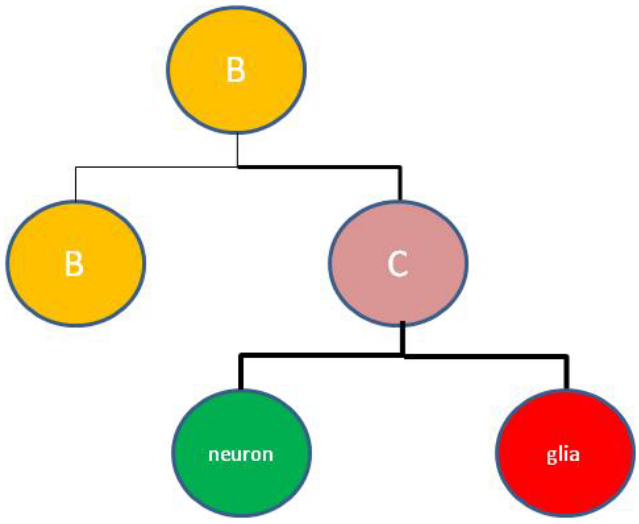

Figure 3. Asymmetric division of multipotent cells from subventricular zone. Line thickness represents velocity of time duplication.

This characteristic reflects the ability to form "clonogenic" **neurospheres** *in vitro.* These free-floating spheroid cell aggregates are highly motile and prone to merge with each other contributing to polyclonal sphere growth. According to the factors used in culture medium, proliferating neurospheres can differentiate into neurons [with nerve growth factor (NGF) and brain-derived neurotrophic factor (BDNF)], astrocytes [glial cell - derived neurotrophic factor (GDNF)] or oligodendrocytes [neurotrophin-3 (NT3) and ciliary neurotrophic factor (CNTF)].

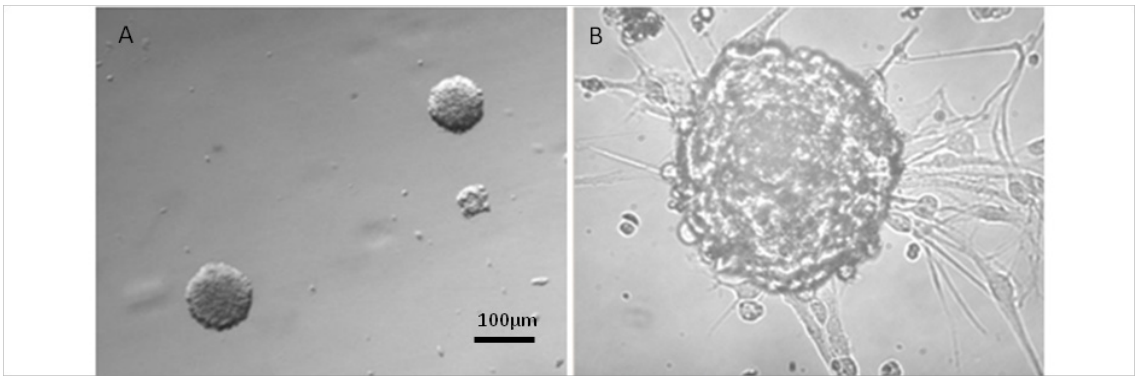

Figure 4. Neurosphere cultures from SVZ (A) Non-adherent proliferating neurosphere culture. (B) Adherent neurosphere culture in differentiation stage. Scale bar = 100 µm.

Four cell types are involved in the activation of neurogenesis from the SVZ, 1) cells of the ependymal layer (E cells), 2) B cells (GFAP positive multipotent cells), 3) C cells (transit amplifying cells) that can differentiate into 4) A cells (neuroblasts) or glioblasts.

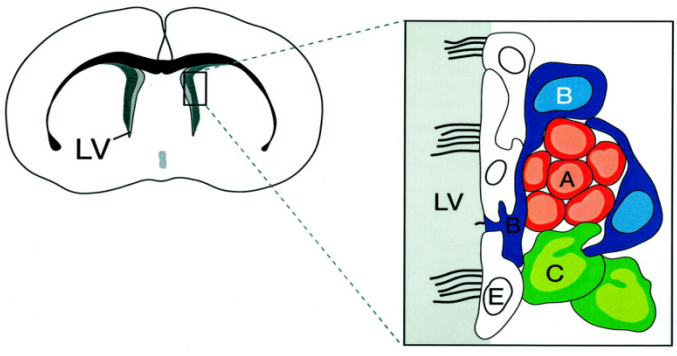

Figure 5. Cellular composition and organization of the SVZ. From (Alvarez-Buylla & Garcia-Verdugo 2002).

Ependymal cells are a monociliated subpopulation of ependymal layer. They are considered from ones as neural stem cells (NSCs) responsible for the neurogenesis in the adult brain (Mirzadeh et al. 2008) in contrast with others that sustain the stemness function of type B cells. Type B cells express different cellular markers, among these the astrocytic glial fibrillary acidic protein (GFAP) or other multipotency markers such as nestin, epidermal growth factor (EGF) receptor or the transcription factor Sox2. B cells are morphologically and functionally different from mature astrocytes despite they derive from embryonic radial glia of the ventricular zone (Alvarez-Buylla & Garcia-Verdugo 2002). The difference between B cells and mature astrocytes reside in the ability to proliferate of the former and the co-expression of additional markers such as nestin or brain lipid-binding protein. Another special feature is the expression of specific genes like thrombospondin 4 (Thbs4) and the GFAP isoform GFAPδ which are preferentially expressed in B cells but not in mature astrocytes (Kamphuis et al. 2012; Benner et al. 2013).

Among these $GFAP^+$ cells, only a monociliated subset protruding cilia into the lateral ventricle is really responsible for neurogenesis (Garcia et al. 2004). More recently, two types of neural stem cells (B cells) have been identified from the adult ventricular-subventricular zone. Quiescent neural stem cells (qNSCs), which are largely dormant *in vivo*, generate olfactory bulb interneurons with slower kinetics and are characterized by GFAP and CD133 expression; and activated neural stem cells (aNSCs). The latter are rapidly cycling, highly neurogenic *in vivo* and positive for GFAP, CD133 and EGFR expression (Codega et al. 2014). In general, B cells possess slower rate of proliferation and are in contact with the C cells (transit amplifying cells) (Fig. 5). These cells, as previously stated, have highest rate of proliferation and can differentiate into A cells (neuroblasts) or glial precursor cells and express predominantly nestin and other multipotency markers until they differentiate into neuro- or glioblasts. Once differentiated in neuroblasts, A cells migrate through RMS into the OB where they disperse radially and differentiate into interneurons (granule cells or periglomerular cells) (Alvarez-Buylla & Garcia-Verdugo 2002). Into the RMS, astrocytes first create a physical route for neuronal migration and then communicate with the migrating neuroblasts and regulate their speed of migration (Bolteus & Bordey 2004). The neuronal linage is characterized by the expression of intermediate neuronal fibers such as polysialylated-neural cell adhesion molecule (PSA-NCAM), doublecortin (DCX), βIII tubulin or AsclI. Expression of these markers overlap during differentiation and the combination of each of these will predict the neuronal phenotype (Fig. 6).

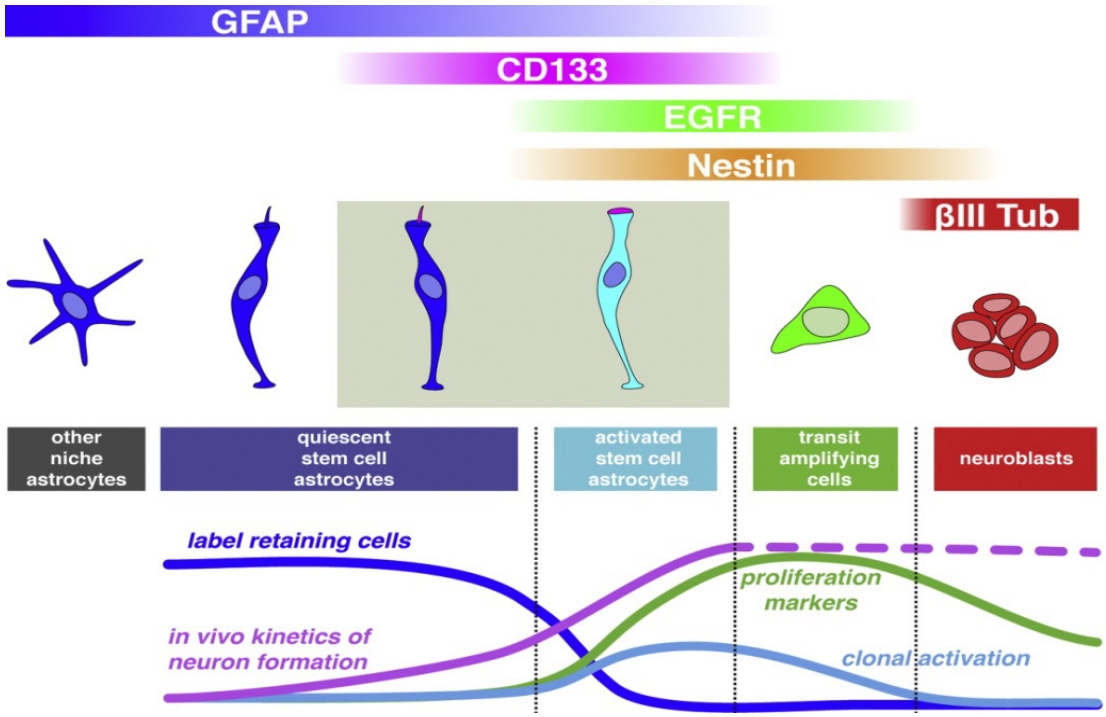

Figure 6. Characterization of cells involved in neurogenesis. From (Codega et al. 2014).

3. THE SVZ AND NEUROGENESIS IN HUMAN BRAIN

Recent studies have revealed significant differences between the rodent and human SVZ. In young children, the SVZ contains many newborn neurons, and there is a prominent RMS to OB (Sanai et al. 2011). The brain of infants also has a medial migratory stream of young neurons from the SVZ to the medial prefrontal cortex, which is a migratory path not evident in the rodent brain. After 18 months of age, few DCX-positive cells are observed in the human SVZ. Instead, there is a prominent gap layer (GAP) consisting of a dense network of interconnected processes from astrocytes and ependymal cells. Adjacent to the GAP is a cellular "ribbon" containing astrocytes, some of which have been reported to have NSC properties *in vitro*. While very few young neurons are observed in the GAP, recent evidence suggests that precursor cells migrate into the adult human striatum and differentiate into local interneurons (Lim & Alvarez-Buylla 2014). However, the claim of neurogenesis in adult human striatum is still controversial, as a very recent study suggests that all interneurons in the adult human and monkey striatum arise during development and not in adult. Thus, while the SVZ clearly has a prominent role during early childhood, the role of the adult human SVZ remains elusive, and available evidence indicates that this neurogenic niche may be largely dormant in the adult human brain (Ernst et al. 2014).

Frisén and colleagues (Ernst et al. 2014) recently showed that new neurons are born every day in the adult human hippocampus and human striatum throughout life. Radiocarbon analysis of deoxyribonucleic acid (DNA) from neuronal and non-neuronal cells showed that both populations are turning over in adulthood. Mathematical modeling of ^{14}C data allows for a detailed analysis of neuronal and non-neuronal turnover. A large proportion (51%) of the non-neuronal cells was found to be continuously exchanged, with a median turnover rate of 3.5% per year. Modeling of the data showed that there are two populations of neurons within the hippocampus, one rather homogenous population (constituting 35% of hippocampal neurons), turning over at a median rate of 1.75% per year, and the other not turning over. The exchange rate of hippocampal neurons corresponds to ~700 new neurons per day in each hippocampus. Generation of new striatal interneurons was shown by the detection of 5-iodo-2´-deoxyuridine (IdU) positive neurons in postmortem tissue from cancer patients who had received IdU as a radiosensitizer. Moreover, carbon dating revealed that neuronal turnover was restricted to the subpopulation of dopamine-releasing protein 23 (DARP23)-negative interneurons, and mathematical modeling indicated a turnover rate of 2.7% per year within this population.

4. NEUROGENESIS MODULATION

Each step in the process of neurogenesis (proliferation, migration, differentiation and network integration) is a possible site of regulation. Neurogenesis is positively modulated by physical activity, growth factors, acute lesions, antidepressant treatments or enriched environment. Thus, a decreased level of neurogenesis occurs in situations like ageing, stress, glucocorticoids administration and neurodegenerative diseases. On the other hand a simple factor can modulate differently distinct NSCs subpopulation. For example, the kainic acid-induced seizures in mice promote proliferation of DCX^+ neuroblasts, but not $nestin^+$ progenitors (Jessberger et al. 2005). Other study showed that low levels of kainic acid led to a radial NSCs activation and conversion into astrocytes. However, higher levels of kainic acid produced symmetrical division of radial NSCs and subsequentely conversion into reactive astrocytes (Sierra et al. 2015). In order to understand and studying adult neurogenesis modulation we must to know how the extracellular environment can maintain the multistep processes (Suh et al. 2009). In general, self-renewal and differentiation are controlled by specialized microenvironment (or niche) in which NSCs reside. Thus, stem cell fate can be modulated by soluble factors, as well as membrane-bound molecules and extracellular matrix (ECM). These soluble and non-soluble niche signals may be derived from the stem cells themselves, their progenitors, and the

neighboring cells. All the niche components must coordinate with each other to orchestrate the complex and precise development of adult NSCs. Following; we will describe these modulating factors under physiological and pathological situations.

5. MODULATION IN PHYSIOLOGICAL CONDITIONS

A large variety of molecular families are responsible for neurogenesis modulation in normal conditions. Here we describe the most relevant molecules:

-Trophic factors. These molecules can stimulate differentiation and survival of progenitor cells. They may be specific for a restricted number of cells types (neurotrophins) or affect many different cell families. Epidermal growth factor (EGF), together with beta-fibroblast growth factor (bFGF) and pigment epithelium-derived factor (PEDF) are the main mitogens used to maintain the neurospheres in a **proliferative status** (Ramírez-Castillejo et al. 2006). As stated previously B- and C cells are characterized for their expression of EGF receptor (EGFr) and when exposed to exogenous EGF during proliferation, progenitor cells are more prone to differentiate into astrocytes (Doetsch et al. 2002). Also the vascular endothelial growth factor (VEGF), released together with PEDF by ependymal and endothelial cells, regulate NSCs self-renewal (Ramírez-Castillejo et al. 2006). Neuronal differentiation is achieved by removal of mitogen factors and addition of neurotrophines like NGF and BDNF. These neurotrophic factors, by acting on their specific receptors p75 and tropomyosin receptor kinase B (TrkB), exert a double role by preventing programmed cell death and enhancing **differentiation** and neurite outgrowth (Ahmed et al. 1995).

-Morphogens. Morphogens are signaling molecules that drive the pattern of tissue development in the process of morphogenesis. These molecules act directly on cells in a concentration-depending manner. Concentration gradients during early development drive the process of **differentiation** of unspecialized cells into different cell types, ultimately forming all the tissues and organs of the body. Nevertheless, they exploit their role also during adult neurogenesis. The main morphogen involved in the modulation of adult neurogenesis is bone morphogenetic proteins (BMP). In general BMP family inhibits neuronal and oligodendroglial differentiation of NSCs and promotes astrogliogenesis (Fukuda et al. 2007). Neuronal inhibition is achieved by a mechanism involving degradation of the pro-neuronal transcription factors Ascl1 (Shou et al. 1999). The natural BMP inhibitor, Noggin, is used to block this cascade and to sustain neuronal differentiation. Hence, a "balance" between BMP and their antagonists may control the levels of neurogenesis and gliogenesis from NSCs in adult brain. In the adult SVZ, Noggin is

highly expressed by E cells, whereas BMP and BMPRs are expressed by type B- and C- cells (Lim et al. 2000). This expression pattern immediately suggests its effects on adult NSCs in promoting neuronal fate specification. In agreement with this hypothesis, the group of Fukuda demonstrated a route of differentiation, where BMP2 is involved in the activation of STAT3 and further activation of Smad1 to promote astrogliogenic differentiation (Fukuda et al. 2007). Astrocyte differentiation in the hippocampus is also modulated by neurogenesin 1 (Ng1) in an autocrine way. The release of Ng1 modulates negatively the astrocyte differentiation acting on BMP, promoting indeed neuronal differentiation (Ueki et al. 2003).

Other morphogenetic factors that positively modulate neurogenesis are Wnts protein family. The members of Wnt family regulate the maintenance of NSC **proliferation**, promoting symmetric against asymmetric division during neural regeneration (Piccin & Morshead 2011). Conversely, Wnt is negatively regulated by glycogen synthase kinase 3 beta (GSK3β) (Mao et al. 2009) and sonic hedgehog (Shh), through activation of Notch (Sims et al. 2009).

-*Transcription factors*. These proteins bind to specific DNA sequences, thereby controlling the rate of transcription of genetic information from DNA to messenger ribonucleic acid (mRNA). Transcription factors perform this function alone or with other proteins in a complex, by promoting or blocking the recruitment of RNA polymerase to specific genes. Transcription factors have a worth role in all the process of neurogenesis (proliferation, differentiation and integration). For example *Sox2* transcription factor, interacting with the PRX1 homeobox is involved both in the formation and **proliferation** of NSCs (Shimozaki et al. 2013). Another factor required for maintenance of neural stem cell niche is c-Myb which promotes the expression of *Sox2* and paired box 6 (*Pax6)* and subsequent cell proliferation (Malaterre et al. 2008). Pax6 is a homeobox transcription factor that promotes SVZ neurogenesis and directs the generation of dopaminergic periglomerular cells (Hack et al. 2005). Its mRNA is present in SVZ cells along the dorso-ventral region, whereas its transcriptional product is restricted only to the dorsal regions. This post-translational regulation of PAX6 expression is determined by regional expression of miR-7a, suggesting that also microRNAs (miRNA) play a key role in determining the regional heterogeneity of the SVZ (de Chevigny et al. 2012).

Also the family class of basic Helix-Loop-Helix (bHLH) transcription factors is involved in sustaining neuronal **differentiation** and **integration**. In general activation of specific bHLH can lead to a specific neuronal phenotype. Activation of Ascl1 generates GABAergic

interneuron in the OB, while activation of Neurog2 stimulates the differentiation of glutammatergic neurons (Kim et al. 2007; Berninger et al. 2007). Another bHLH factor is Olig2, which is expressed in qNSC (B1 cells) and type C cells and is deputed to stimulate oligodendrogliogenesis (Hack et al. 2005).

-Small heat shock proteins: The small heat shock proteins (sHsps) are oligomeric structures of about 32 subunits. They are present in the cytosol of most cells and tissues even in the absence of stress factors and exert pleiotropic effects. Interestingly, expression levels under physiological conditions have been correlated to **cell growth** and **differentiation**. Among the variety of small heat shock proteins, *Hspb8* expression increases during differentiation and has a pro-survival effect (Ramírez-Rodríguez et al. 2013). Furthermore, this small heat shock protein family has been largely studied as a potent modulator of cytokines release and inflammatory modulator (Shao et al. 2013).

Other factors can contribute to the modulation of neurogenesis from SVZ like cytokines (Perez-Asensio et al. 2013), epigenetic mechanisms (Wu et al. 2010; Ramos et al. 2013) or neurotransmitters.

-Cytokines: Cytokines are a group of proteins acting as chemical messengers between the immune cells. However, some of them participate in the neurogenic process. Of particular note for neurogenesis modulation is IL-10, which is a general anti-inflammatory molecule that is present at low levels in circulating blood. It exerts key functions for the maintenance of the pro- and anti-inflammatory balance to prevent inflammatory and autoimmune pathologies. Apart from these known effects, IL-10 acts as a growth factor on dorsal SVZ progenitors and regulates neurogenesis in adult brain (Perez-Asensio et al. 2013).

-Neurotransmitters: A number of different neurotransmitters regulate the neurogenesis from SVZ in normal and pathological conditions. Glutamate is the most prominent neurotransmitter in the body and is involved in oligodendrocyte **differentiation** from SVZ NSCs. This effect occurs through the stimulation of N-methyl-D-aspartate (NMDA) receptor and subsequently through the activation of PKC. In turn, stimulation of PKC activate NOX cascade generating reactive oxygen species (ROS) that leads to the generation of new oligodendrocytes (Cavaliere et al. 2012; Cavaliere et al. 2013).

The 5-hydroxytryptamine (5-HT, serotonin) neurotransmitter acts through receptors in the SVZ regulating cell **proliferation** and OB neurogenesis. The inhibition of serotonin

synthesis is associated with the decrease in the number of newly generated cells in the SVZ and also in the dentate gyrus (Brezun & Daszuta 1999). Young neuroblasts from SVZ spontaneously release gamma-amino butyric acid (GABA), activating GABA-A-receptors on precursor cells. This GABA-dependent depolarization inhibits cell proliferation and neuronal differentiation (Liu et al. 2005). Neurogenesis from SVZ can be modulated also by external inputs like in the case of dopaminergic innervations from the midbrain. In this case modulation can occur through the activation of D2 and D3 receptors on the Type C cells. Indeed, it has been demonstrated that dopaminergic denervation results in downregulation of proliferation and decreased OB neurogenesis (Höglinger et al. 2004).

-Epigenetic mechanisms: Among epigenetic mechanisms involved in neurogenesis modulation the most studied are histone acetylation, a covalent chromatin modification associated with active transcription; and DNA methylation, which is well known for its role in transcriptional repression at gene promoters. The methyltransferase DNMT3A is prominently expressed in the SVZ and is required for non-promoter DNA methylation, which facilitates the transcription of key neurogenic genes like *Dlx2* (Wu et al. 2010).

Emerging evidences indicate that long non-coding RNAs (lncRNAs), transcripts >200 nucleotides with no evidence of protein coding potential, have been associated with specific SVZ cell types and lineage specification, e.g. *Six3os* (Ramos et al. 2013).

-Other molecules: **extracellular matrix** (ECM) components like chondroitin sulfate proteoglycans and laminin facilitate neuroblast migration through the RMS. The ECM constitutes for the adult NSCs an important component of regulation. Functionally, the ECM can provide support and anchorage for NSCs, sequester and present a variety of growth factors, and regulate intercellular communication. Some of the main molecules involved in neural precursor cell migration include β1-integrin, reelin, tenascin-R, PSA-NCAM. This last and reelin are expressed in the neuroblasts and its expression is critical for SVZ-RMS migration in post-natal mice (Hu et al. 1996; Hack et al. 2002).

In addition to the above mentioned molecules, we want to mention the role of SLIT-ROBO pathway in neuroblasts migration. SLIT is a secreted protein which is most widely known as a repulsive axon guidance cue and Robo its transmembrane receptor. SLITs proteins are expressed by the septum and choroid plexus and the Robo-2/Robo-3 receptors are expressed in the SVZ and RMS. This distribution generates a gradient of SLIT2 chemorepulsive signal -with the highest concentration in the posterior SVZ- which parallels the directionality of type-A cells migration (Hu 1999).

Chemoattraction is a mechanism also used to move type-A cells from SVZ to the OB. Prokineticin-2 (Ng et al. 2005) and Netrin-1 (Astic et al. 2002) are both expressed in the OB and can attract type-A cells *in vitro*. Netrin-1 is required for efficient migration of precursors from the LV walls into the RMS and OB. In line with this, the Netrin-1 -/- OBs showed a decrease in the numbers of specific types of ventrally derived interneurons (Hakanen et al. 2011).

Apart from the factors that modulate proliferation, migration and differentiation other molecules can regulate **integration** into preexisting neuronal network like, for example, NMDA. NMDA receptors are expressed in neuroblasts along the RMS and participate to the migration and further integration in existing OB circuitry (Platel et al. 2010).

Finally, the system of **blood vessels irrigation** in the SVZ, consisting of endothelial cells, pericytes, fibroblasts, and macrophages and the associated extravascular basal lamina can also modulate neurogenesis by concentrating and/or modulating cytokines or growth factors release. Thus, any factor modifying architecture of blood vessels will indirectly regulate the growth factors level and consequently the neurogenesis (Honda et al. 2007). For example, betacellulin, an EGF-like growth factor secreted by endothelial cells is a modulator of SVZ cell proliferation and neuroblast production (Gómez-Gaviro et al. 2012). Further, it has been demonstrated that neuroblasts can migrate along blood vessels (Honda et al. 2007).

Moreover also the **cerebrospinal fluid** (CSF) provides extrinsic regulatory cues to the SVZ niche. The IGF-2 present in the CSF binds to the apical membrane and primary cilia of progenitors regulating their proliferation. The proliferation–inducing effects of IGF-2 are age dependent with the highest levels at the end of neurogenesis and a decrease postnatally (Lehtinen et al. 2011).

6. MODULATION IN PATHOLOGICAL CONDITIONS

In pathological conditions such as ischemia (Kokaia et al. 2006), the local environment influenced by cellular stress plays a crucial role in modulating the neurogenetic mechanisms of proliferation, migration and differentiation. After brain damage, such as traumatic brain injury, ischemic stroke or other neurodegenerative diseases, neural precursors cells from the SVZ, can migrate from their normal route along the RMS to the site of neural damage. This response to neural damage is mediated by release of endogenous factors, including cytokines and chemokines produced by inflammatory response at the injury site, and by the production of growth and neurotrophic factors. In

particular, the inflammatory response involves production of proinflammatory cytokines and chemokines such as interleukin-1β (IL-1β), tumor necrosis factor-α (TNF-α), interferon-γ (IFN-γ), interleukin-6 (IL-6), interleukin-18 (IL-18), monocyte chemoattractant protein-1 (MCP-1), and various reactive nitrogen and oxygen species (Rock et al. 2004).

The response of NSCs to damage-induced inflammation varies, depending on injury type, region of neural damage, animal species and likely a range of other factors that will be analyzed later on. The diverse composition of neurogenic niches and their multiregulatory roles for adult NSC development suggest that niche is not merely a static microenvironment to house NSCs but should also be regarded as a highly dynamic center for complex biochemical signal and cellular interactions events. This dynamic property further implicates another important feature of neurogenic niche: plasticity for remodeling in response to pathologic conditions.

Several neuropathologies have been studied considering the factors that modify neurogenesis. Among them, we will analyze acute insults like brain ischemia and neurodegenerative disorders such as Alzheimer´s and Parkinson´s diseases. The common characteristic of these neurodegenerative disorders is the generation of inflammation. Inflammation, characterized by activation of microglia and astrocytes in a lesser extent, indeed plays a dual role in causing neuronal death in Alzheimer´s and Parkinson´s diseases, or sustaining the formation of new neurons.

These findings indicate that brain following disease has the capacity to regenerate new neurons to compensate the neuronal loss. This aptitude leads us to investigate new strategies for therapeutic targets that stimulate endogenous neurogenesis and counteract neurodegeneration.

Here, we will show some of the most important factors modulating neurogenesis during pathological conditions:

-*Proinflammatory mediators*: This group includes cytokines, chemokines, reactive oxygen and nitrogen species, and prostaglandins.

-Cytokines: The proinflammatory cytokines are produced by activated microglia as a part of the innate immune response. Among these IL-6 is released by activated microglia and promote astrocytic **differentiation** of NSCs via activation of Janus kinase (JAK)/ signal transducer and activator of transcription (STAT) and mitogen activated protein kinase (MAPK) pathways (Nakanishi et al. 2007). In the hippocampus, IL-6 inhibits

neurogenesis in two different ways: directly, by stimulating the progenitor cells expressing IL-6 receptor, and indirectly by central stimulation of the hypothalamo-pituitary-adrenal axis, giving rise to increased circulating glucocorticoids, which in turn inhibits cell proliferation and neurogenesis in the dentate gyrus (Gould et al. 1992; Cameron & Gould 1994). On the other hand, the gp130-associated cytokines, ciliary neurotrophic factor (CNTF) and leukemia inhibitory factor (LIF), activate JAK/STAT3, MAPK and PI-3K/Akt pathways following ligand binding. These cytokines have been shown to regulate NSC **proliferation** and differentiation.

Another proinflammatory cytokine can modulate neurogenesis is TNF-α, which is up-regulated in most of all immune responses as well as in a spectrum of neurodegenerative diseases. After an insult to the brain, activated astrocytes and microglia produce TNF-α, this then exerts its biological functions via interaction with TNF-α receptors (TNF-R1 and TNF-R2). Depending on which receptor is activated, TNF-α generates two different effects: suppression of neural progenitor proliferation by TNF-R1 activation or proliferation and survival of newly formed hippocampal neurons by TNF-R2 activation (Iosif et al. 2006). Even if related with apoptosis, prolonged treatment of neurosphere cultures with TNF-α has no significant effect on apoptosis, but increase their proliferation without affecting their differentiation. (Widera et al. 2006). In relation with these results, the use of a blocking antibody to TNF-α reduced the number of striatal and hippocampal neuroblasts generated after stroke (Heldmann et al. 2005).

-Chemokines*:* Chemokines form a family of small (8-14kD), mainly basic, secreted molecules that are primarily known for regulating chemoattraction of immune cells to sites of tissue damage. They have been reported to have widespread non-immunological effects in the central nervous system (CNS), including regulation of neural cell proliferation, migration, survival, and synaptic transmission and can act in a paracrine or autocrine manner (Bajetto et al. 2002). Adult NSCs express a range of chemokine receptors that receive chemokines input from different brain regions, among which the OB. This suggests a role of chemokine system in regulating neuroblasts **migration** in adult brain (Turbic et al. 2011).

Chemokines produced by astrocytes are RANTES (CCL5), MCP-1 (CCR2), IP-10 (CXCL10), SDF-1α (CXCL12) whereas microglia is the major producer of MIP-1α (CCL3). The brain also expresses a wide array of chemokine receptors (and their correspondient ligands), such as CCR3 (for CCL5, CCL7, CCL13, CCL26 and CCL11 ligands), CXCR4 (SDF-1/CXCL12), CXCR2 (IL-8) and CX3CR1 (CX3CL1) on neurons; CXCR4 on astrocytes, and

CCR3 and CCR5 on microglia. In particular, SDF-1α and its receptor CXCR4 are upregulated at the ischemic area (Imitola et al. 2004; Robin et al. 2006) and is a modulatory molecule in neuroblast migration after *in vitro* oxygen and glucose deprivation (Vergni et al. 2009). The expression of several other chemokines and their receptors are upregulated on adult NSCs in response to inflammatory cytokines, like IFN-γ and TNF-α (Turbic et al. 2011).

MCP-1 is another important chemokine, for leukocyte trafficking into the brain, whose levels increase dramatically in any neuroinflammatory condition. Its receptor, CCR2, is widely expressed on NSCs and the stimulation with MCP-1 led to activation of the **migration** potency of NSCs (WIDERA 2004).

-Nitric oxide (NO): NO, a short-lived diffusible gas that acts in an autocrine and/or paracrine manner is produced by the enzyme nitric oxide synthase (NOS). The neuronal NOS (nNOS) expressed by neuroblasts, has been related with neurogenic inhibition in the adult mouse SVZ and olfactory bulb. Inhibiton of nNOS increases the number of mitotic cells in the SVZ, RMS, and OB. Contrary, the NO synthesized by endothelial NOS (eNOS) and inducible NOS (iNOS) stimulates neurogenesis (Zhu et al. 2003; Reif et al. 2004). In ischemic conditions, infusion of NO donors promotes **proliferation** and neurogenesis (Zhang et al. 2001).

-Complement system: the complement system is essentially a part of the humoral immune system, and, via its involvement in inflammation, opsonization and cytolisis confers protection against infectious agents. The most important molecules are C3a and C5a, whose receptors are expressed by neural progenitors and immature neurons. In experiments by Rahpeymai, mice lacking C3a or C3a receptor show impaired basal neurogenesis in the SVZ as well as attenuated ischemia-induced neurogenesis in the infarcted area. The intracerebral complement system thus has beneficial effects on CNS regeneration after brain injury (Rahpeymai et al. 2006).

Speaking of inflammatory mediators makes necessary to describe the role of **microglia in neurogenesis modulation**. It is conceivable that early detrimental action of microglia after acute injury can in some situations be converted into a supportive state during the chronic phase. In particular, it has been demonstrated that after stroke, the microglial population changes over time with respect to the morphology, phenotype and cytokine expression. Subsequently after the insult, microglia exploits a cytotoxic action, thus the inhibition of inflammation by indomethacine improves the **survival** of the neuroblasts in the striatum (Hoehn et al. 2005). The microglial M1/M2 classification has the following characteristics: an M1 phenotype represents pro-inflammatory activity,

including the production of pro-inflammatory cytokines, such as TNF-α and IL-1β and M2 microglia exhibit an anti-inflammatory phenotype expressing IL-10 and transforming growth factor-β (TGF-β). Regarding its morphology characterizes the inflammatory state of damaged tissue. Ramified microglia or with intermediate morphology, sustain the down-regulation of inflammatory mechanisms, whereas phagocytic microglia with amoeboid or rounded morphology are frequent in the peri-infarct striatum. On the other hand, if injury is extended for longer times, the activated microglia changes into a chronic profile. The cells either maintain their acute phenotype or divert into another activation state, potentially more maladaptative or neuroprotective. This transition is exemplified by alteration in cytokine production, which means that there is a progressive reduction in the production of TNF- α, IL-1β, IL-6 and free radicals such as nitric oxide (NO). In contrast, IL-10 and prostaglandin E2 (PGE2) are fully retained or enhanced, both factors being potent suppressors of the pro-inflammatory function of microglia (Cacci et al. 2008).

-Growth factors: Ischemia and traumatic brain injury increase some growth factors expression, thus modulating neurogenesis. It has been demonstrated that stem cell factor (SCF) and FGF2 are released following ischemic insults (Jin et al. 2002). In mouse ischemia, EGF promoted NSC **proliferation** in the SVZ with consequent production of neuroblasts in the SVZ and striatum. EGF also sustained neuroblast migration and further long term (13 weeks) **survival** of derived-parvalbumin interneurons (Teramoto et al. 2003). Other studies in rat ischemia showed that treatment with EGF alone induced proliferation and some NSC migration but did not promote regeneration unless combined with a later administration of erythropoietin (Epo) (Kolb et al. 2007). It is clear that, there is a species-specific mechanism of EGF action on neurogenesis modulation probably due to EGF-induced dysplasia in rat but not in mouse SVZ (Lindberg et al. 2012).

Another factor that modulates neurogenesis in pathological conditions (stroke) is insulin-like growth factor I (IGF-1). When overexpressed by adeno-associated virus (AAV) it mitigates apoptosis and promotes **proliferation** and **differentiation** of neural progenitors increasing neurogenesis from the SVZ (Zhu et al. 2008).

Likely, intranasal delivery of NGF after focal ischemia in rats did not promote proliferation of SVZ progenitors but sustained newborn neuron **survival** in the ipsilateral SVZ and injured striatum (Zhu et al. 2015).

In addition, it has been showed that a combination of factors such as BDNF and EGF is more effective than either factor alone at promoting long term new striatal neuron survival following ischemic injury in mice (Im et al. 2010).

Also GDNF increases cell proliferation in ipsilateral SVZ and stimulates the recruitment of new neuroblasts into striatum after middle cerebral artery occlusion (MCAO), improving survival of new mature neurons (Kobayashi et al. 2006).

-Morphogens: intrathecal administration of sonic hedgehog (Shh) following rat ischemia promoted NSC **proliferation** in the SVZ and improved behavioral recovery (Bambakidis et al. 2012). Astrocytes are the main cellular types producing Shh in the adult brain. Following brain injury activated astrocytes upregulate Shh expression in response to pro-inflammatory stimuli, which subsequently stimulates the generation of oligodendrocyte precursor cells (Amankulor et al. 2009).

BMP signaling promotes the astroglial phenotype and inhibits oligodendrogliogenesis and neurogenesis. The effect of BMP inhibition was shown in different animal models of neural injuries by noggin infusion into the lateral ventricles of rodents. In cuprizone-induced demyelination models BMP4 upregulation was inhibited by noggin infusion with following decrease of SVZ astrocytes, increased of oligodendrocytes and promoted remyelination of corpus callosum (Cate et al. 2010; Sabo et al. 2011).

7. MODULATION OF NEUROGENESIS IN ISCHEMIC CONDITIONS

HUMAN BRAIN ISCHEMIA

Stroke is a common and devastating disease. It is the second leading cause of death in developed countries and a major cause of disability in adults (Donnan et al. 2008). According to National Institute of Neurological Disorders and Stroke (NINDS, 1990), the cerebrovascular disease can be divided into hemorrhagic and ischemic (Díez-Tejedor et al. 2001). **Hemorrhagic strokes** result from the rupture of a blood vessel releasing blood inside parenchyma and originating damage.

In general, **ischemic stroke** is generated by a blood clot that blocks a blood vessel in the brain generating a deficit of oxygen and glucose. According to the cerebral affected region, ischemic stroke is divided into focal and global ischemia (Lee et al. 1999):

Focal ischemia: In this case the vascular obstruction due to thrombosis or embolism produce injury in a specific brain area. If the length of disruption is less than 24 hours, effects can be reversible and without permanent neurological deficit (Díez-Tejedor et al. 2001). But, if occlusion extends more than 24 hours it produces tissue necrosis, and is called ischemic stroke. Focal ischemia produces two regions with different characteristics. The infarct core where the blood flow is completely restricted and the lack of oxygen and

glucose produce irreversible damage. In this area the cellular death is due to necrosis. While in the area surrounding the core, ischemia is incomplete and the residual flow is enough decreased to maintain physiological function, but not to cause the loss of morphological integrity. This area is known as ischemic penumbra and there is an imbalance between pro- and antiapoptotic factors (Heiss 2012). Thus, ischemic penumbra represents the therapeutic target for cellular repair when cerebral flow is reestablished. This lesion is accompanied by extensive inflammation with edema and gliosis. In the case that ischemia prolongs, cells start apoptosis and die inevitably in the penumbra.

Global ischemia: It is originated when the reduction in blood flow is produced simultaneously in all brain. Global ischemia affects both hemispheres. This type of ischemia is the result of a decrease in systemic circulation due to a reduction of the volume or blood pressure, cardiac arrest or systemic hypoperfusion, or because there is a occlusion of the main arteries irrigating the brain. The global ischemia can be complete, when the reduction of flow is total; or incomplete, when there is a residual blood flow.

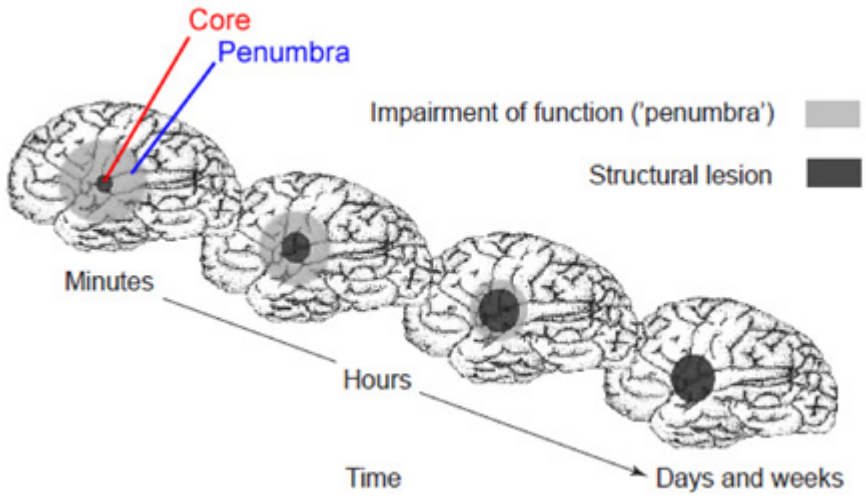

Figure 7. Ischemic damage evolution. After ischemic insult two areas are produced: core, with irreversible damage and penumbra, where the decreased residual flow is enough to maintain physiological function. As time passes, the lesion in the infarct core increases. This process is known as delayed-death. The outer areas recover their function, becoming this region in a perfect therapeutical target. Adaptated from (Dirnagl et al. 1999).

8. EXPERIMENTAL *IN VIVO* MODELS

Brain ischemia constitutes a very high social spending, which is estimated to increase in coming years, due to the ageing of our population. For this reason, appropriate animals models that mimic human disease are imperative in understanding the efficacy of different treatment strategies for the human brain. These models aim to satisfy the following criteria: (1) to mimic the pathophysiological changes found in human stroke (motor, sensory and cognitive deficits), (2) to create reproducible lesions, (3) to employ procedures that are relatively simple and noninvasive, (4) to be of low financial cost, and (5) to enable monitoring of physiologic parameters and analysis of brain tissue for outcome measures. Actually, 85% of human strokes are ischemic in origin. Thus, several ischemic stroke models have been developed in a variety of species, including rodents, canines, rabbits, pigs, cats, and even nonhuman primates. However, rodents are the most commonly used animals for several reasons, including: (1) their resemblance to humans in their cerebral anatomy and physiology, (2) their small size which enables easy analysis of physiology and brain tissue, (3) their low cost, (4) the remarkable genetic homogeneity within strains, and (5) the available broad spectrum of transgenic models.

All in all, experimental models of cerebral ischemia have been developed in an attempt to closely mimic the changes that occur during and after human ischemic stroke. There are models for both ischemic insults: global and focal. Among the **global ischemic model** we can distinguish: four-vessel occlusion procedure (4-VO), which begins with permanent occlusion of the vertebral arteries prior to temporary ligation of the two common carotids, and the two-vessel occlusion method (2-VO), in which temporary disruption of both common carotid arteries is coupled with hypotension to produce ischemia in the forebrain region. These models are considered limited in their translational clinical application as they do not closely approximate the evolution of stroke events in human aside from cardiac arrest (Tajiri et al. 2013).

Focal brain ischemia models can be categorized into two groups: permanent and transient ischemia. Permanent ischemia results in a region of severe ischemic damage (core) surrounded by a zone of less damaged tissue (penumbra). Reestablishment of perfusion after 3 hours does not reduce infarct size in all animal models. On the other hand, transient focal ischemia produces various degrees of ischemic damage depending on the duration of ischemia. Importantly, brain damage caused by transient ischemia results from both the ischemia and the effects of reperfusion. Compared to permanent occlusion, which mimic only a minority of human strokes where there is no recanalization, transient

models better represents what occur after a stroke (therapy-induced thrombolysis or spontaneous thrombolysis).

The cortex and striatum are the main target of focal ischemic damage. This is performed by ligation or occlusion of the proximal and distal middle cerebral artery (MCA) using sutures/filaments, photothrombotic approaches, and arterial or intracerebral placement of autologous blood and clot forming agents. These techniques can be achieved by craniectomy (more invasive) or intravascular approach via the carotid artery. Moreover, the occlusion can be proximal or distal, depending of site of occlusion. In case of proximal occlusion of a long segment of the MCA, including the lenticulostriate branches, the infarct size covers cortical and subcortical structures; whereas distal occlusion induce a smaller region of infarct, mainly confined to the cortex (Fig. 8). Now, we summarize some of the procedures used in literature with main emphasis on filament technique, which was used in this work:

In **thromboembolic** models the MCA occlusion is induced by an injection of a fibrin-rich clot or, for example, by the insertion of microspheres (Hossmann 2008; La Torre et al. 1991). However, lesions are multifocal and have low reproducibility. Also, the permanency of the ischemia does not simulate most clinical situations that limit the applicability of this model.

The **photothrombotic** method, uses the photosensitizing dye *rose bengal*. After systemic injection, irradiation of the intact skull with green light (560 nm) induces thrombotic plugs (Watson et al. 1985). This technique causes severe damage to affected blood vessels and substantial early vasogenic edema uncharacteristic of human stroke. Another procedure of thrombus formation involves the intravascular catheter **injection of thrombin**, at the MCA; however, this method may also not produce total arterial occlusion (Zhang et al. 1997). Moreover, clot breakdown can generate secondary micro-clot formation with possible artifact of MCA occlusion with consequent less control over ischemia location and duration.

MCA occlusion can be generated also pharmacologically through the peptide **endothelin-1** (ET-1). It induces profound and prolonged vasoconstriction of cerebral vessels. Stereotaxic intracerebral injection of ET-1 adjacent to MCA decreases significantly cerebral blood flow. This model may be useful in restorative drug studies but a main disadvantage is the high variability of occlusion. Advantages include visual confirmation of ischemia, a gradual reperfusion and low mortality.

Electrocoagulation is used to permanently occlude MCA. The occluded portion of the artery is then cut ensuring complete occlusion. This technique is more invasive because requires craniectomy. However, one of the advantages is its control over infarct size and location obtained by occluding different segments of MCA.

Alternative MCA occlusion models use devices such as microaneurysm clips, hooks, ligatures to occlude the artery. These models have the advantage of controlling the duration of the ischemia and allow subsequent reperfusion of tissue. The disadvantage is the greater variability in infarct size compared with electrocoagulation models (Macrae 2011).

We decided to occlude MCA by using **intra-luminal suture model** because of its highly reproducibility in outcome measures (infarct size and neurological deficit). Moreover, it is suitable for permanent or transient ischemia and the surgery does not involve craniectomy. Further, this model reproduces the neuronal cell death, glial activation, and blood brain barrier (BBB) damage, which is produced after an ischemic insult. In this technique a surgical filament is introduced through the internal carotid artery to the origin of the MCA. The procedure may provide a model of transient ischemia with reperfusion or permanent occlusion according to whether the suture is left inside. In the case of transient ischemia, recirculation is restored by withdrawal of the filament. Depending on the duration of the occlusion, the size lesion will be different; e.g., 30 minutes MCAO will produce damage to only the dorsolateral part of the rat striatum, while 2 hours MCAO will cause injury to overlying parietal cortex too.

The selection of the most pertinent model will depend on the class of drug under study and its perceived mechanism of action. For example, embolic stroke model is used to test new thrombolytic drugs; transient focal ischemia is commonly used to test free radical scavengers and anti-inflammatory agents. However, given the heterogeneity of human stroke, tested drugs should demonstrate preclinical efficacy in a range of different models and species before being considered for translation through the clinical trials.

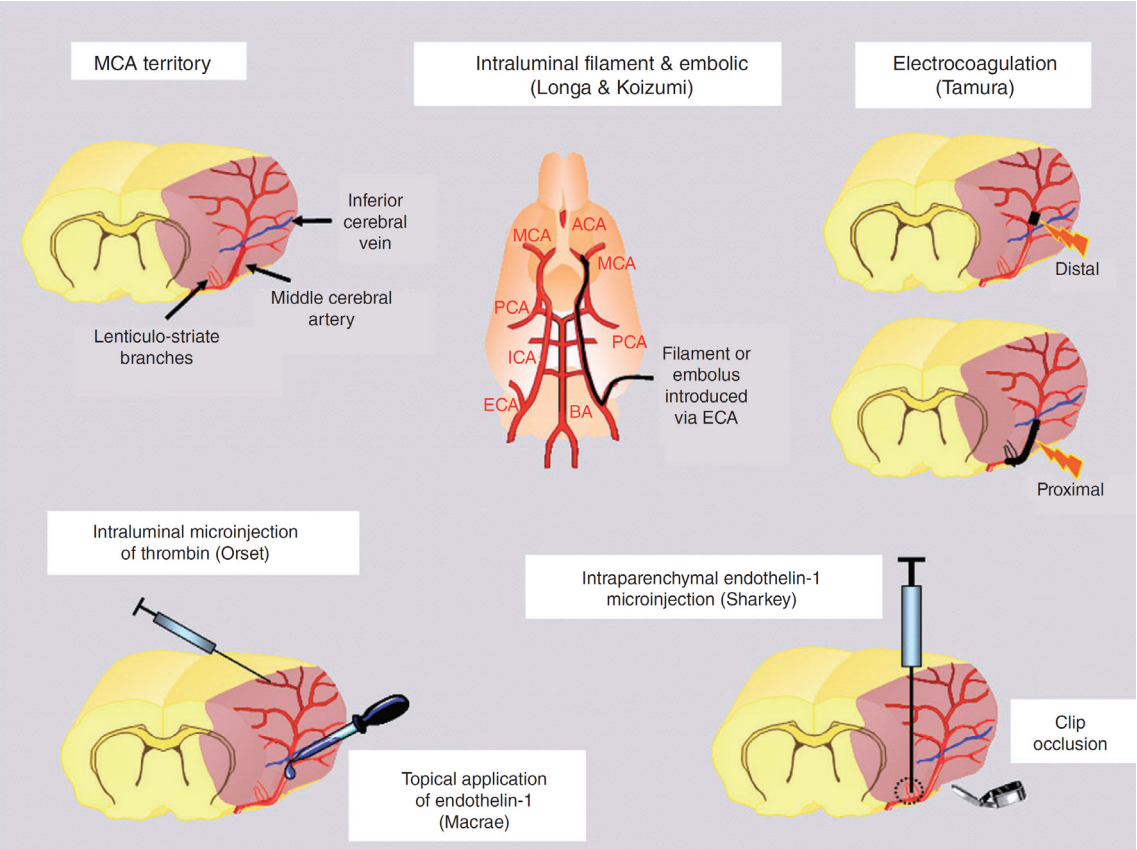

Figure 8. Several MCAO models (Beside the name of the models appears the author´s name of referring bibliography). Pink shading represents ischemic region. Electrocoagulation diagram shows the difference between proximal occlusion inducing cortical and subcortical damage and distal occlusion injuring only the cortex. Adaptated from (Macrae 2011).

9. PATHOPHYSIOLOGY OF ISCHEMIA-REPERFUSION INJURY

The brain is particularly vulnerable to ischemia. Complete interruption of blood flow to the brain for only 5 minutes triggers the death of vulnerable neurons in several brain regions. This vulnerability to ischemic damage is due to its high metabolic rate, which is 25% of basal metabolism. In addition, neurons have a near-exclusive dependence on glucose as an energy substrate, and brain stores of glucose or glycogen are limited. Because nerve cells do not store alternative energy sources, these hemodynamic reductions can result in the reduction in the metabolites such as intracellular ATP, leading to metabolic stress, energy failure, ionic perturbations, and ischemic injury. Cells that undergo ischemia may die within minutes of the insult or display a delayed vulnerability. Although depending on how early reperfusion is initiated, metabolic and ionic homeostasis can return and cell survived maintained in the ischemic penumbra.

Following ischemic insult, the neuronal vulnerability is accompanied by a typical glial reaction involving astrocytes and microglia. Reactive astrocytes display hypertrophy and hyperplasia and microglia proliferate showing increased expression of major histocompatibility complex. Finally, microglia transform into intrinsic brain phagocytes, removing neuronal debris. Reactive astrocytes and microglia undergo specific functional changes, among these secretion of cytokines and growth factors, which may mediate tissue damage (Eddleston & Mucke 1993; Gehrmann et al. 1995).

Regarding molecular changes, immediately after cerebral ischemia is produced a shutdown of neural activity induced by K^+ efflux from neurons, leading to a transient hyperpolarization. A few minutes later, a redistribution of ions occurs across the plasma membrane, associated with membrane depolarization (efflux of K^+ and influx of Na^+, Cl^-, and Ca^{2+}). This depolarization results in the excessive release of neurotransmitters, in particular glutamate, promoting further cellular depolarization, depletion of energy stores, and advancement of injury cascades. The released glutamate under ischemic conditions overstimulates N-methyl-D-aspartate (NMDA), alpha-amino-3-hydroxy-5-methyl-4-isoxazolepropionic acid (AMPA), and kainite-type glutamate receptors, promoting Na^+ influx and K^+ efflux through glutamate receptor-activated membrane channels. As consequence of glutamate release, marked neuronal cell body swelling and dendrite swelling occur, hallmarks of necrosis death. Other event triggering deleterious cytotoxic cascades is elevations in neuronal intracellular free Ca^{2+} due to glutamate increase. This increase in intracellular Ca^{2+} leads to activation of Ca^{2+}-dependent catabolic enzymes such as phospholipases, calpains, endonucleases,… which contribute to destruction of structural components of cells. Further, it has been observed an increase in ATP levels as a consequence of the release from cytosol of damaged cells or from exocytotic vesicles (Braun et al. 1998). Apart from ATP, there is an increase in its metabolic product adenosine, which exerts neuroprotective actions by inhibiting glutamate release via presynaptic receptors (Schubert & Kreutzberg 1993). Other studies have suggested that neuroprotective effect is through adenosine A1 receptor (von Lubitz 1999). In addition to glutamate and ATP other molecules released to extracellular space such as dopamine, serotonin or gamma-aminobutyric influence resultant brain injury.

Regarding downstream mediators, protein kinase C (PKC) is rapidly activated during ischemia and it may enhance neuronal excitotoxicity by increasing vesicular glutamate release. The highly conserved mitogen-activated protein (MAP) kinases, including p38 and extracellular signal-regulated kinases (ERK) can modify processes relevant to cellular injury and programmed cell death.

After ischemic insult, post-ischemic reperfusion induces further tissue damage mediated by the accelerated formation of several reactive oxygen species and nitric oxide radicals. Anaerobic metabolism releases lactic acid, increasing concentration of H^+, which leads to formation of reactive oxygen species (H_2O_2) and disruption of the normal acid-base balance in the brain. One of the consequences of ROS formation is DNA breakage (Doyle et al. 2008). Furthermore, reperfusion of ischemic tissue is associated with microvascular disfunction, which is showed as impaired endothelium-dependent dilation in arterioles, adhesion molecules on endothelial cell surface are also induced, enhancing neutrophils adhesion and passage through the vascular wall into the brain parenchyma, which is followed by invasion of macrophages and monocytes. Activated endothelial cells in all segments of microcirculation produce more oxygen radicals, but less nitric oxide, in the initial period following reperfusion. The superoxide/nitric oxide imbalance in endothelial cells leads to the production and release of inflammatory mediators and enhances the biosynthesis of adhesion molecules that mediate leukocyte-endothelial cell adhesion (Carden & Granger 2000). This inflammatory response may exacerbate initial levels of tissue injury. In particular, elevation of mRNA levels of cytokines TNF-α and IL-1β have been observed as early as 1 hour after induction of ischemia.

In relation with endothelial alterations, it has been observed acute alterations in the blood-brain barrier during early periods of post-ischemic reperfusion (Bramlett & Dietrich 2004).

Ischemia is capable of producing necrosis, fulminant cell death associated with plasma membrane failure, and swelling of cell body and internal organelles. This necrosis occurs mainly in the ischemic core. Furthermore, several molecular signatures of apoptosis such as translocation of cytochrome c from mitochondria to cytosol or activation of caspase 3 have been identified in the ischemic brain, in particular in the ischemic penumbra. Neuronal death can be demonstrated within a few hours after the insult. However, it can be taken as long as 2-3 days to mature (Du et al. 1996) (Fig. 9).

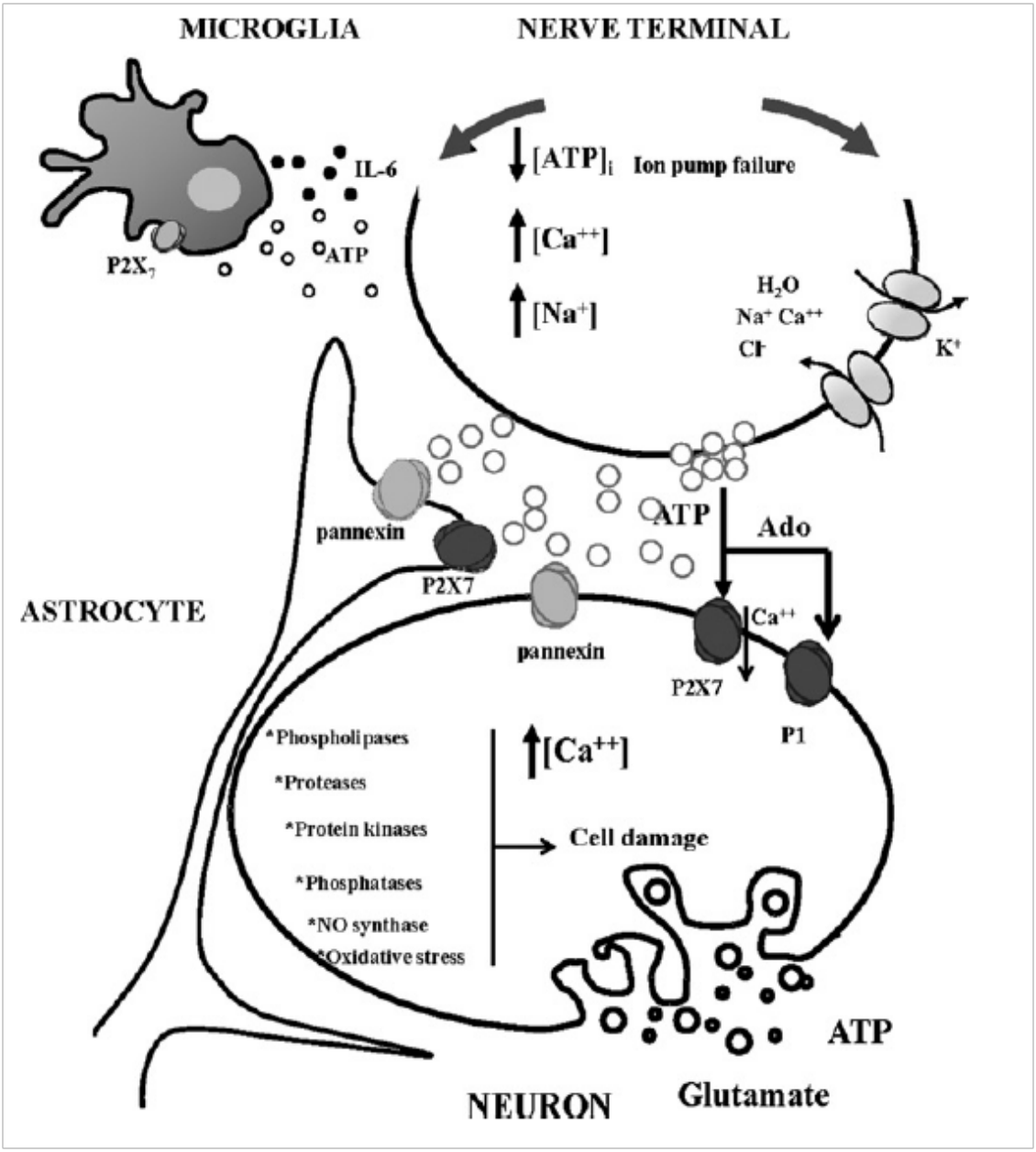

Figure 9. Pathophysiological mechanisms in ischemia. Excess of ATP and of glutamate release during ischemia leads to purinergic receptor (P2X7) activation and subsequently calcium overload in the cytosol. It triggers to activation of enzymes resulting in mitochondrial failure and cell death, and extravasation of ATP and glutamate from dying cells, which propagates damage. Release of ATP may occur by exocytosis from neurons and astrocytes, or from alternative mechanism including P2X7 receptors and pannexin hemichannels both of which are expressed in neurons and glia. Microgliosis also be detrimental by releasing proinflammatory cytokines such as interleukin-6 (IL-6). In parallel, adenosine (Ado) directly releases from neurons and astrocytes interacts with P1 adenosine receptors. From (Matute & Cavaliere 2011).

10. NEUROGENESIS IN ISCHEMIC CONDITIONS

Ischemic insults can activate neurogenesis in the adult brain from the SVZ and the SGZ. Regarding the mechanisms involved in stroke-induced neurogenesis, there are evidences demonstrating that ischemic insult leads to an increase of **cell proliferation** in the ipsilateral SVZ and a reduction in cell cycle length (R. L. Zhang et al. 2006). Nevertheless, only a small fraction of the newborn neurons will **survive** long-term. It has been estimated that about 80% of the stroke-generated striatal neurons die during the first 2 weeks after their formation (Arvidsson et al. 2002). Also endothelial cells of the blood vessels support neuroblasts activation as evidenced by the presence of neuroblasts surrounding mice endothelial cells 18 days after the insult (Yamashita et al. 2006). The importance of blood vessels in promoting survival and **differentiation** of neuroblasts is suggested also by endothelial release of factors such as SDF-1α and BDNF (Ohab et al. 2006; Wang et al. 2006). The extension of the damage is critical for the extent of recruitment of new neuroblasts to striatum after stroke. The less extensive is the lesion, fewer striatal neuroblasts are generated. Thus, the number of neuroblasts correlates significantly with the volume of striatal injury (Thored et al. 2006). Interplay between SVZ and damaged cortex has been demonstrated by Cavaliere (Cavaliere et al. 2006) in *in vitro* experiments during oxygen and glucose deprivation. They demonstrated that soluble heat-labile factors released by the subventricular zone in the media can lead to protection specifically in the cortical area.

The final step in neurogenesis process is the functional **integration** into pre-existing neuronal network. The group of Yamashita (Yamashita et al. 2006) has reported that the axons of the new striatal neurons contain abundant presynaptic vesicles and form synapses with neighboring cells, indicating some level of integration into existing neural circuitries. Although it remains unclear whether the new neurons develop their functional synaptic connectivity to improve or worsen function in the diseased brain. Nevertheless, the loss of reliable techniques to record electrophysiological properties in stroke-generated neurons is the main obstacle in demonstrating clearly the existence of synaptically integrated neurons.

Ischemia-induced neurogenesis is triggered both in neurogenic and non-neurogenic areas e.g., the striatum. This last is confirmed by some evidences summarized as follows: (1) cells coexpressing the thymidine analog bromodeoxyuridine (BrdU) and markers of immature (DCX, PSA-NCAM…) and mature neurons (NeuN) are detected in the damaged striatum. (2) Cells expressing neuroblasts markers such as DCX are detected in the stroke-

damaged striatum and coexpress transcription factors specific for developing striatal projection neurons (Arvidsson et al. 2002). Other studies have described cortical neurogenesis showing the presence of new cells expressing markers of neuroblasts or mature neurons in the ischemia-damaged cerebral cortex (Leker et al. 2007).

The latest discovery in neurogenic niches is focused on reactive astrocytes during pathological conditions such as stroke. These astrocytes close to the damaged region are able to dedifferentiate, display neural stem cell properties and subsequently, they can be forced to either convert into or produce neurons when reprogrammed by ectopic expression of transcription factors *in vivo*. Recently it has been proposed that this function can be exploited also by astrocytes newly generated from the NSCs of SVZ (Faiz et al. 2015; Grégoire et al. 2015). In addition, other studies have demonstrated the role of inflammation in dedifferentiation process (Gabel et al. 2015) as well as purinergic modulation in reactive gliosis (Boccazzi et al. 2014).

One of the factors that can modulate neurogenesis after ischemia is extracellular ATP, as previously demonstrated in our lab (Vergni et al. 2009). In fact, ATP is massively released in the extracellular milieu during ischemia and it is one of the modulating factors of neuronal survival. Thus, here we studied the role of adenosine, one of the metabolic products of ATP, in basal and pathological neurogenesis.

11. PURINERGIC SYSTEM

Purinergic system includes nucleotides and nucleosides molecules, mainly ATP and adenosine, their receptors and enzymes implicated in metabolism of nucleotides and signaling pathways. ATP was established by Fritz Limann and Herman Kalckar as the main donor of metabolic energy in biological systems. Until 1970s ATP was considered as an intracellular molecule, but Geoffrey Burnstock, pioneer in the study of nucleotides signaling, postulated that ATP could act as a transmitter in the synaptic space. In general, extracellular purines, are potent signaling molecules of the CNS eliciting a wide array of physiological effects. These can range from neurotransmission, smooth muscle contraction, pain, inflammatory response, insulin secretion, platelet aggregation, neurogenesis... Apart from these effects, they play an important role as second messengers in signaling transduction (cyclic adenosine monophosphate, cAMP).

Extracellular ATP can exert its effect as a neuromodulator when released alone or co-released with other neurotransmitters such as acetylcholine, noradrenaline, glutamate, GABA or dopamine. This founding generated the hypothesis of **purinergic**

cotransmission postulated by Burnstock in 2009 (Burnstock 2009). The release of ATP to extracellular space can occur through diffusion (due to a difference in electrochemical gradient between extracellular and intracellular medium) or exocytosis. More specifically, ATP can be released by several mechanisms in physiological and pathological conditions (Cavaliere et al. 2015): 1) passive release from damaged cells through the injured membrane e.g. in necrotic cell death, 2) active release from large storage vesicles, 3) via connexin/pannexin "hemichannels" (Domercq et al. 2010), 4) from transport vesicles delivering proteins to the cell membrane, and 5) from a subset of lysosomes.

12. EXTRACELLULAR RECEPTORS

Once released into the extracellular environment, purinergic ligands behave as signals mediators, activating different subtypes of **purinergic receptors** or are captured by the cells through specific transporters. There are four subtypes of adenosine P1 receptors (A1, A2A, A2B and A3), seven subtypes of nucleotide P2X ligand-gated ion channel receptors (P2X1-7) and eight subtypes of nucleotide P2Y metabotropic receptors (P2Y1, P2Y2, P2Y4, P2Y6, P2Y11, P2Y12, P2Y13, and P2Y14). P2X and P2Y receptors can be activated by dinucleoside polyphosphates such as Ap4A, adenosine triphosphate (ATP), uridine triphosphate (UTP)… Both subtypes receptors, P1 and P2, can activate the purinergic signal directly, through second messengers activation, or indirectly through the release of other signals mediators (such as glutamate, BDNF, LIF,…) that may determine the final functional outcome.

Purinergic receptors are expressed by almost every cell type, including prokaryotes, protozoa and early plants (Burnstock & Verkhratsky 2010). In the CNS all types of cells (oligodendrocytes, neurons, microglia, astrocytes) express purinergic receptors. The expression of all P2Y receptors, with the exception of P2Y4 and P2Y11, and essentially all P2X receptors have been identified by RT-PCR in cultured and adherent adult neural progenitor cells or neurospheres. In addition, A1, A2A and A2B adenosine receptors were found to be expressed by cultured neurospheres (Stafford et al. 2007; Lin et al. 2007). The expression of specific subtypes of receptors or catabolic enzymes can vary transiently with developmental stage, suggesting that nucleotides and nucleosides affect stage-specific developmental processes.

Apart from purinergic receptors, adenosine can be cellularly internalized or released through specific **purinergic transporters**. There are two subgroups of transporters: 1) equilibrative nucleoside transporters (ENT), independent of Na^+ and which moves nucleotides by facilitated diffusion according to gradient concentration; and concentrative

nucleoside transporters (CNT), dependent of Na^+ and which contribute to nucleotides accumulation inside the cell by active transport. Among the concentratives transporters we can distinguish two families, CNT1 and CNT2, even if their role is still debated. Regarding equilibrative transporters, there are four groups, ENT1 and ENT2, which are expressed in the CNS; and ENT3 and ENT4 less studied in brain but considered as candidate gene of tumors (Griffith & Jarvis 1996; Li et al. 2010).

13. IONOTROPIC RECEPTORS

Ionotropic receptors are classified as P2X receptor (from P2X1-P2X7), which are Na^+, K^+, and Ca^{2+} permeable ion channels. They respond to extracellular ATP with a rapid depolarization and further activation of intracellular Ca^{2+}-dependent signaling cascades. They have two hydrophobic domains going through plasmatic membrane joined by a long chain of polar amino acids. These receptors posses the amino and carboxi terminal orientated to cytosol. They can be homomerics or heteromerics, which results in altered pharmacological properties.

All P2X receptors are activated by ATP, which is the most potent of naturally-occurring nucleoside triphosphates (NTPs). Other NTPs can work at certain receptor subtypes [e.g. cytidine-5´-triphosphate (CTP) at P2X1, guanosine-5´-triphosphate (GTP) at P2X5 and UTP at P2X3]. There are a number of synthetic analogues that activate P2X receptors, among them 2-(Methylthio)adenosine-5′-triphosphate (2-MeSATP), α,β-methyleneadenosine-5′-triphosphate (α,β-meATP) and *2*'(*3*')-O-(4-Benzoylbenzoyl)adenosine-5'-triphosphate (2´,3´-BzATP). Among the P2X receptors antagonists we want to mention the suramin analogues, pyridoxal-phosphate-6-azophenyl-2',4'-disulfonate (PPADS), 2',3'-*O*-(2,4,6-trinitrophenyl)adenosine-5'-triphosphate (TNP-ATP), diinosine pentaphosphate (Ip5I), Coomassie Brilliant blue G and Reactive blue 2.

P2X receptors are dynamically expressed in the pre- and postnatal central and peripheral nervous system as well as endothelium, epithelium, vascular muscle, leukocytes, platelets and macrophages. Specifically in the CNS, these receptors are located in presynaptic and post-synaptic neurons and glial cells. In addition, their expression varies depending on the stage of development. In rodent, P2X3 receptor is expressed at different embryonic stages in cranial motor neurons and then its expression changes to other regions during the development until declining its expression at P14 stage. Conversely, P2X4, P2X5, and P2X6 are expressed from P1 stage onward (Zimmermann 2006).

The role of several P2X receptor subunits have been examined in several mice models. Null mutations for P2X1, P2X3 and P2X7 subunits, and overexpression of P2X1 in transgenic mice implicated the P2X receptors in processes as diverse as fertility, thrombosis, pain and cytokine production.

One important feature of P2X receptors is that they can interact with cell-adhesion molecules, physically cross-talk with other receptor channels or interact with G protein couple receptors (GPCRs). In particular, the extended C terminus of P2X7 receptor interacts with multiple proteins forming a large signaling complex, activating several second messengers and enzyme cascades as Akt, extracellular signal-regulated kinases (ERKs), p38 MAP kinase… There are splice variants of P2X7 receptor that may have different effects e.g. the splice variant of the P2X7A receptor is related to pore formation and cell death whereas the P2X7B variant stimulates cell growth (Adinolfi et al. 2010).

P2X7 receptor can regulate the homeostasis of the neurogenic niche by means of an inhibition of **proliferation** and stimulation of NSC **differentiation** (Tsao et al. 2013). Conversely, ATP has an inhibitory effect on motor **axon outgrowth** in neural tube explants via P2X3 receptors (Zimmermann 2011). Moreover, the P2X7 receptor expressed on neuroblasts can contribute to the clearance of apoptotic cells by activating innate phagocytosis during early stage of neurogenesis (Lovelace et al. 2015).

The P2X7 is also involved in pathological conditions, being the principal receptor of purinergic-induced excitotoxic **cell death**. As we described previously, after an insult high concentration of extracellular ATP is released from neurons, glia and damaged cells. In particular P2X7 contributes to the cell toxicity by inducing the formation of large pores, allowing the passage of cations and sustaining the release of ATP. This determines a sustained activation of purinergic receptors and an increase in intracellular calcium in target cells. In microglia the imbalance of calcium homeostasis results in the release of different interleukins, triggering a neuroinflammatory reaction (Sperlágh et al. 2006).

Indeed, during an insult a lot of molecules are released to extracellular medium acting on different receptors. Extracellular ATP can interact with P2 receptors expressed in neuroblasts inhibiting the **migration** of neuroblasts to the damaged cortex (Cavaliere et al. 2006; Vergni et al. 2009). The inhibitory effects of cytotoxic levels of extracellular ATP during OGD can be rescued *in vitro* by the use of specific antagonists (Cavaliere et al. 2001; Cavaliere et al. 2007).

14. METABOTROPIC RECEPTORS

The P1 and P2Y subtypes are classical seven-transmembrane domain receptors, whose action is mediated through G-proteins and intracellular second messengers, including Ca^{2+}, cAMP, and inositol triphosphate ($InsP_3$) (Burnstock 2007), activating a considerable variety of intracellular signaling pathways, including gene activation. Unlike ionotropic receptors, metabotropic receptors posses the amino terminal fragment orientated to the extracellular medium and carboxi terminal inside the cell. As for P2X receptors, P2Y receptors form homo-oligomers or heterooligomers with other GPCRs that could impact on both ligand properties and intracellular signaling. In particular, the P2Y1 receptor can forms hetero-oligomers with the A1 adenosine receptor (Zimmermann 2006).

P2Y receptors. There are eight P2Y receptors with different ligand preferences: P2Y1 [adenosine diphosphate (ADP), ATP], P2Y2 (UTP, ATP), P2Y4 (UTP, ATP), P2Y6 (uridine diphosphate, UDP), P2Y11 [ATP, nicotinamide adenine dinucleotide (NAD^+)], P2Y12 (ADP), P2Y13 (ADP), and P2Y14 (UDP-glucose and other nucleotide sugars). A number of synthetic nucleotides and dinucleotides can activate the recombinant P2Y receptors such as adenosine-5′-O-(2-thiodiphosphate) (ADPβS), and uridine-5´-O-(2-thiodiphosphate (UDPβS). Some of the agonists for P2X receptors such as 2-MeSADP, 2-MeSATP, BzATP also activate P2Y. This feature occurs for antagonists, being the most important suramin, Reactive blue 2, PPADS,…

Nevertheless developing brain expresses only P2Y1 and P2Y4 receptors (Cheung et al. 2003), with P2Y4 receptor as the main expressed early in the olfactory system, diencephalon, amygdale and brain stem (Zimmermann 2006).

The main functions of P2Y receptors are: 1) activation of intracellular signaling cascades, via the catalytic G protein α-subunit, and 2) modulation of membrane ion-channels, via regulatory G protein βγ-subunits. A third, less understood process involves the physical interaction of P2Y receptors with membrane proteins in their close proximity.

Depending on subtype, P2Y receptor activation can induce several intracellular signaling cascades, most notably activation of phospholipase C, activation or inhibition of adenylyl cyclase, activation of phospholipase A2, coupling to ion channels, activation of MAPK pathways, and induction of immediately early genes. In particular, P2Y1, P2Y2, P2Y4 and P2Y6 receptors coupling to G_q protein induce the activation of phospholipase C and generate $InsP_3$ and dyacilglycerol (DAG). $InsP_3$ promotes Ca^{2+} mobilization from intracellular stores and DAG activates protein kinase C (PKC). On the other hand, P2Y12,

P2Y13 and P2Y14 receptors typically couple to G_i protein, inhibit adenylate cyclase and reduce intracellular levels of cAMP (Zimmermann 2011). As for P2X receptors, the effect of P2Y receptors vary with cell type, with the coexpression of receptors and with the associated intracellular signaling molecules.

The most P2Y receptors involved in adult neurogenesis are P2Y1 and P2Y2 receptors. These stimulate cell **proliferation** in neurospheres sharing the same intracellular signaling cues of EGF.

In particular, the effect of P2Y1 in modulating neurogenesis depends on the physiological conditions and the concomitant presence of EGF and FGF. If the growth factor concentration is low, cell proliferation and migration dependent by P2Y1 increased; whereas a higher growth factor concentration has an antiproliferative effect (Mishra et al. 2006; Stafford et al. 2007). Recent findings demonstrate that stimulation of P2Y1 after infusion of ATP in rat SVZ increases the proliferation of type C cells but not of type B or A (Suyama et al. 2012). P2Y1 signal intervene also in embryonic neurogenesis sustaining the **migration** of SVZ progenitors and the subsequent proper formation of the SVZ (Liu et al. 2008).

The human P2Y2 receptor contains two C-terminal consensus Src-homology-3 (SH3) binding domains that promote recruitment and activation of Src. The Src family of tyrosine kinases is important for embryonic **stem-cell renewal** (Zimmermann 2006) suggesting a role of the P2Y2 in this function. The relationship between P2Y2 and Src family kinase is suggested also for the modulation of neuronal differentiation. In fact, synergistic activation of P2Y2 and TrkA receptor tyrosine kinase enhances neuronal **differentiation** from SVZ NSCs (Zimmermann 2011).

Other function where P2Y receptors participate together with NGF is **neurite outgrowth**. These effects vary, however, between cell type or cell line investigated. In particular, UTP acting via the P2Y4 receptor in human neuroblastoma SH-SY5Y cells increased the contribution of neurite-bearing cells. Transient transfection of these cells with the P2Y4 receptor facilitated neuritogenesis. This was accompanied by an increased transcription of immediate early genes linked to differentiation (Cavaliere et al. 2005).

***P1 adenosine receptors* (ARs)**. As we described previously, there are four subtypes of P1 receptors: A1, A2A, A2B and A3. In this case all receptors are activated by adenosine. Adenosine levels rise in stress and distress and tend to minimize the risk for adverse outcomes by increasing energy supply and decreasing cellular work, by stimulating

angiogenesis, and having multiple effects on immune competent cells (B B Fredholm 2010). The functions of adenosine receptors depend on activated pathway signaling. All receptors couple to adenylate cyclase modulating the production of cAMP. A1 and A3 are negatively coupled to adenylate cyclase through the $G_{i/o}$ protein α-subunits (downregulating cAMP), whereas A2A and A2B are positively coupled to adenylate cyclase through G_s protein (increasing the production of cAMP).

The affinity of adenosine on ARs is different, being A1, A2A and A3 receptors activated by physiological concentrations of adenosine, whereas pathophysiological concentrations of adenosine are required to activate the A2B receptor (Fredholm et al. 2001). The potency of endogenous adenosine depends both on receptor number, and on type of response measured (B B Fredholm 2010). Apart from adenosine, other synthetic agonists like NECA (5´-N-ethylcarboxamido-adenosine), CPA (N^6-cyclopentyladenosine, the most selective agonist for A1 subtype) can activate ARs. CGS 21680 is the most selective A2A agonist and, IAB-MECA and CI-IB-MECA are mainly used as A3 receptor selective agonists. In addition, A1 and A3 receptors can also be activated by inosine that acts as a partial agonist. Regarding AR antagonists, we want to mention caffeine (which has biphasic effects-stimulatory and causing slightly euphoria in low doses-inhibitory and dysphoric at high doses), methylxantines, 1, 3-dipropyl-8-cyclopentylxanthine (DPCPX) and PSB36, the two last are modified methylxantines specific for A1 receptor. In the case of A2B receptor, the most selective antagonist is MRS1754. Other AR antagonists are SCH58261, ZM241385, MRE3008F20 and MRS1523.

Adenosine receptors are widely expressed in the CNS, being the A1 and A2A the most expressed receptors. A1 receptor is mainly expressed in cerebral cortex, cerebellum, hippocampus and spinal cord, the A2A receptor shows high level in olfactory bulb and GABAergic neurons of the striatum. On the other hand, A2B and A3 receptor have low expression in the brain, with exception for A3 receptor which is observed in the hippocampus and cerebellum (Ribeiro et al. 2002).

The role of adenosine in neurogenesis is still debated due to a low bibliographic production and controversial data. It was either found to sustain or to inhibit progenitor cell **proliferation**. Stimulation of A1 receptor through the activation of MEK/ERK and Akt signaling pathways can activate whereas stimulation of A2A inhibits proliferation (Zimmermann 2011). Adenosine has a potential in modulating **neuritic differentiation** as demonstrated *in vitro* with PC12 cells after ecto-5´-nucleotidase-dependent reduction of extracellular adenosine. Effect of adenosine is not dependent by A1 receptors which

inhibits rather than activates the neuritic differentiation. On the other hand has been also reported that A1 receptors can induce neuritogenesis in SH-SY5Y cells apparently via differential intracellular signaling pathways (Zimmermann 2006).

15. NUCLEOTIDE METABOLISM

Extracellular nucleotides' life span is controlled by cell surface-located ectonucleotidases. These enzymes are located at the plasma membrane with an extracellularly oriented catalytic site. Extracellular nucleotides can be inactivated or interconverted by a multiplicity of enzymes. The regulation of extracellular nucleotides concentration hampers that purinergic receptors are permanently activated leading even to receptor desensitization when the stimulation of a ligand is extended. In the catabolic process, extracellular ATP is eventually degraded to adenosine. As a consequence of the metabolism of ATP, a variety of molecules are produced such as ADP, AMP (adenosine monophosphate), adenosine, IMP (inosine monophosphate), inosine…

There are four major groups of ectonucleotidases: 1) **Ectonucleoside triphosphate diphosphohydrolases or apyrases** (NTPDases, CD39) and ectonucleotide pyrophosphatase/phosphodiesterases, hydrolyze nucleoside tri- and /or diphosphates to the respective nucleoside monophosphates. 2) **Alkaline phosphatases** (AP) degrade nucleoside 5´-tri-, -di- and –monophosphates to the respective nucleoside, releasing inorganic phosphate. 3) **Ectonucleotide pyrophosphate/phosphodiesterase** (E-NPPs) hydrolyzes 5´-monodiester bonds in nucleotides and their derivatives, resulting in the release of 5´-nucleotide monophosphate and pyrophosphate. Physiological substrates include ATP, NAD^+, nucleotide sugars, and also dinucleoside polyphosphates. Typically, ATP is directly degraded to AMP with the release of inorganic pyrophosphate. 4) **Ecto-5´-nucleotidase (CD73)** catalyzes the hydrolysis of nucleoside monophosphates to the nucleoside (Zimmermann 2011) and it is thus of major importance for extracellular formation of the P1 receptor agonist adenosine.

Furthermore, there are other crucial enzymes: **adenosine deaminase** (ADA) transforming adenosine into inosine (other nucleoside that can activate A1 and A3 receptor (Fredholm et al. 2001)) and **adenosine kinase** (ADK), which produces AMP. The inosine can be metabolized to hypoxanthine, xanthine and uric acid. Both enzymes are important to regulate the levels of adenosine in the cell.

In the CNS, the ecto-5´-nucleotidase has predominantly glial location. However, there is considerable evidence that this enzyme is associated with the neural surface during

development and plasticity. Ecto-5´-nucleotidase is transiently associated with synapses during synaptogenesis and synapse remodeling. Other characteristic of this enzyme is that it also binds to the extracellular components laminin and fibronectin and may mediate cellular adhesion. Its expression is increased by NGF and retinoic acid. Other factors modulating its expression are Wnt and β-catenin, suggesting a role of extracellular adenosine in neuronal development (Zimmermann 2006). On the other hand, it is worth to mention that the tissue nonspecific form of alkaline phosphate (TNAP) is expressed in mouse and human undifferentiated embryonic stem cells (Czyz et al. 2003). These enzymes are powerful tools to fine tune the effects mediated by extracellular purines, hydrolyzing ATP into adenosine and, as a consequence, activating P1 pathway and switching off P2 signaling. One of the evidence for a role of nucleotides in adult neurogenesis come from the observation that type B cells of the SVZ and the glial tube cells of the rostral migratory stream express the ectonucleotidase NTPDase2 (Zimmermann 2011). TNAP is expressed by type B, type A and type C cells of the SVZ and throughout the rostral migratory stream. Deletion of ectonucleotidases results in increased extracellular nucleotide concentration, which leads to an increase in cell proliferation due to a stimulatory role of ATP in progenitors as we will point below.

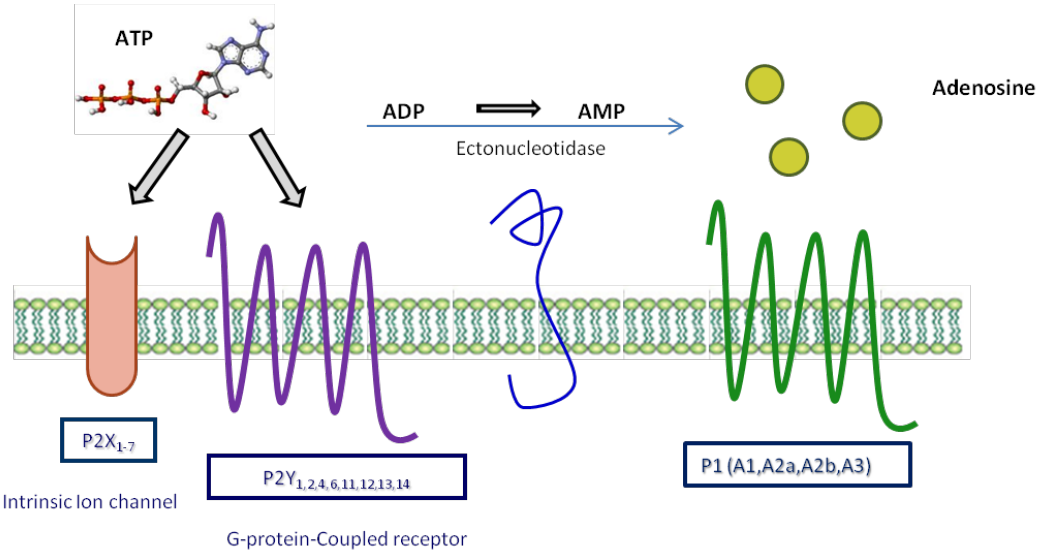

Figure 9. Potential pathways of extracellular nucleotide metabolism and the interaction with their receptors. Released ATP is metabolized by ectonucleotidases to adenosine in a stepwise manner (ADP and AMP). Some of the ectonucleotidases directly degrade ATP to AMP without intermediate formation of ADP. ATP is an agonist at P2X receptors as well as at some P2Y receptors (P2Y1, P2Y2, P2Y4 and P2Y11). Adenosine activates P1 receptors (A1, A2A, A2B, and A3).

16. FUNCTIONS OF THE PURINERGIC SYSTEM

Nucleotides act as intercellular mediators through autocrine and paracrine mechanisms. This involves that nucleotides can induce a multiplicity of cellular signaling pathways and are involved in multiple molecular interactions, thus opening the possibility of cross talk between several signaling pathways, including growth factors, cytokines, and extracellular matrix components. This means that this system is involved in a great variety of functions. In general, some of the functions are related with cardiovascular system (reducing heart rate through A1 receptor (Headrick et al. 2013)), pain (via A1 receptor (Araldi et al. 2016)), mouthfeel (via P2X2 and P2X3 receptors) or urothelium distension (via P2X3 receptor) (Burnstock 2004).

Other important function is related with platelet aggregation, which occurs through P2Y1 and P2Y12 receptors. The platelet plug is mediated by the release of ADP and as a result the activation of P2Y receptors. In this context, it is necessary to note that the activation of A2A receptor inhibits platelet aggregation. Thus, a balance between the activation of one or other receptors will allow an accurate control in platelet aggregation (Iyú et al. 2011).

Regarding the purinergic role in the immune response, the effect is mediated by P2Y2 receptors. The activation of neutrophils, which express this receptor, leads to the release of ATP and subsequently activation of P2Y2 receptor, enlargement of immune response and migration to the infectious focus. The hydrolysis of ATP to adenosine triggers to stimulation of A3 receptors, increasing immune signal (Jacob et al. 2013). On the other hand the activation of A2A receptor causes a chemotaxis inhibition (immunosuppression) (N. Zhang et al. 2006).

In addition to the functions described before, the adenosine can act as depressant agents through the activation of A1 and A2A receptors. For this reason, many of the psycho-stimulant actions of caffeine are due to the target of this antagonist. Sleep deprivation leads to accumulation of adenosine in areas such as basal forebrain nuclei. This explains why A1 receptor knock-out mouse showed normal sleep wake cycles (Bertil B Fredholm 2010).

The purinergic system also has a crucial role in some diseases such as epilepsy, ischemia, multiple sclerosis, Alzheimer disease or Parkinson disease. In *epilepsy*, seizures result from the recurrent firing of excitatory neurons as a consequence of an imbalance favouring hyperexcitability which leads to excessive release of glutamate. Thus, treatment

is based on activity-dependent inhibitors of voltage-gated sodium channels, enhancers of GABA signaling, as well as antagonists of ionotropic glutamate receptors. In this context, seizure activity can be suppressed by administration of P1 (A1) and P2 (P2X2, P2X4 and P2X6) antagonists.

As we mentioned previously, *ischemia* leads to the loss of nutrients and oxygen and causes ionic imbalance and cell death. These events result in membrane depolarization and the release of glutamate and ATP which induce calcium overload of the cytosol. ATP release during ischemia generates an unfavorable environment in which migration and proliferation of SVZ-neuroblasts to the damaged area is impeded and facilitated by the blockade of P2X1 and P2X7. On the other hand, adenosine generated by ectonucleotidases exerts a dual role in the metabolism and surviving of cells in the neurogenic niches. It can result neurotoxic through the activation of A2A receptor and further production of proinflammatory cytokines or neuro-protective if A1 receptor is activated. In this last case neuroprotection is achieved by a fine regulation of calcium influx, glutamate release and membrane potential.

Multiple sclerosis (MS) is characterized by focal lesions with inflammation, demyelination, infiltration of immune cells, oligodendroglial death and axonal degeneration. Its etiology is unclear but has autoimmune and inflammatory derivation. However, genetic and environmental factors contribute to MS susceptibility such as alterations in glutamate signaling, which contributes to oligodendrocytes death, demyelination and tissue damage. Accordingly, the A1 receptor is highly involved in the modulation of neuroinflammation and tissue protection whereas P2X7 receptors participate in the development of the disease triggering oligodendrocyte excitotoxicity.

Parkinson´s disease (PD) is characterized by the loss of dopamine innervations in the striatum and the subsequent degeneration of dopaminergic neurons leading to tremor, slowness of movement, rigidity and postural instability. In this case, A2A receptor is involved to inherent characteristics of these receptors, which were mentioned above. In addition, the heteromers formed by A2A with dopamine D2 receptor serve as a therapeutical target in this illness as they allow controlling motor function. This can be achieved by means of A2AR antagonists and/or dopaminomimetic drugs.

One of the most common neurodegenerative disorders is Alzheimer disease (AD). It affects the elderly so that the major risk factor is advanced ages. AD is characterized by a progressive impairment of memory and other cognitive skills leading to dementia. The neurophatological hallmarks of AD include: 1) selective synaptic and neuronal loss in

several brain regions, including the cerebral cortex and hippocampus; 2) senile plaques, mainly composed of amyloid-β peptide and 3) neurofibrillary tangles. The role of adenosine in this illness occurs through A1 and A2A, which show a different pattern of localization and levels in several brain regions. Benefits for cognitive deficits can be achieved by manipulating A2AR and A1R with antagonists.

Apart from these functions of the purinergic system in pathological and normal situations, it remains to mention its important role in neurogenesis. A lot of studies have demonstrated its implication in the major steps involved in the formation of the functional mature central and peripheral nervous system. In particular, the purinergic system regulates specific stages of neurogenesis like proliferation, migration of young neurons, their differentiation and cell type specification, neuritogenesis, axon growth and guidance, synapse formation and stabilization, the death of neurons that failed to integrate successfully, and finally neural network formation (Burnstock & Ulrich 2011). These effects may vary depending on receptor subtype activated, brain region where this receptor is expressed, the presence of other receptors (heteromers)… (Fig. 10)

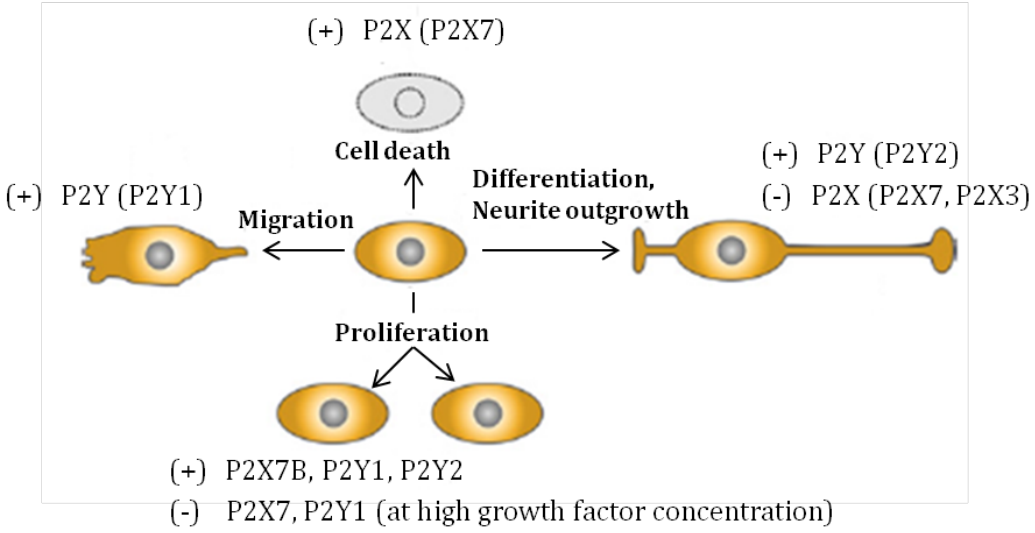

Figure 10. Principles functions of nucleotides during neurogenesis. Nucleotides were found to stimulate (+) or also to inhibit (-) cell proliferation, migration, differentiation, neurite outhgrowth and cell death via different purinergic receptors. Adaptated from (Zimmermann 2011a).

Objectives

The knowledge of adult neurogenesis modulation by the purinergic system has developed in the last years. However, numerous variables as concentration threshold, time of receptor stimulation and development stage modify the role of purinergic molecules in adult neurogenesis. Thus, the specific function of these molecules, in the different steps of basal and pathological neurogenesis, remains to be identified. Previous results from our laboratory found that ATP released after oxygen and glucose deprivation modulates neuroblasts migration and neuronal differentiation. In this context, the general objective of this project is to elucidate the role of extracellular adenosine, one of the metabolic products of ATP, in modulating adult neurogenesis in basal and pathological conditions. For this purpose we used as a cellular model neurosphere cultures and the animal model of ischemia transient middle cerebral occlusion artery (tMCAO). The specific research objectives of this PhD project are as follows:

Objective I

To analyze the effects of adenosine in neurogenesis from SVZ

Objective II

Identification of the adenosine receptor subtype involved in modulating neurogenesis

Objective III

Identification of the cellular target of adenosine

Objective IV

Characterization of the mechanisms involved in neurogenesis after adenosine receptor activation

Objective V

To test the effect of blocking adenosine receptor on neurogenesis induced after ischemia in *in vivo* models

Materials and Methods

1. *IN VITRO* CULTURES

1.1. Neurosphere culture

Neurosphere cultures were prepared from P7 and P42 Sprague-Dawley rats as previously described (Cavaliere et al. 2012). Briefly, the subventricular zone (SVZ) from 2-3 brains was isolated and minced with a Mc Illwain tissue chopper (Campden Instrument, www.campdeninstrument.com). SVZ tissue was digested for 10 minutes at 37ºC in 5 ml of trypsin/EDTA (Sigma, Madrid, Spain). Digestion was stopped by adding an equal volume of trypsin inhibitor (Sigma) and 0.01% DNAse I (Sigma) for 5 minutes at room temperature. The cell suspension was centrifuged for 10 minutes at 900×g and the pellet mechanically dissociated 25 times in NeuroCult medium (Stem Cell Inc., Grenoble, France) using a glass Pasteur pipette and 20 times using 1 ml pipette tips. Undissociated cells were decanted for 30 minutes and the single cell suspension counted using the Neubauer chamber. Cells were seeded in proliferation medium [NeuroCult with 10% neural stem cell factors both from Stem Cell Inc., 2 mM glutamine, penicillin/streptomycin mix, 20 ng/ml EGF (Promega, Madrid, Spain), 10 ng/ml bFGF (Promega)] at a density of 10^4 cells/cm^2 and cultivated in suspension for 7 days at 37ºC and 5% CO_2. EGF and bFGF were added freshly every 2-3 days.

1.2. Neuronal differentiation

After 7 days, cells were aggregated as primary clonogenic neurosphere. Floating neurospheres were attached on plastic or glass coverslips previously treated with poly-ornithine (Gibco, Madrid, Spain) and differentiated for different time in differentiation medium (DM) [Neurocult basal medium, 10% differentiation factors (both from Stem Cells Inc.), 2 mM glutamine, penicillin/streptomycin mix, 50 ng/ml NGF and 50 ng/ml BDNF (Biovision, Madrid, Spain)].

Differentiation was evaluated by *Single Sphere assay*. Briefly, after neurosphere formation one single spheres (approximately 100 μm of diameter) were picked under sterile condition and seeded in a 12 mm poly-ornithine glass coverslips; differentiation experiments were performed in triplicate in DM. Differentiation was evaluated after 7-12 days by immunofluorescence for different neuronal markers as shown in Tab. 1 (NMDAR1, calbindin, synaptophysin, tyrosine hydroxylase…). Neuronal differentiation was quantified by densitometry after immunofluorescence as a ratio of βIII tubulin (AbCam) signal vs total nuclei staining with DAPI (Gibco) by using the ImageJ software or by cytofluorimetric assay (see below).

1.3. Astrogliogenesis *in vitro*

Neurosphere cultures were differentiated for 7 days in DM in the presence of the proliferation marker BrdU (Sigma). After 7 days in culture, cells were fixed in 4% para-formaldehyde (PFA) for 10 minutes and processed for immunofluorescence (see below). We evaluated the amount of mature astrocytes by direct count of $S100\beta^+/BrdU^-$ cells; whereas $S100\beta^+/BrdU^+$ cells were considered as undifferentiated neural progenitor cells.

1.4. Organotypic culture

The organotypic culture is a valid and reliable model between monocultures and *in vivo* models. This type of culture resembles *in vivo* models better than dissociated cultures. In fact, individual cells are in tight contact with each other, maintain their organotypic architecture, and preserve neuron–glia interactions, tissue-specific transport, and ion diffusion systems. This model has allowed culturing for weeks or months CNS tissue. In our case, the objective of the experiment was analyzing the expression of some proteins related with differentiation and synapses in 3D explants. They were prepared from Wistar rat pups (4-7 days old) using a modification of the method by Plentz and Kitai (Plenz & Kitai 1996). Rat pups were decapitated and skulls opened along the commissural lines. Brains were separated in two hemispheres and the lateral third of each hemisphere, together with cerebellum, were removed (Fig. 11). The resulting brain blocks were cut dorso/ventrally (350 μm of thickness) in a tissue chopper (Mickle Laboratory Engineering, Ireland). Finally, slices containing cortex-corpus callosum- subventricular zone- striatum (approximately 6 slices/rat) were selected morphologically under dissection microscope taking as a reference the subventricular zone. Slices were cultivated in liquid-air interface on Millicell CM culture inserts (Millipore, Schwalbach, Germany) and maintained at 37ºC and 5% CO_2 in medium: 50% Neurobasal-B27, 25% HBSS, 25% inactive horse serum (Gibco, Eggenstein, Germany), 1 mM L-glutamine (Biochrom, Berlin, Germany), 25 mg/ml penicillin/streptomycin mix and 5.5 mM glucose. This medium was removed instead of fresh medium the following day. Slices were shifted to fresh medium every 2-3 days. Organotypic cultures were used after 7-12 days *in vitro* in order to avoid apoptotic cell death in the inner layers due to loss of oxygen and nutrients and to allow proper maturation. After 7-12 days *in vitro*, slices were fixed for 40 min in 4% PFA. The immunofluorescence protocol will be described later.

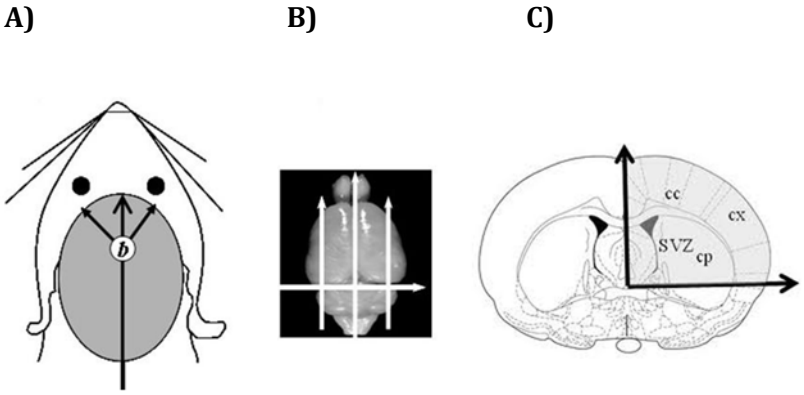

Figure 11. **Schematic view of organotypic culture preparation.** A) Lines indicate the location and direction of cut to open the skull and remove the brain for further dissection. **b** inside the circle indicates the Bregma point. B) The outer third of the lateral cortex and the entire cerebellum were removed (arrows). C) Schematic view of explant structure, which includes corpus callosum (cc), cerebral cortex (cx), subventricular zone (SVZ) and striatum-caudate putamen (cp).

2. CELL VIABILITY

We differentiated $5x10^5$ cells in DM for 7-9 days. Cells were detached and disaggregated with Accutase (Sigma) for 3 minutes and counted by the **automatic cell counter Scepter** (Millipore) in 1 ml of phosphate buffered saline (PBS). This system uses the Coulter principle of impedance based on particle detection to reliably and accurately count the cells. As cells flow through in the sensor, resistance increases, and, this increase in resistance causes a subsequent increase in voltage.

3. Ca^{2+} RECORDINGS

Calcium imaging technique shows the calcium (Ca^{2+}) status of a cell by means of calcium indicators, like fura-2, indo-1, fluo-3, fluo-4,… These fluorescent molecules respond to the binding of Ca^{2+} ions by changing their fluorescence properties. In our experiment we used the citosolic calcium quelate fura-2, which is excited to 340 nm and 380 nm of light, and the ratio of the emissions at those wavelenghts is directly related to the amount of intracellular calcium [Ca^{2+}i]. We wanted to verify the functionality of neurosphere-derived glutamatergic neurons by analyzing the Ca^{2+} entrance after 100 μM glutamate stimulation. Specifically, neurospheres, after 7 days of differentiation, were loaded with 5 μM fura-2 AM (Invitrogen) for 45 min at 37°C. Cells were washed in HBSS containing 20 mM HEPES (pH 7.4), 10 mM glucose, and 2 mM $CaCl_2$ (incubation buffer) for

5 min at room temperature. Experiments were performed in a cover slip chamber continuously perfused with incubation buffer at 1 ml/min. Single cells were selected using a high-resolution digital black/white CCD camera (ORCA; Hamamatsu Photonics Iberica, Barcelona, Spain), and image acquisition and data analysis were performed using the AquaCosmos software program (Hamamatsu Photonics Iberica).

4. IMMUNOLABELING

4.1. Immunofluorescence

Immunocytochemistry technique is used to visualize the localization of a specific protein in cells by antigen-antibody reaction. It combines the use of primary antibodies, which are specific for a particular protein, and secondary antibodies, which recognize primary immunoglobulins and are linked to different fluorescent dyes. In this study, cell cultures on glass coverslips were fixed in 4% PFA and permeabilized with 0.05% Triton and 5% normal goat serum in PBS. In the case of organotypic culture, slices were permeabilized and saturated with 0.5% Triton and 10% normal goat serum in PBS. Primary antibodies were incubated at different concentrations (see tab.1 for specification) overnight at 4ºC and then washed three times with 0.1% Triton in PBS. Secondary conjugated antibodies were incubated for 1 hour in the dark at room temperature. All secondary antibodies were diluted at 1:500 (see tab.1 for specification). After three washes with 0.1% Triton in PBS, nuclei were counterstained for 1 minute with DAPI and further washed with PBS. Finally, cover slips were mounted with Glycergel (Dako, Barcelona, Spain) and analyzed by fluorescence using the Apotome system (Zeiss, Goettingen, Germany) or by confocal imaging (Leica TCS SP8 STED CW confocal laser scanning microscope).

Antibody	Host	Technique	Dilution	Company
A1 receptor	Rabbit	IF	1/200	AbCam, UK
A1 receptor	Rabbit	WB	1/1000	AbCam, UK
A2a receptor	Rabbit	IF	1/100	Alomone, Israel
A2b receptor	Rabbit	IF	1/100	Alomone, Israel
A3 receptor	Rabbit	IF	1/100	Alomone, Israel
Synapthophysin	Mouse	IF/WB	1/500	Millipore, Germany
VGLUT2	Mouse	IF	1/300	AbCam, UK
Calbindin	Rabbit	IF	1/300	AbCam, UK
NMDAR1	Mouse	IF	1/200	AbCam, UK
Tyrosine hydroxylase	Rabbit	IF	1/1000	Millipore, Germany
Nestin	Mouse	IF	1/500	Cell Signaling, Germany
βIII tubulin	Rabbit	IF	1/300	AbCam, UK
GFAP	Mouse	IF	1/1000	Sigma, Spain
GAPDH	Mouse	WB	1/1000	Millipore, Germany
β-actin	Rabbit	WB	1/5000	Sigma, Spain
aIL10	Rabbit	IF	2μg/ml	Antibodies on-line, Germany
IL10R	Mouse	IF	1/500	Santa Cruz Biotech, Germany
IL10R	Rabbit	CF	1μg/10^6 cells	Santa Cruz Biotech, Germany
NeuN	Rabbit	IF	1/500	Millipore, Germany
pSMAD1/5	Rabbit	CF	1μg/10^6 cells	Cell Signaling, Germany
DCX	Rabbit	IF	1/500	AbCam, UK
S100β	Rabbit	IF	1/500	Santa Cruz Biotech, Germany
BrdU	Rat	IF	1/400	Invitrogen, Spain
Alexa Fluor	Goat	IF,CF	1/500	Invitrogen, Spain

Table 1. Antibodies used in immunofluorescence (IF), Western blot (WB) or cytofluorimetry assay (CF).

4.2. Cytofluorimetry assay

Flow cytometry is a laser-based, biophysical technique used in cell counting, cell sorting and biomarker detection by suspending cells in a stream of fluid and passing them by an electronic detection apparatus. Flow cytometry allows multiparametric analysis of the physical and chemical characteristics of up to thousands of particles per second.

We used cytofluorimetry assay to count cells expressing biomarkers for neuronal and astrocyte differentiation. Neurosphere cultures were differentiated for 7 days under different condition and suspended in 0.3 ml PBS/0.5 mM EDTA/1% BSA at single cell level after trypsin dissociation.

We have performed two types of cytofluorimetric experiments.

4.2.1. The objective of first experiment was to identify the **cellular target** of adenosine. For this purpose, neurospheres were differentiated under different conditions (no treatment, 100 mM adenosine, 100 μM CPA, 1 μM PSB36 and CPA+PSB36). Newborn neurons were labeled 48 hours before cytofluorimetry assay by transfection with 3 μg of the plasmid pEGFP-NFM (Addgene). Whereas multipotent cells were labeled for 2 hours with 20 ng/ml EGF complexed to Alexa Fluor® 647 (A640EGF, Molecular Probes, Cambridge, UK). Staining with pEGFP characterized newborn neurons, staining with A640EGF characterized B cells and double staining with A640EGF/pEGFP intermediate progenitor cells (C cells). Cells were suspended at single cell level in 0.3 ml of PBS/0.5 mM EDTA/1% BSA after 0.01% trypsin-EDTA (Gibco) dissociation. Cells were analyzed with a Gallios analyzer (Beckman Coulter). For GFP analysis cells were excited with 488 laser while A640EGF with a 633 laser.

4.2.2. The second experiment was performed for studying **intracellular expression of pSMAD and IL10R,** molecules involved in astrogliogenesis pathway**.** After 7 days of proliferation neurospheres were differentiated for different times under different conditions. Cells were detached with 0.01% trypsin-EDTA (Gibco) and dissociated as described above. Primary antibodies (anti-IL10R and pSMAD1/5) were incubated (see Tab.1 for concentration) for 1 hour at 4ºC after three fast washes in 0.1% Triton. Immunoreactivity was revealed after Alexa Fluor 488 (Life Technologies) incubation for 30 min at 4ºC. Cells were finally suspended in 0.3 ml of PBS/ 0.5 mM EDTA/1% BSA and analyzed with the sorter FACS Jazz (BD, Madrid, Spain) by using 488 blue lasers. For IL10R localization, cells were gated as described in (Azari et al. 2011) under morphological characteristics.

5. GENE EXPRESSION ANALYSIS

5.1. RNA extraction and quantification

Total RNA from approximately $2x10^6$ of cells was extracted after 3, 7 or 15 days of differentiation under different conditions with the commercial kit (Pure link-RNA mini kit) from Ambion-Life technologies (Madrid, Spain) using column-based affinity methodology. The quality of extracted RNA was checked on agarose gel. Quantification was performed using a Nanodrop 2000c spectrophotometer (Thermo-Scientific, USA).

5.2. Retrotranscription

RNA samples were retrotranscribed to complementary DNA (cDNA) by means of a retrotranscriptase enzyme. In each reaction, 400 ng of total RNA were incubated with 0.25 µg random primers (Promega, Spain); 1 µl of a mixture of 10 mM dinucleotidetriphosphate (dNTPs; Invitrogen, Life Technologies, Thermo Fisher Scientific, USA); 200U of the retrotranscriptase SuperScript III (SSIII; Invitrogen, Life Technologies, Thermo Fisher Scientific, USA); 40U of ribonucleases inhibitor (RNase OUT; Invitrogen, Life Technologies, Thermo Fisher Scientific, USA); 1 µl of 0.1 M dithiothreitol (DTT), a cofactor for the RNase; and 4 µl of 5X buffer (250 mM Tris-HCl, 375 mM KCl, 15 mM $MgCl_2$), being the final volume 20 µl. The enzymatic process was performed in a Verity 96 well thermal cycler (Applied Biosystems, Life Technologies, Thermo Fisher Scientific, USA) by initially incubating the mixture for 5 min at 25ºC, then activating the SSIII for 60 min at 50ºC, and finally inactivating the enzyme by incubation at 70ºC for 15 min.

5.3. Quantitative real time polymerase chain reaction (qRT-PCR)

This technique amplifies and simultaneously detects or quantifies a target gene using fluorescent reporter dyes. The first cycles of a PCR lead to an exponential generation of cDNA copies, which is reflected in an exponential increase in the fluorescent signal, reaching finally to a plateau stage. During exponential stage is when it can be defined the threshold cycle or Ct (cycle where the amplification of your sample crosses with the threshold line). The more abundant is the target in the starting material, the lower the Ct. An aliquot (0.5 µl/well) of each cDNA was incubated with primers (1.3 µl/well) and (5.2 µl/well) the fluorescent reporter dye (SSoFast™ EvaGreen® Supermix; BioRad, Madrid, Spain) in a final volume of 10 µl. Specific primers for the different adenosine receptors (Adora1, Adora2a, Adora2b, Adora3), crystallin alpha B (CRYAB), IL10, Bmp2 were all acquired from Qiagen (QuantiTect Primer Assay, Barcelona, Spain). Primers of the housekeeping genes hypoxanthine phosphoribosyl-transferase 1 HPRT1 (Qiagen

(QuantiTect Primer Assay, Barcelona, Spain) and glyceraldehydes-3-phosphate dehydrogenase GAPDH (forward sequence, GAAGGTCGGTGTCAACGGATTT; reverse sequence, CAATGTCCACTTTGTCACAAGAGAA) were used for normalization. Cycling conditions included a initial denaturation step for 3 min at 95ºC followed by 40 cycles which consisted in a) denaturation and enzyme activation step of 10s at 95ºC, b) annealing/extension step of 30s at specific anneling temperature for each primer pair. Finally we ran the melting curve to corroborate that a unique and specific PCR product was amplified. Real-time quantitative PCR reactions were performed in a CFX96 Detection System (BioRad, Madrid, Spain). Quantification was performed using the $2^{-\Delta\Delta Ct}$ algorithm.

5.4. PCR gene expression array

The PCR array system combines the quantitative performance of SYBR® Green-based real-time PCR with the multiple gene profiling capabilities of a microarray. It is a reliable tool for analyzing the expression of a focused panel of genes. The specificity of the system is based on the combination of SYBR Green primers and PCR master mixes, which guarantees a single product of the predicted size from every reaction. The cDNA retro-transcribed from $2x10^6$ cells (see above), was analyzed in a 96 multiwell plate for the expression of 88 different neurogenesis-related genes (Qiagen, Barcelona, Spain). This array includes genes related to the regulation of key neurogenesis processes such as the cell cycle and cell proliferation, differentiation, motility and migration. Each well contains replicates of different probes; results were analyzed and quantified as aΔΔCt system with the software "PCR Array Data Analysis Software" (Qiagen). Only changes by more than a ±30% of threshold was considered in this study.

5.5. Adora1 silencing

The silencing mechanism leads to the degradation of a target messenger ribonucleic acid (mRNA). It is induced by small interfering RNAs (siRNAs) or short hairpin RNAs (shRNAs), in both it is formed a double-strand structure, which lead to degradation of target RNA. In this experiment, we have used plasmids, which contain a sequence that encodes for a shRNA, which contains a loop structure that is processed to siRNA by Dicer proteic complex. It hybridizes with target RNA impeding its translation. Plasmid was transfected with Nucleofector® system (AMAXA-Lonza, Madrid, Spain), which allows integration into host cell genome, reaching stable expression.

Expression of adenosine A1 receptor (Adora1) was silenced after transfection with specific shRNAs. Briefly, after 7 days of proliferation neurospheres were dissociated with

accutase and transfected with specific shRNA. We used two specific shRNA to increase effectiveness (A1-shRNA1: CCgggAAggTTATCAgCATggAgTACTCgAgTACTCCATgCTgATAACCTTCTTTTT and A1-shRNA2: CCggCCCggAAATgTACTggTgATTCTCgAgAATCACCAgTACATTTCCgggTTTT both from Sigma). Transfection was performed with 3 μg of each plasmid by electroporation (AMAXA-Lonza, Madrid, Spain). A scrambled plasmid was used as a control. Silencing efficiency was evaluated by Western blot analysis 6 days after transfection by using Adora1 antibody (Abcam). Differentiation was evaluated after 7 days by immunofluorescence with βIII tubulin vs total cells (DAPI).

6. PROTEIN EXPRESSION

6.1. Protein extraction and Western blot

Western blot is a semi-quantitative technique which is able to identify specific proteins from a complex mixture of proteins extracted from cells. The technique is summarized in three stages: (1) separation by size in an electric field (electrophoresis), (2) transfer to a solid support (membrane), and (3) marking target protein using proper primary and secondary HRP-conjugated antibodies that ensure the detection of the molecules.

Total protein was extracted on ice using RIPA buffer (50 mM Tris-HCl pH 7.4, 1% NP-40, 0.25% Na-deoxycholate, 150 mM NaCl, 1 mM EDTA, 1 mM PMSF, 1 μg/ml of each aprotinin, leupeptin, and pepstatin,1 mM Na3VO4, 1 mM NaF) in the presence of protease inhibitor cocktail (Complete, Mini EDTA-free tablets, Roche, Leganes, Spain) and subjected to centrifugation (12.000 rpm at 4ºC for 5 min) to remove insoluble material. Solubilized proteins were quantified using the BioRad Protein Assay (USA), based on Bradford´s method. This colorimetric assay is based on the absorbance shift in the dye Coomassie induced by protein binding (change from red to blue). The absorbance was read at 595 nm in a Spectronic 501 spectophotometer and the obtained values were plotted to a standard curve made using bovine serum albumin (BSA).

Proteins were denatured for 5 min at 90ºC in the presence of sample buffer (6.25 mM Tris pH 6.8, 12.5% glycerol, 2.5% SDS, 0.025% bromophenol blue, and 5% β-mercaptoethanol). After that, samples (10 μg/lane) were separated by electrophoresis in a Criterion TGX pre-cast gel (BioRad, USA). A prestained standard molecular weight ruler was included (EZ-Run PreStained *Rec* Protein Ladder, Thermo Fisher Scientific, USA) to figure out the molecular weight of the target protein. Electrophoresis was carried out in a

Criterion Cell cuvette (BioRad) at a voltage of 125V for 15 min (to allow the package of the proteins) and at 250V for the rest of the running phase.

Separated proteins in the gel were transferred into a nitrocellulose membrane (Trans-Blot Turbo, Midi Format 0.2 µm, BioRad) in a semi-wet transference system (Trans-Blot® Turbo, Bio-Rad) for 7 min. Protein transfer was evaluated by Ponceau staining. All membrane incubations were performed in TBST buffer (50 mM Tris Base, 200 mM NaCl, 0.1% Tween-20, pH 7.4). Membranes were saturated in blocking solution (TBST, 5% BSA) for 1 hour at room temperature and successively hybridized overnight at 4ºC with the different primary antibodies (see tab.1 for specification). Membranes were washed three times for 10 min with washing solution (TBST) and incubated for 1 hour with different HRP secondary antibodies (all 1:5000, Sigma, Madrid, Spain), washed three times, and revealed with peroxidase using ECL (Super Signal West Dura, Pierce). The luminescence of the reaction product was detected by the ChemiDoc XRS Imaging System (Bio-Rad), and the intensity of the bands was quantified using Quantity One® (Bio-Rad) software corrected by Gaussian curves. Results were normalized to β-actin or GAPDH to correct errors in sample loading and/or protein transfer.

6.2. Synaptosome preparation

Synaptosomes are artificial, membranous sacs that contain an enriched fraction of synaptic proteins. They are created during nerve tissue homogeneization and contain the complete presynaptic terminal, including mitochondria and synaptic vesicles, with the postsynaptic membrane and the postsynaptic density. In our case synaptosomes preparation were used to study axo-dendritic transport to synapses.

Synaptosomes were prepared from $2x10^6$ differentiated cells under different conditions by using the commercial solution Syn-PER (Pierce-Thermo Scientific). Once cells have differentiated completely to form synapses for 10 days, Syn-PER Reagent (Thermo Fisher Scientific, USA) containing protease/phosphatase inhibitors was added to cells and these were scraped from the plate. Cell suspension was centrifuged at 1200×g for 10 minutes and pellet discarded. Supernatant was centrifuged at 4ºC for 20 minutes at 14000×g; supernatant was the cytosolic fraction and pellet synaptosome. Both cytosolic fraction and synaptosomes were analyzed by Western blot for the expression of synaptophysin, GAPDH, Ezh2 and total ERK. The quality of preparation was evaluated as an enrichment of GAPDH and the nuclear protein Ezh2 in the cytosolic fraction respect to the synaptosomal. Quantification was evaluated by densitometry after normalization with total ERK1/2 as a ratio between the expression in the synaptic vs cytosolic fraction.

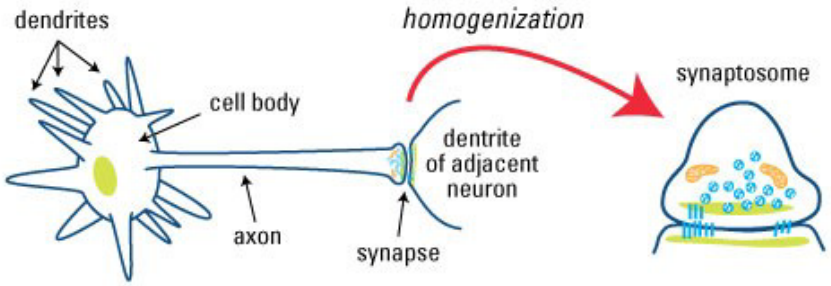

Figure 12. Schematic of a synaptosome formed from the detached nerve terminal and part of the postsynaptic membrane during mechanical homogenization.

7. LUMINISCENCE ASSAYS

We performed two types of luminescence assays: ELISA assay to analyze the release of different interleukins; and STAT3 assay, in which it was measured protein activity.

7.1. ELISA assay

Enzyme-linked immunosorbent assay (ELISA) is a biochemical technique used to detect the presence of an antibody or antigen in a sample. In sandwich ELISA, the antigen is quantified between two layers of antibodies (capture and detection). In this study, we analyzed several interleukins (IL-6, IL-10, IL-1 and TNF-α). Elisa assays were performed by using commercial kits from Peprotech (London, UK). $5x10^5$ cells were differentiated in the presence of 100 μM CPA for 5 days. Supernatants were collected and concentrated with Amicon ultra-4 (cut-off 10KDa, from Millipore). ELISA reaction was performed in multi-well plate, where capture antibody is fixed. Afterwards, dilutions of each interleukin standard and supernatants were incubated at room temperature for 2 hours. Plate is aspirated, washed four times and incubated with detection antibody for 2 hours. Newly, solution was removed and plate washed. The signal was amplified by avidin-HRP conjugate, we incubated for 30 min, washed and immediately incubated with ABTS substrate until solution color became blue. The reaction was stopped adding 1N HCl. Signal was read in luminometer Synergy-HT (BioTek, Bad Friedrichshall, Germany) at 450 nm.

7.2. Luciferin/luciferase assay

In this experiment, we studied one of the components of astrogliogenesis pathway, STAT3. For that, 10^6 cells from neurosphere cultures were transfected with 3 μg of the

plasmid 4xBwt-pGL3 (Fukuda et al. 2007) using Nucleofector® technology. After 3 days of differentiation, cells were stimulated for different times with 100 µM CPA in the presence or absence of 1 µM PSB36 or blocking antibody against IL10 (2 µg/ ml). The plasmid contains STAT3 binding sites in the Bmp2 promoter fused with the luciferase gene. The gene translation produces luciferase, which oxidize luciferin and transform into oxyluciferine and energy in the form of light. So, transfected cells whose plasmids are expressed show luminescence. Differentiated cells medium was removed. Immediately, cells were washed with PBS containing 1mM Mg^{2+} and 1mM Ca^{2+}; and incubated at room temperature for 10 min with a mixture of different buffers which contain luciferin substrate (Tropix Luc-screen for firefly luciferase, Life Technologies). Luciferin/Luciferase reaction was read in the luminometer Synergy H4 hybrid (BioTek, Bad Friedrichshall, Germany).

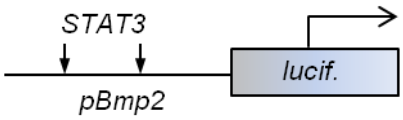

Figure 13. Schematic representation of the plasmid 4xBwt-pGL3 that contains the luciferase reporter gene under the control of Bmp2 promoter with two STAT3 consensus sequences.

8. *IN VIVO* EXPERIMENTS

All animals for *in vitro* and *in vivo* studies were handled in accordance with the European Communities Council Directive (2010/63/EU). All possible efforts were made to minimize animal suffering and the number of animals used.

Regarding *in vivo* experiments we have distinguished two types according to the drug administered (the A1 agonist CPA or the A1 antagonist DPCPX).

8.1. Osmotic pumps releasing CPA

For these *in vivo* experiments we analyzed the effect of A1 receptor agonist (CPA) in the brain for 14 days. We used adult male Sprague Dawley (200-250g, 6-8 weeks). Two experimental groups (vehicle and treated) were considered. Before surgery, osmotic pumps (Alzet®, model number 1002) were filled with PB (Vehicle) and CPA (treated, 16 µg/100 µl (500 µM); 250 nl/h/14 days) and they were immersed in PBS solution at 37ºC until the following day. Proliferating cells in both groups were labelled the day before the experiment with 3 intra peritoneal injections of 100 mg/kg BrdU (Sigma). At the day of the experiment rats were anesthetized with an intraperitoneal injection of a mix of ketamine

(80 mg/Kg) (Merial, Lyon, France) and xylazine (10 mg/Kg) (Bayer, Pennsylvania, USA). Animals were placed on a stereotactic instrument and it was made an incision on the skin which allowed visualize the skull. Once it was located the injection point according to Bregma coordinates (implantation: 2mm lateral to the midline; 1mm posterior to the Bregma; 4mm from the brain surface); the canula connected to osmotic pump was inserted subcutaneously in the right ventricule. Immediately, it was sutured by means of surgical staples. Animals were sacrificed after 14 days.

8.1.1. Sacrifice and tissue processing

After 14 days, animals were anesthetized with intraperitoneal injection of 20% chloral hydrate (200 mg/ml, 0.5 g/kg, Panreac) to proceed to transcardial perfusion. This technique consists in making two incisions; one of them at right auricle, to allow the removal of the blood, and the other one at left ventricle, to allow the perfusion by means of a canula. A 0.1M PBS solution followed by 4% PFA solution in phosphate buffer (PB: 25 mM $NaH_2PO_4 \cdot H_2O$; 7.5 mM $NaHPO_4$) was administered with the canula to aorta artery for 10-15 min. Peristaltic pump 70 18-20 (MasterFlex, USA) controlled the flow speed. After extraction, brains were postfixed in 4% PFA for 3 hours, and then changed to PBS solution with 0.02% sodium azide to prevent contamination.

Afterwards, olfactory bulb and SVZ were sliced at 40 μm of thickness in a Leica VT 1200 S vibratome (Leica Microsystems) for immunofluorescence (see below Immunohistochemistry: Double flourescence immunolabelling). All images were obtained in a Leica TCS SP8 STED CW confocal laser scanning microscope. For the analysis, we counted the total number of double-labeled positive cells (DCX/βIII tubulin/S100β + BrdU) in three slices/condition (each at 60 μm) of the olfactory bulb using the proprietary Leica Confocal LAS-AF Software (v 3.3.0.10134). Neurogenesis was assessed in the granular layer of olfactory bulb (GrL) in the case of DCX/$BrdU^+$ cells or in the glomerular layer (GL) for NeuN/BrdU cells. Astrogliogenesis (S100β/$BrdU^+$ cells) was assessed in the GL.

8.2. Ischemic animals treated with DPCPX

For these *in vivo* experiments we analyzed the effect of the antagonist of A1 receptor 1, 3-dipropyl-8-cyclopentylxanthine (DPCPX, 0.1 mg/Kg, Sigma) in ischemic animals. We realized transient middle cerebral artery occlusion (tMCAO) procedure to generate ischemia in adult C57BL/6 mice. This technique uses a filament to arrest flow proximal to the lenticulo-striate arteries, thus lesions are produced in the cortex and striatum.

In this case two groups of animals were used, sham and tMCAO animals. In the sham group, arteries were visualized but not disturbed. The other group was animals subjected to tMCAO. In both cases, it was established 2 set of animals, one of them was injected with a vehicle solution (PBS) and the other one with DPCPX (treated animals). In a separate set of experiments anesthetized animals from all groups underwent cerebral blood flow (CBF) measurements using a laser Doppler perfusion monitor. All CBF measurements were conducted with the mouse fixed in a plastic frame with the probe placed in the region of cerebral cortex perfused by MCA.

Previously to tMCAO procedure, surgical tools were sterilized, and surgery table and other equipment were sanitized using 70% ethanol. Adult animals (25g of weight) were anesthetized with isofluorane (B. Braun, Melsungen, Germany) and oxygen (induction of anesthesia with 4% isofluorane and maintenance for surgery at 1.5% isofluorane). Furthermore, they underwent analgesia (buprenorphine, 0.03 mg/kg body weight intraperitoneally every 12 hours for 24 hours) (Animalcare Ltd, Nether Poppleton, United Kingdom). Animals were laid on heating plate to maintain body temperature during surgery at 37ºC. Firstly, we disinfected the skin and surrounding fur with 70% ethanol and dry it afterwards. Immediately, a midline incision was made in the neck and the soft tissues were pulled apart. The left external carotid and pterygopalatine arteries were isolated (without harming the vagal nerve) and ligated with 6-0 silk thread (B. Braun). The internal carotid artery (ICA) was occluded at the peripheral site of the bifurcation of the internal carotid artery and the common carotid artery (CCA), and both were ligated with 6-0 silk thread. The external carotid artery (ECA) was cut, and a 6-0 nylon monofilament (Ethicon, Inc, Somerville, USA) with a tip that was blunted (210-220 μm) with a coagulator was inserted into the ECA. After the knot at the ICA was removed, the nylon thread was advanced into the middle cerebral artery (MCA) until light resistance was felt. The monofilament and the CCA ligature were removed after 50 minutes of occlusion to initiate the restoration of blood flow (reperfusion). The wound was sutured and animals removed from anesthesia. Animals were put in a heated cage for two hours to control body temperature. After surgery, mice were checked daily for signs of discomfort.

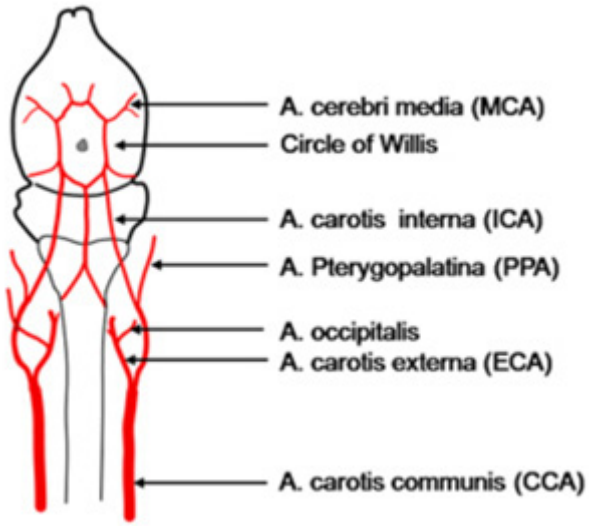

Figure 14. Scheme of the vessel architecture supplying the brain in the mouse.

8.2.1. Parameters

Several parameters were measured to check daily the animal state. We evaluated **body weight** and the functionality of the animal, which was checked by neurological score and pole test. These parameters are modified in ischemic conditions. Thus, we wanted to analyze if the treatment causes any modification on them.

-Neurological score. Motor deficits were assessed in each animal one hour after tMCAO and later, on intervals of 24 hours. A system with five-point scale was used (Bederson et al. 1986) in a blinded fashion:

Grade 0: No observable deficit. The animal is active.

Grade 1: Failure to extend right paw.

Grade 2: Decreased resistance to lateral push and circling to the right.

Grade 3: Falling to the right. The animal presents rotating or revolving.

Grade 4: Unable to walk spontaneously.

Grade 5: Dead animal.

Animals without neurological deficits were excluded from the study.

-Pole test. Pole test evaluates simple motor function and has been used in animal models of focal ischemia. It successfully distinguishes between sham and tMCAO animals in early and relatively late time points.

The procedure consists in placing the animals on top of vertical pole and forcing to descend down (snout first) until the ground of a mouse cage. A 50 cm metal pole with a diameter of 10 mm is used for this purpose. The surface of the pole was covered with an adhesive tape to ensure a rough surface to enable traction.

The measurement is the time to reach the floor of cage. This time is higher in ischemic animals due to its mobility is reduced. If an animal falls immediately, the longest time of the group is assigned. On the other hand, animals that do not descend were encouraged to do it by gently pushing to a side. Each animal was subjected to 3 trials and the average of 3 trials was used as final score. Before and after each trial, mice were allowed to explore the cage for 15s and then returned to their home cage. Animals had an interval of at least 5 minutes between the three repetitions of measurements. In a successful run, the animal must not pause or stop once it starts moving. If it does a pause, the trial is repeated.

For the correct procedure, it was necessary training one day before ischemia. The trials were carried out alternative days post-ischemia (day 1, day 3, day 5... until sacrifice) in order not to disturb too much animals.

8.2.2. Experimental protocol and drug treatment

Three types of tMCAO experiments were performed at different times (7 days, 15 days and 30 days) in order to establish when maximum neurogenesis occurs in this pathology.

The antagonist of A1 receptor DPCPX (0.1 mg/Kg) was administered intraperitoneally every day each animal. The first injection was immediately administered just after the monofilament was removed. In the case of vehicle animals, daily injections of PBS (500 µl) were administered.

In addition, the S-phase marker BrdU (100 mg/Kg) was injected to be able to follow the proliferating cells in vehicle and treated animals. Three BrdU injections (i.p.) every two hours were administrated one day before ischemia and one per day during the treatment. Once different times of treatment finished, animals were perfused and tissue processed for histology.

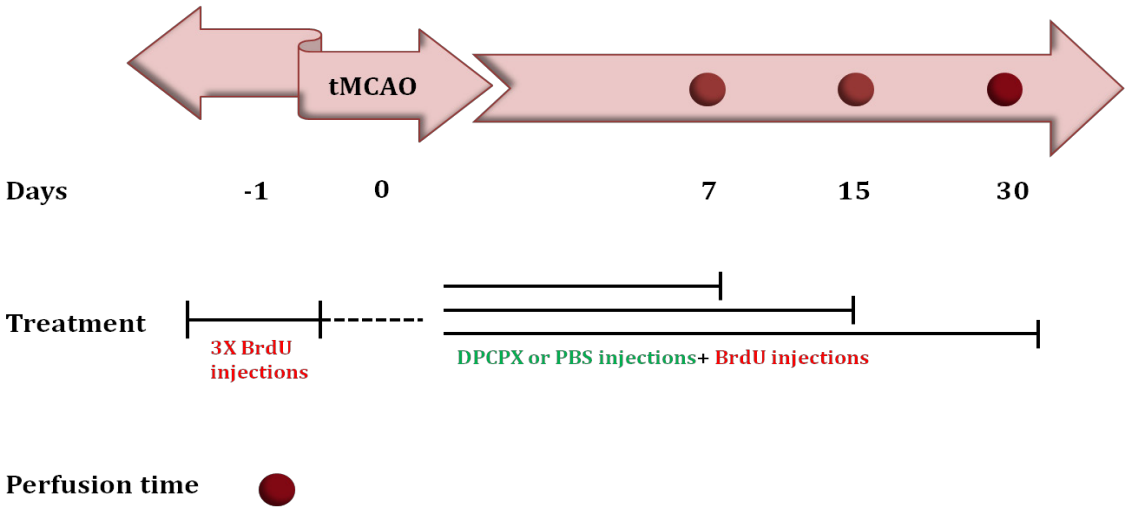

Figure 15. Schematic description of administration procedures. Ischemic animals were treated with BrdU injections before and after tMCAO to label proliferating cells. Also, daily injections of DPCPX or PBS were administered for different times (7, 15 and 30 days).

8.2.3. Tissue fixation, dissection and vibratome

After established times (7, 15 and 30 days) animals were anesthetized with 20% chloral hydrate and transcardially perfused with 4% PFA in 0.1M PB (pH 7,4), as previously we described. Brains were removed and immediately post-fixated in 4% PFA for 3 h. They were washed with PBS and transferred to a 20% aqueous sucrose solution at 4ºC until brains decanted (approximately 2-3 days). Tissue was changed to a cryoprotection solution (30% glycerol, 30% ethylene glycol, 10% 0.4M PB, 30% water) and stored at -20ºC until use. Brains were cut in coronal sections of 40 µm of thickness in a Leica VT 1200 S vibratome (Leica Microsystems). Coronal sections were used for immunohistochemistry and to measure infarct volume.

8.2.4. Measure of infarct volume

Infarct volume is an essential indicator of the severity of the ischemic damage. There are several techniques to measure it. One of them is 2,3,5-triphenyltetrazolium chloride (**TTC**) staining, which is used to determine the infarct size on living tissue after focal cerebral ischemia. The colorless TTC is enzymatically reduced to a red formazan product by dehydrogenases, which are most abundant in mitochondria. As a result, viable tissue is stained red while dead tissue is left unstained.

In our case the infarct volume was measured by **cresyl violet** staining, which is used for non living tissue. This compound labels Nissl substance in the cytoplasm of neurons in para-formaldehyde or formalin-fixed tissue. The neuropil will be stained a granular purple-blue. The cresyl violet method uses basic aniline dye to stain RNA blue. Viable tissue turns into deep blue/purple colour and infarcted tissue into pale blue/white.

A representation of slices of the brain was analyzed to measure the infarct volume. Six-seven slices (40 μm of thickness) with a distance of 1 mm between them were stained with 0.5% cresyl violet (Sigma) solution: 25 % methanol, 75 % distilled water. Slices were placed on slides (covered with 2% gelatine) and maintained at 37ºC for 30 minutes until they were dried. The tissue was deepened into water and then dehydrated-rehydrated by immersion into different concentration alcohols. Firstly, 70%-96%-100% alcohols were used to dehydrate; afterwards 100%-96%-70% alcohols to rehydrate. Finally, slides were deepened into cresyl violet solution and once again into growing concentration alcohols (70%-96%-96% with 3% acetic acid-100%). Tissue was clarified with xylol and mounted with DPX Mountant for Histology (Sigma).

The infarcted area of each slice was assessed blindly and delineated by the relative paleness using ImageJ. Also, both hemispheres were measured. Infarct volume was calculated according to Storini (Storini et al. 2006). In this equation the ischemic area and the percentage of swelling were determined by subtracting the area of the healthy tissue in the ipsilateral hemisphere from the contralateral hemisphere on each section.

8.2.5. Immunohistochemistry: Double fluorescence immunolabeling

Brain coronal sections (40 μm thickness) from tMCAO and osmotic pumps experiments were used to study the expression of different neural markers (NeuN, DCX, S100β…) and BrdU. Tissue sections were pretreated to display BrdU staining with HCl 2N (Merck, Darmstadt, Germany) for 15 minutes at 37ºC and following PBS washing. Subsequently, sections were permeabilized with 0.1% Triton and 10% normal goat serum in PBS. Primary antibodies were incubated at different concentrations (see tab.1 for specification) overnight at 4ºC and then washed three times with 0.1% Triton in PBS. Following extensive washing, primary antibodies were detected by incubation with appropriate Alexa Fluor® 568 and 488 conjugated goat antibodies (1:500 Invitrogen, Life Technologies, Thermo Fisher Scientific, USA) for 1 hour in the dark at room temperature. After three washes with 0.1% Triton in PBS, sections were stained for 5 minutes with DAPI and further washed with PBS. Finally, cover slips were mounted on slices with

Glycergel (Dako, Barcelona, Spain). In all cases, the analysis of sections was carried out using a confocal microscope, as describe below.

8.2.6. Image acquisition and analysis

Confocal microscopy of dual-labeled tissue sections was performed using a Leica TCS SP8 STED CW confocal laser scanning microscope. In the case of tMCAO experiments, we selected 6 coronal sections representing complete striatum. In each section, six regions were analyzed: 3 from striatum and 3 from cortex (all of them were nearby of injured zone). Series of optical sections (z-stacks) were taken through each slice at spacing of 8.4 µm using a 40X oil immersion objective (zoom 2.9). The analysis speed was 600 Hz using 488 and 568 lasers. Image size was 100.22x100.22 µm. For co-localization analysis, we counted positive cells for neuroblasts (DCX/BrdU), newborn neurons (NeuN/BrdU) and new astrocytes (Thbs4/GFAP/BrdU) through z-stack of each slice using the proprietary Leica Confocal LAS-AF Software (v 3.3.0.10134). We calculated cellular density (number of cells/ striatum volume), although this parameter it is modified due to the volume changes in ischemia. Thus, we calculated the total number of cells in the striatum.

8.3. Positron Tomography Emission (PET)

Positron Tomography Emission is a non-invasive technique used *in vivo* research and in diagnosis. PET technology is used to trace the biologic pathway of any compound in living humans or animals. It shows metabolic activity by means an image and it is based in detection and tridimensional distribution analysis of a radiotracer with short half-lives. PET scanners are able to detect gamma photons given off by the humans or experimental animals and transform into electric signals. This generates an image which has been processed previously.

The radiotracer works as an antibody joining protein of interest. In this case, we have used the radiotracer 3'-deoxy-3'-[^{18}F]-fluorothymidine ([^{18}F] FLT). This molecule is used to study cellular proliferation because it is trapped in cells in proportion to thymidine-kinase 1 enzyme expression, which is up-regulated during DNA synthesis. The tracer is phosphorylated by the enzyme thymidine kinase 1 (TK1), which is expressed with the onset of S-phase during DNA synthesis, its activity thus being a read-out for cellular proliferation. After phosphorylation by TK1, [^{18}F] FLT is trapped within the cell and can therefore be visualized by PET.

8.3.1. Radiochemistry

The synthesis of 3'-Deoxy-3'-[^{18}F]-fluorothymidine ([^{18}F] FLT) was performed as described earlier (Blocher et al. 2001) using a TRACERlab FX_{FN} synthesis module (GE Healthcare). After purification by HPLC (stationary phase: VP125/10 Nucleosil 100-7 C18 column, Macherey-Nagel; mobile phase: 0.01M aqueous NaH_2PO_4/ethanol, 90/10; retention time: 13-14 min) and sterile filtration, injectable [^{18}F]FLT solution was obtained with non-decay corrected radiochemical yield of 7.5±1.1% in an overall production time of 62 min. Radiochemical purity was above 95% in all cases.

8.3.2. PET scans and data acquisition

In this work PET scans were repeatedly performed in DPCPX-treated (n=8) and vehicle-treated (n=7) ischemic male Sprague-Dawley rats at 0, 8 and 21 days after ischemia using a General Electric eXplore Vista CT camera. Scans were performed in rats anaesthetized with 4% isofluorane and maintained by 2-2.5% of isofluorane in 100% O_2. Animals were subjected to [^{18}F] FLT PET scans to assess neurogenesis, in particular cellular proliferation. Around 20 MBq of [^{18}F] FLT were injected in a tail vein and placed into a mouse holder compatible with PET acquisition systems and maintained normothermic using a water-based heating blanket. Brain dynamic images were acquired (24 frames: 1x5, 1x15, 3x30, 5x60, 5x120, 3x180, 6x300 seconds) in the 400-700 keV energetic window, with a total acquisition time of 55.4 minutes, providing 0.387 mm thick 175 transaxial and 0.775mm thick 61 axial slices. After each PET scan, CT acquisitions were also performed (140μA intensity, 40kV voltage), providing anatomical information of each animal as well as the attenuation map for the later image reconstruction. Dynamic acquisitions were reconstructed (decay and CT-based attenuation corrected) with filtered back projection using a Ramp filter with a cutoff frequency of 0.5 mm^{-1}.

8.3.3. PET Image Analysis

PET images were analyzed using PMOD image analysis software (PMOD Technologies Ltd, Zürich, Switzerland). For the analysis of PET signal in cerebral striatums, PET images were coregistered to the anatomical data of a MRI rat brain template. Volumes of Interest (VOIs) were automatically generated in both striatums (ipsilateral and contralateral) by using the region proposed by the PMOD rat brain template to study the evolution of [^{18}F] FLT binding. For quantification of VOIs, summed binding uptake during the last 15 minutes of acquisition was expressed in percent of injected dose per cubic centimeter of tissue (ID/cc). Finally, PET signal frames were summed and voxels outside the selected

VOIs were masked to better represent the PET binding in ipsilateral and contralateral striatums using PMOD software.

These experiments were carried out with the collaboration of Dr. Abraham Martín Muñoz at the CIC Biomagune, San Sebastian, Spain.

9. Statistical analysis

Data obtained in this work were analyzed with programs Prism v 4.0 (GraphPad, La Jolla, USA) and Excell 2007 (Microsoft).

Analysis of differences between treated and controls were carried out with different statistical tests according to *in vitro* or *in vivo* experiments. In all instances, a value of $p < 0.05$ was considered significant. Data are presented as mean ± the standard error of the mean (SEM).

For *in vitro* experiments, determination of the significance between treated and control was by means of Student´s t test or ANOVA. Each experiment was repeated at least three times and each condition was always evaluated in triplicate.

For *in vivo* experiments, we used one-way and two-way ANOVA followed by Bonferroni post-hoc test. The number of animals was indicated in the epigraph of each experiment ($n>6$).

Results

1. CHARACTERIZATION OF NEUROSPHERE CULTURES

First of all, we characterized neurosphere cultures to assess **the expression of adenosine receptors** in multipotent cells from rat SVZ by using RT-PCR (Fig. 16A), Western blot (Fig. 16B) and double labeling immunofluorescence (Fig. 16C) with specific antibodies. Both mRNA and protein of A1, A2a, A2b and A3 receptors are present in those multipotent cells before differentiation. Thus, PCR analysis revealed a similar qualitative pattern of expression of all the receptor subtypes in the SVZ cultures to that present in the brain (used as positive control; Fig. 16A). In turn, immunofluorescence staining showed that the receptors were present in cells labeled with the multipotency marker nestin (Fig. 16C).

Neurosphere cultures are a heterogeneous mix of different neural progenitors for this reason one should standardize the culture to be able to analyze it correctly. One way is performing different **neurosphere passages**. We checked different protocols and dissociation agents (Tab. 2). Neurosphere cultures after 5-7 days in proliferation were dissociated by mechanical treatment with a fire polished glass Pasteur, or enzimatically with different concentration of trypsin-EDTA (0.1% and 0.5%), with papain or accutase. The efficiency of disgregation was evaluated under different parameters: cell dissociation, cell survival and differentiation. As shown in Tab. 2 only 0.5% trypsin-EDTA, papain and accutase treatment could disgregate primary neurospheres but only accutase treatment resulted viable. Primary neurospheres treated with accutase could be disgregated and expanded to form up to secondary and tertiary neurospheres (Fig. 17A). The analysis of cell linage markers in different cellular passages showed a decreased in the multipotency marker nestin and an increase in neuroblast marker doublecortin (DCX). Nevertheless, after three passages we obtained a small number of cells as a selection of the original pool of progenitors (Fig. 17B). Due to all this technical impedance and according to the neurosphere analysis performed previously by Gil-Perotin by which their biological properties can change with passage (Gil-Perotín et al. 2013), we decided to test neuronal differentiation by single sphere assay (see material and methods section).

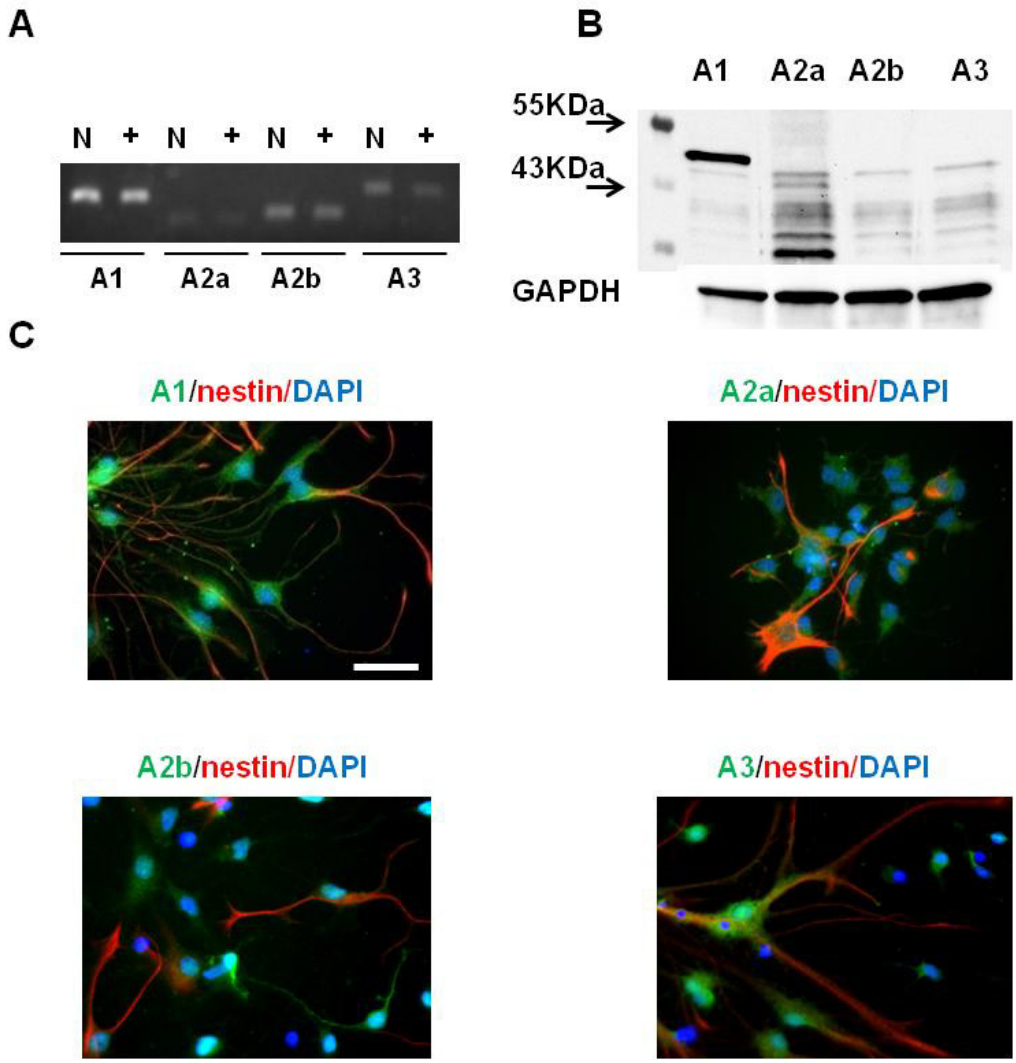

Figure 16. Neurosphere cultures express adenosine receptors. A) Total RNA from 7 days proliferating neurospheres (N) was retro-transcribed and adenosine receptor genes (A1, A2a, A2b and A3) amplified by PCR. RNA from total brain (+) was used as a positive control. B) Total protein from 7 days proliferating neurospheres were analyzed for adenosine receptors expression by Western blot. GAPDH antibody was used to normalize protein loading C) Neurospheres after 7 days of proliferation were analyzed by double immunofluorescence for adenosine receptors (green) and nestin (red). Nuclei were counterstained with DAPI. Scale bar = 40 µm.

	Mechanical disgregation	0.5% Trypsin-EDTA	0.1% Trypsin-EDTA	Papain	Accutase
Cell dissociation	✗	✓	✗	✓	✓
Survival	NT	✗	NT	✗	✓
Differentiation	NT	NT	NT	NT	✗

Table 2. Different methods to disgregate and passage primary neurospheres. Green V, efficient; red cross, not efficient; NT, not treated.

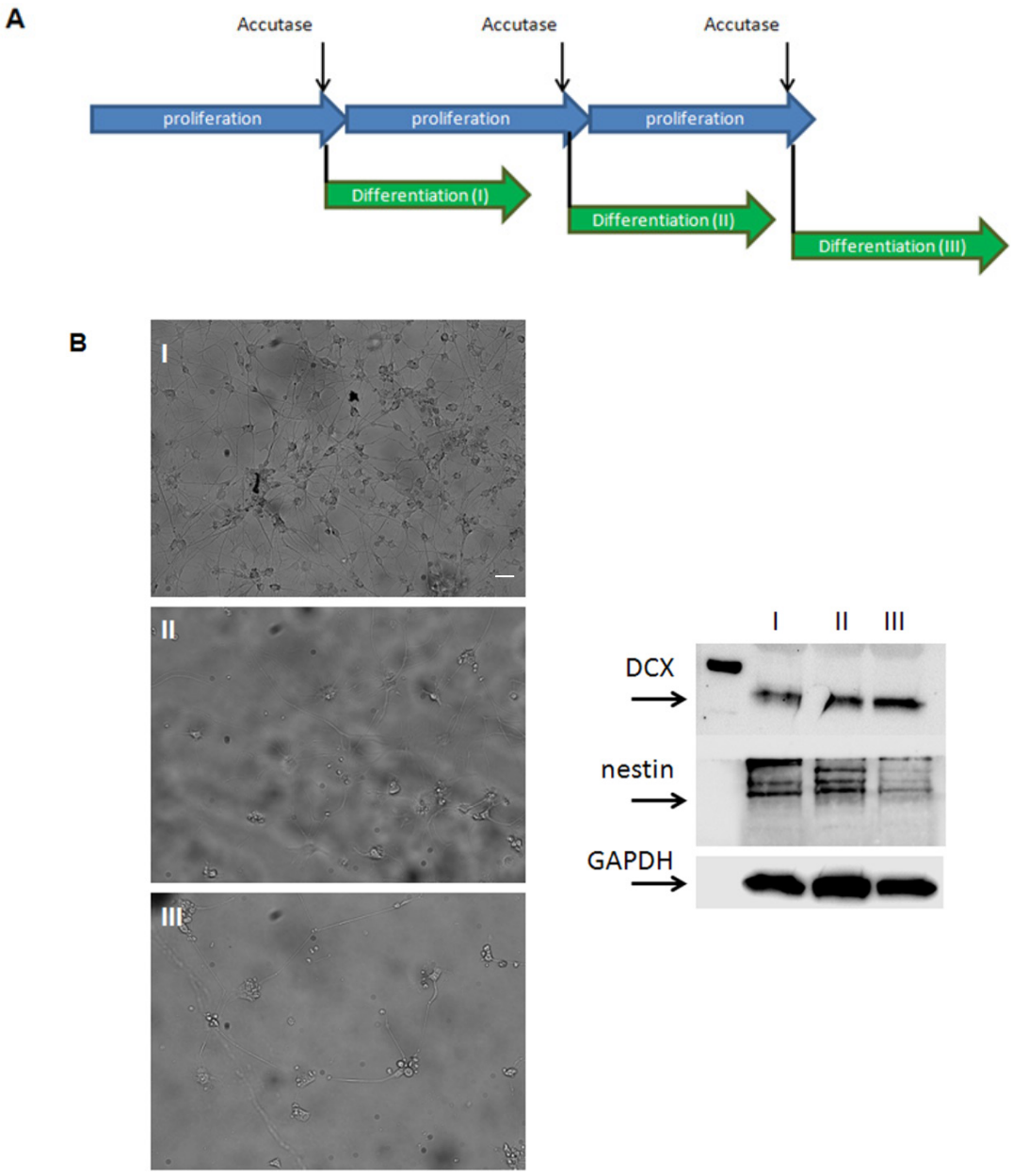

Figure 17. Protocol setting. A) After 7 days of proliferation neurospheres were dissociated with accutase generating primary (I), secondary (II) and tertiary (III) neurospheres. B) To test the efficiency of differentiation, each neurospheres passage (I, II and III) was differentiated for 7 days in the presence of 50 ng/ml NGF and 50 ng/ml BDNF and total protein extracted. Left panel shows the culture passages before protein extraction. On the right panel, proteins extracted from different neurospheres passages, were analyzed by Western blot for the expression of doublecortin (DCX, marker of neuroblasts) and nestin (marker of multipotentiality). Figure shows that neurosphere passages enrich DCX expression while decreasing nestin but drastically affecting the cell number (left panel). Scale bar = 30 µm.

Functional neuronal differentiation was assessed after 7-10 days by immunofluorescence for **the expression of different neuronal markers** (NMDAR1, tyrosine hydroxylase, synaptophysin and calbindin). The presence of functional NMDA receptor was also demonstrated by the intracellular calcium entry after glutamate stimulation (Fig. 18 and 19). Immunocytochemical results showed that neurosphere cultures can differentiate into several cellular types, among these glutamatergic and dopaminergic neurons. Furthermore, these cells express synaptophysin, suggesting, together with calcium entry analysis, that neurons are functional.

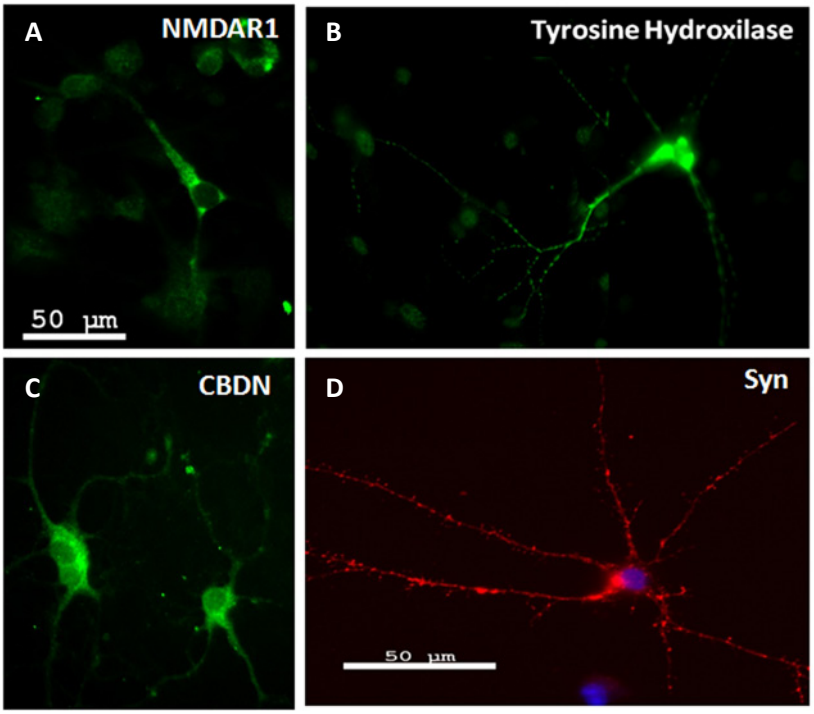

Figure 18. Differentiated neurospheres express neuronal markers. Primary neurospheres were differentiated in the presence of NGF and BDNF and stained with different neuronal markers: A) NMDAR1 B) tyrosine hydroxylase, C) calbindin (CBDN) D) synaptophysin (Syn). Scale bar = 50 µm.

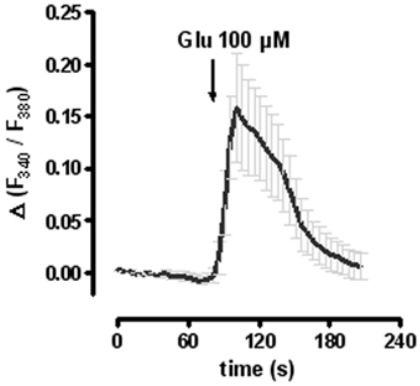

Figure 19. Glutamate receptors expression in differentiated neurospheres. Neurospheres were differentiated in the presence of NGF and BDNF. After 7 days of differentiation cells were loaded with 5 µM fura-2 AM for 45 min at 37°C. The Ca^{2+} entrance was analyzed after 100 µM glutamate stimulation (arrow) and expressed as the difference of F340 vs F380 ratio.

2. EXTRACELLULAR ADENOSINE NEGATIVELY MODULATES NEURONAL DIFFERENTIATION

Extracellular ATP released at high concentration during tissue injury may have a pivotal role in inhibiting adult neurogenesis (see i.e. (Vergni et al. 2009)). Here, we have extended our investigation to adenosine which is one of the metabolic products of ATP hydrolysis. The adenosine effect on neuronal differentiation was quantified on single spheres by densitometry after immunofluorescence, as a ratio between βIII tubulin expression (newborn neuron marker) *vs* total cells, stained with DAPI. As shown in figure 20A-B, we tested increasing concentrations of adenosine (1, 10 and 100 μM) and we observed a dose-dependent effect in inhibiting neuronal differentiation. Thus, neuronal differentiation was significantly inhibited with a maximum effect (61% of inhibition) after 100 μM adenosine treatment (Fig. 20B).

Next, we verified if adenosine was inhibiting neuronal differentiation through adenosine receptors (A1, A2A, A2B and A3) or through equilibrative nucleoside transporters (ENT). We differentiated neurospheres in the presence of 100 μM adenosine plus 50 μM caffeine, a broad spectrum antagonist of adenosine receptors or dipyridamole, inhibitor of ENTs. Caffeine and dipyridamole reduced the effect of 100 μM adenosine (25% vs 60% of neuronal inhibition) (Fig. 20C). This suggested that adenosine signal is mainly mediated by adenosine receptors but also by nucleoside transporters.

Other evidence about adenosine leads to a differentiation inhibition was by controlling the cellular concentrations of Ado through adenosine kinase (ADK). This enzyme transfers a phosphate from ATP to Ado leading to AMP formation. We differentiated neurospheres in a culture medium with A-134974 dihydrochloride hydrate (100 nM), a selective adenosine kinase inhibitor, which generates a higher concentration of intracellular adenosine and the subsequently release to extracellular medium. The endogenous adenosine release achieved a reduction in neuronal differentiation, although its effect was lower than generated by 100 μM adenosine (30% vs 60% of neuronal inhibition).

Then, we wanted to check if reduction of βIII tubulin depended from a reduction of neuronal differentiation or from neuronal death. We differentiate neurospheres in the presence of adenosine with or without the caspase inhibitor ZVAD-FMK (100 μM) (Fig. 20A-C). The caspase inhibitor ZVAD-FMK was ineffective in modulating the effect of adenosine suggesting that the loss of βIII tubulin did not depend from neuronal apoptosis. In order to explore more deeply cellular death, we analyzed the effect of adenosine on

total cell death by direct count. The results showed that adenosine (100 μM) causes a small but significant portion of apoptotic-independent cell death (15%, Fig. 21).

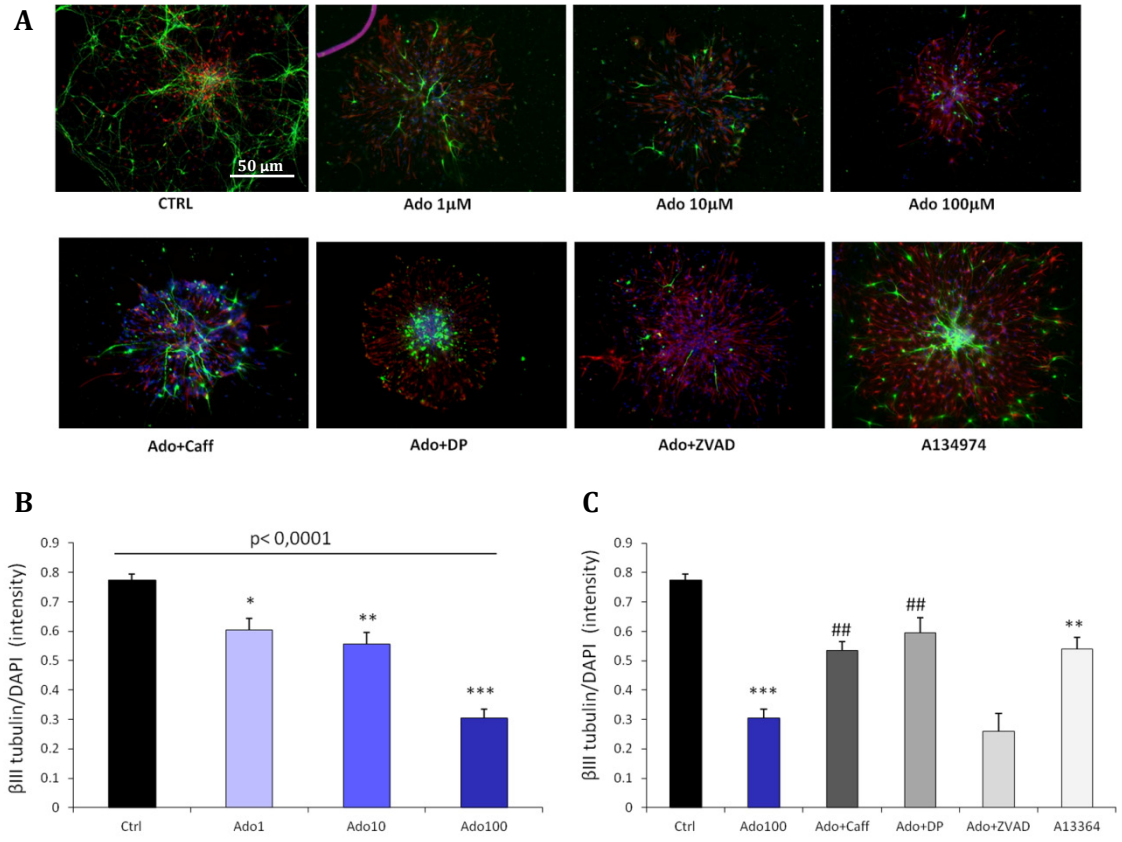

Figure 20. Extracellular adenosine reduces neuronal differentiation. Single neurospheres were differentiated for 7 days in the presence of increasing concentrations of adenosine (1, 10, 100 μM in A, B), the adenosine receptor antagonist caffeine (50 μM caff), the inhibitor of the nucleoside transporter dipyridamole (10 μM), the caspase inhibitor ZVAD (100 μM) or in the presence of the adenosine kinase inhibitor A-134974 (100 nM) (A, C). Neuronal differentiation was visualized by immunofluorescence with βIII tubulin (green), and quantified in (B and C) by densitometry as a ratio between βIII tubulin vs total cells stained with DAPI (blue). GFAP (red) was used as a marker for multipotentiality. Counts represent means ± SEM (n = 6 independent experiments); 3 single spheres of each experimental condition were counted in every experiment. *** $p < 0.001$, ** $p < 0.01$ and * $p < 0.05$ vs. Ctrl; ## $p < 0.01$ vs. 100 μM Ado. One-way ANOVA. Scale bar = 50 μm.

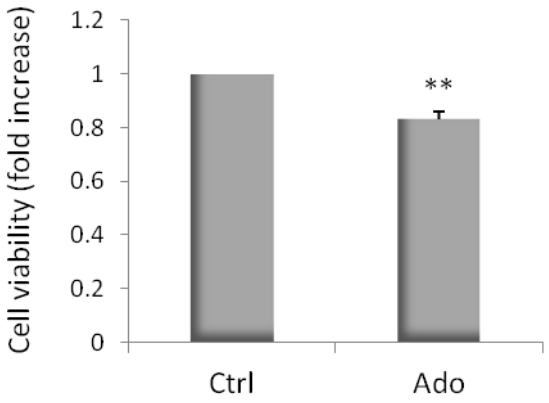

Figure 21. Apoptotic-independent cell death. $5x10^5$ cells were seeded and differentiated in DM in the absence (Ctrl) or presence of 100 μM adenosine (Ado). Cell viability was measured automatically by direct count of cells with Scepter (Millipore). The data represent means ± SEM (n = 6 independent experiments). ** $p < 0.01$ vs. Ctrl. T test.

3. STIMULATION OF ADENOSINE RECEPTORS DURING DIFFERENTIATION INHIBITS THE TRANSPORT OF SYNAPTIC VESICLE

Previous studies affirmed that activation of adenosine receptors, particularly A1, can negatively modulate synaptic activity through the inhibition of multiple voltage-gated Ca^{2+} channel (McCool & Farroni 2001). So we decided to investigate if inhibition of differentiation driven by adenosine can also depend by autocrine mechanisms like the block of synaptic activity. For this reason, we analyzed by immunofluorescence two synaptic markers: synaptophysin and vesicular glutamate transporter 2 (VGLUT2). The results showed that neuronal progenitors differentiated in the presence of adenosine accumulated synaptophysin in the cytoplasm (Fig. 22). We postulated that adenosine could block the axo-dendritic transport to the synapses. In the case of VGLUT2, this marker also accumulated in the cytoplasm.

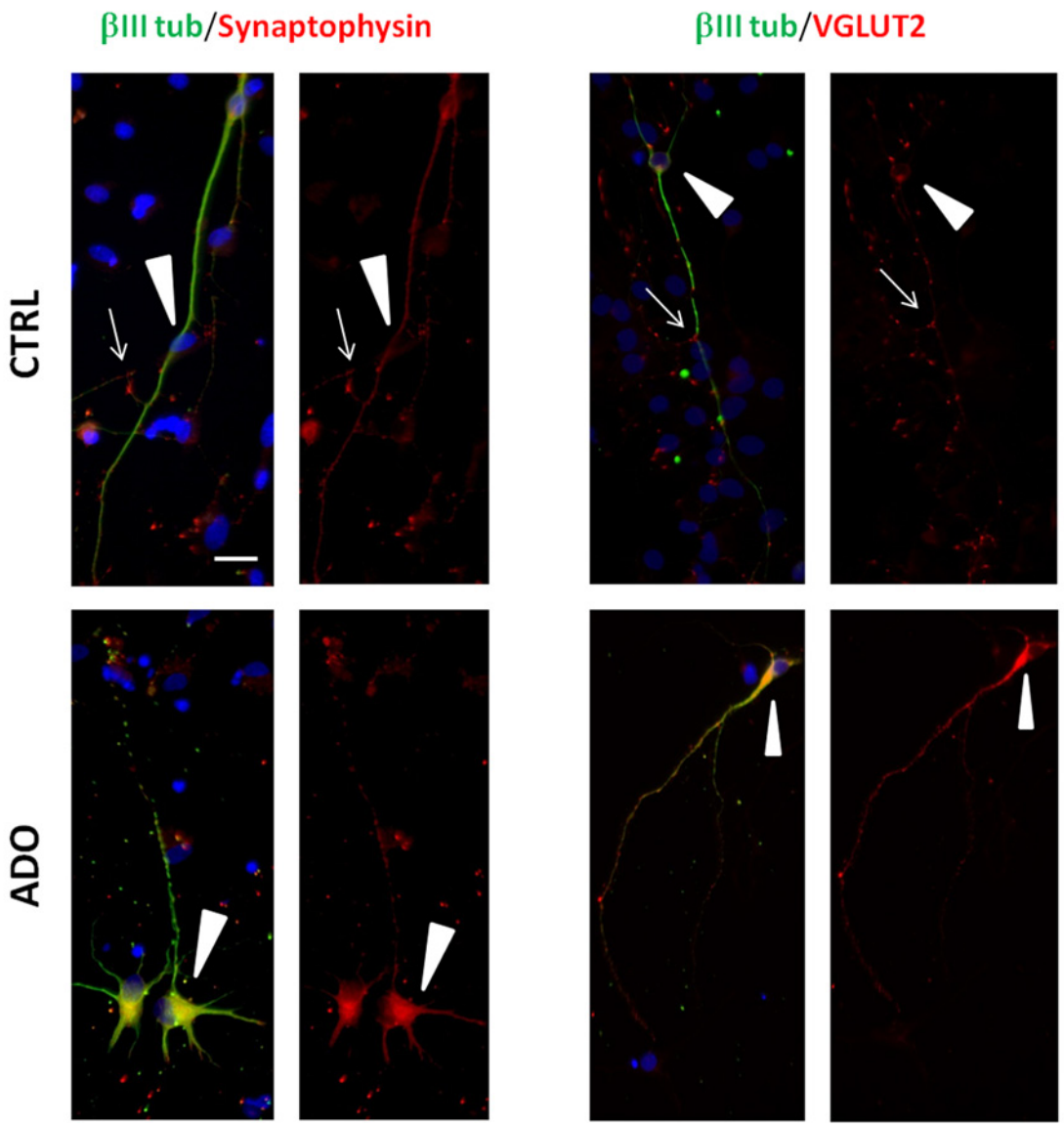

Figure 22. **Adenosine provokes cytoplasmic retention of synaptic vesicle.** Cells after 10 days of differentiation in the presence of adenosine 100 μM (Ado) were labeled with βIII tubulin (green), synaptophysin (red, left) or VGLUT2 (red, right) and counterstained with DAPI. Arrowheads=cytoplasm. Scale bar = 20 μm.

The inhibition of vesicular transport also occurred in cellular models more complex like organotypic cultures. The organotypic cultures from subventricular zone were maintained for 7-12 days in the absence (Ctrl) or presence of adenosine 100 μM. Also in this case, the treatment with adenosine produced an accumulation of synaptophysin in the cytoplasm (Fig. 23).

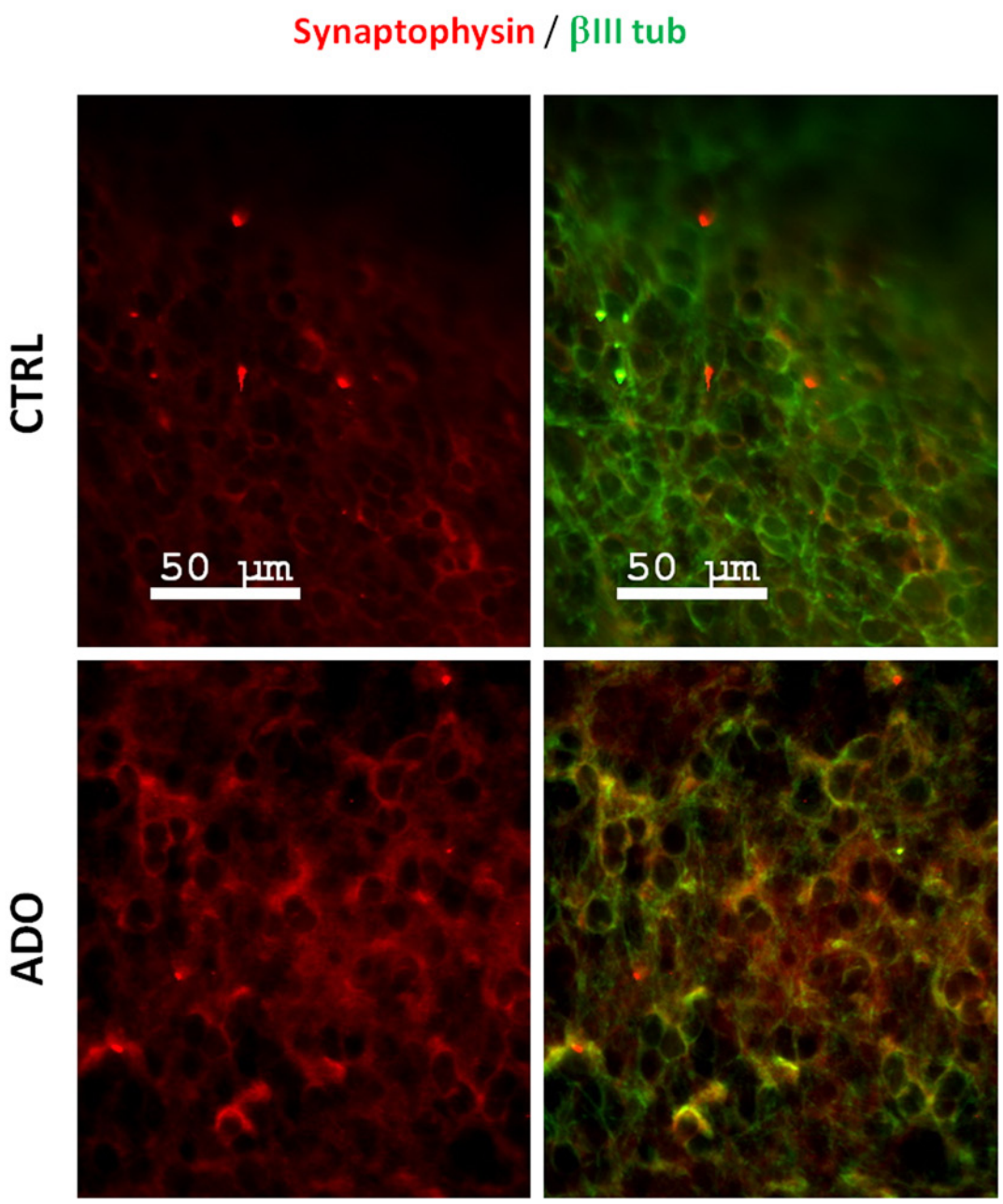

Figure 23. Adenosine provokes cytoplasmic retention of synaptic vesicle: organotypic cultures. Organotypic cultures were maintained in a liquid-air interface for 7-12 days in the absence (Ctrl) or presence of adenosine 100 µM (Ado) and stained with βIII tubulin (green) and synaptophysin (red). Scale bar = 50 µm.

Inhibition of vesicular transport was also confirmed by Western blot analysis of synaptophysin in cytosol fractionation in neurospheres differentiated in the presence of 100 µM adenosine. After treatment we separated cytosolic from synaptic proteins and analyzed the localization of synaptophysin by Western blot as a mean of the ratio between synaptic vs cytosolic fraction. The quality of preparation was evaluated as an enrichment

of GAPDH and the nuclear protein Ezh2 in the cytosolic fraction respect to the synaptosomal. As shown in figure 24, adenosine induced a decrease of the synaptic synaptophysin (47% respect to control).

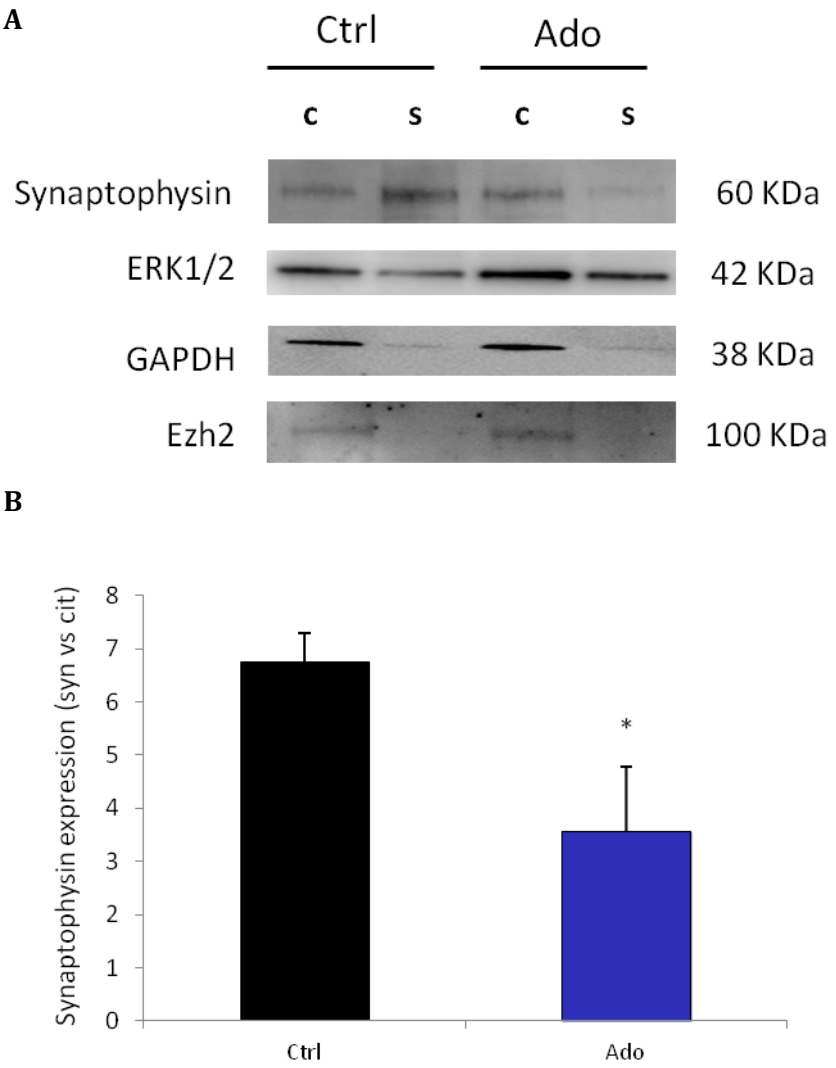

Figure 24. Adenosine provokes cytoplasmic retention of synaptic vesicle: synaptosome analysis. A) Neurospheres were differentiated for 10 days in the absence (Ctrl) or presence of 100 μM adenosine (Ado). Synaptic proteins (s) were separated from the cytosolic fraction (c) and analyzed by Western blot for the expression of synaptophysin. B) Quantification was evaluated by densitometry after normalization with total ERK1/2 as a ratio between the synaptic vs cytosolic fraction. The quality of synaptic preparation was confirmed by the expression of the nuclear protein Ezh2 and the enrichment of GAPDH in the cytosolic fraction. Counts represent means ± SEM (n = 3 independent experiments). * $p < 0.05$ vs control. T test.

Finally to demonstrate that block of vesicular transport in se, is able to inhibit neuronal differentiation, we treated neurospheres with brefeldin A (BfdA) (Benedetti et al. 1995) during differentiation and evaluated neuronal differentiation by

immunofluorescence with βIII tubulin. BfdA inhibits the protein transport from the endoplasmic reticulum to the Golgi apparatus. As confirmed in figure 25 the block of vesicular transport by BfdA drastically reduced the expression of βIII tubulin.

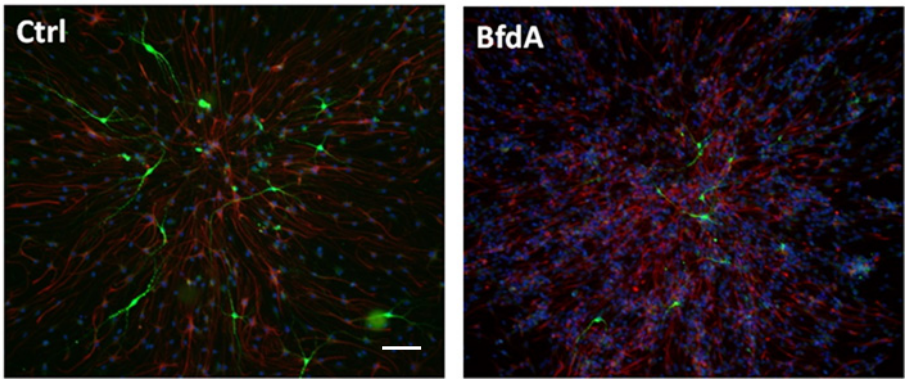

Figure 25. Inhibition of synaptic transport by brefeldin A decreased neuronal differentiation. Neurospheres were differentiated for 10 days in the presence of 10 nM brefeldin A (BfdA). Cells were stained with βIII tubulin (green), GFAP (red) and counterstained with DAPI (blue). Scale bar = 100 μm.

4. ADENOSINE INHIBITS NEURONAL DIFFERENTIATION THROUGH THE ACTIVATION OF A1 RECEPTOR

In order to confirm that extracellular adenosine inhibits neuronal differentiation, we analyzed the transcription profile of 88 mRNAs related to neurogenesis expressed in neurosphere cultures after 3 days of differentiation with 100 μM adenosine (Table 3). We decided to analyze gene expression after three days of differentiation because all are expressed early. We analyzed only changes by more than a ±30% of threshold; among those transcripts 36 were down regulated and only 6 up-regulated by adenosine. The latter include adenosine receptors Adora1 (A1) and Adora2a (A2a) (increased by 126% and 44% respectively) as well as Bmp2, Bmp15, Ep300 and EGF.

Gene	Ado modulation	Gene	Ado modulation	Gene	Ado modulation
Ache	0,482400206	Erbb2	0,371600421	Nog	0,567191684
Adora1	**2,26010333**	Fez1	0,521967013	Notch2	0,58754334
Adora2a	**1,444730767**	Fgf13	0,467848303	Nrcam	0,500560352
Apbb1	0,354769203	Fgf2	0,657248829	Nrg1	0,44071186
Ascl1	0,465918804	Flna	0,530736817	Ntn1	0,520876591
Brp15	**1,556044527**	Gnao	0,482775649	Pou3f3	0,485023776
Brp2	**1,474945544**	Gpi	0,523898595	Pou4f1	0,680206522
Cdk5rap2	0,605760114	Grin1	0,627232162	Ptn	0,636209665
Cdk5rap3	0,393261091	Hdac4	0,648444011	Robo1	0,587510115
Cxcl1	0,412867298	Hdac7	0,690511453	Sema4d	0,50054681
Dlg4	0,700606394	Heyl	0,609378723	Sox8	0,460273406
Drd2	0,516456956	Ncoa6	0,606512829	Tnr	0,573956022
Egf	**1,492055986**	Ndn	0,637702152	Vegfa	0,496203699
Ep300	**1,561556945**	Ndp	0,618852557	Ywhah	0,381533652

Table 3. List of genes modulated by adenosine treatment during neuronal differentiation. Cells were differentiated for 3 days in the presence of 100 µM adenosine. Transcription of different genes related with neurogenesis was assayed by quantitative RT-PCR. Values represent the modulation of ΔΔCt respect to the control, and only changes by more than a ±30% of threshold was considered. Up- and down-regulated genes are depicted in red and black, respectively.

To confirm the Adora1 and Adora2a up-regulation shown in the PCR array we performed quantitative RT-PCR in the presence or absence of 100 µM adenosine (Fig. 26) and evaluated mRNA levels of Adora1, Adora2a, Adora2b and Adora3 after 3 and 15 days of differentiation. Transcripts of A1r (Adora1) and A2br (Adora2b) receptors were expressed at higher levels than the other two receptor subtypes. Adora1 was more intensely modulated by adenosine and the modulation was maximal (43% increase respect to the control) after 3 days of treatment (Fig. 26).

Afterwards, we verified if the level of A1 receptor protein is also up-regulated by adenosine during differentiation. We selected protein extracts after 3 days, according to maximum expression peak obtained in qRT-PCR, and analyzed the expression of adenosine A1 receptor after treatment with adenosine and the specific A1 antagonist PSB36 (1 µM) (Müller & Jacobson 2011). Adenosine increased 52 % the expression of A1 receptor, whereas the antagonist reverted this effect (Fig. 27).

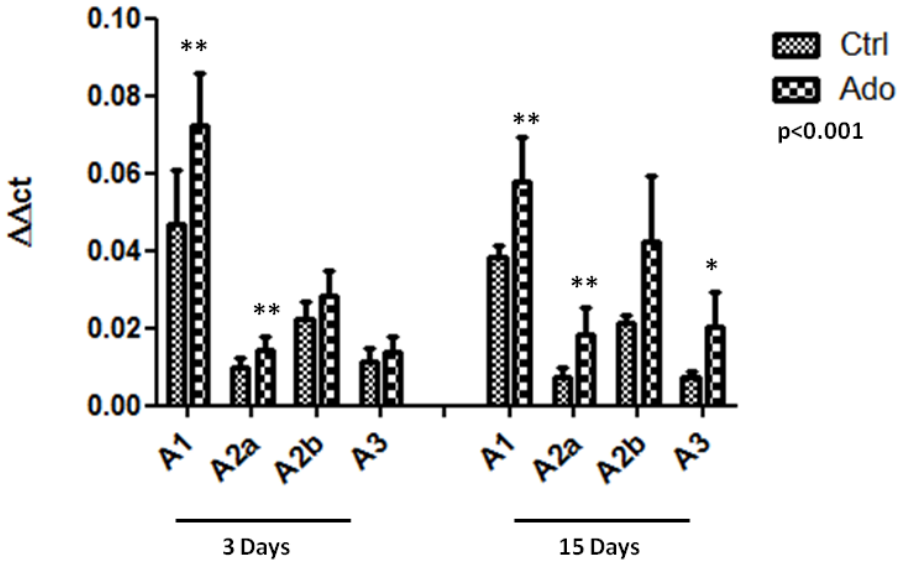

Figure 26. Adenosine receptor A1 modulates neuronal differentiation: gene analysis. qRT-PCR of total RNA extracted after 3 and 15 days of differentiation in the absence (Ctrl) or presence of 100 μM adenosine (Ado). mRNA encoding adenosine receptors were amplified by using commercial primers and expression was quantified by the ΔΔCt method. Counts represent means ± SEM (n = 3 independent experiments). ** $p < 0.01$ or * $p < 0.05$ vs. respective control. Two-way ANOVA followed by Bonferroni post-hoc tests.

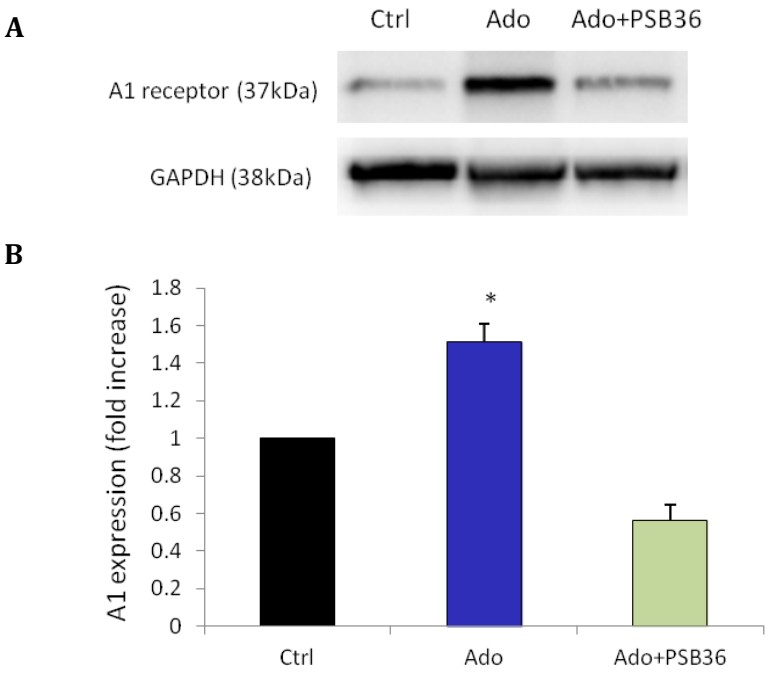

Figure 27. Adenosine receptor A1 modulates neuronal differentiation: protein analysis. A) Western blot of total protein extracted after 3 days of differentiation (Ctrl), in the presence of 100 μM adenosine (Ado) or Ado plus the A1 antagonist PSB36 (1 μM). The antagonist was added 30 minutes before Ado treatment. GAPDH was used to normalize protein expression. B) Protein expression of A1 receptor was quantified as a ratio between A1/GAPDH expression. Counts represent means ± SEM (n = 3 independent experiments). One-way ANOVA.

The involvement of the A1 receptor in modulating neuronal differentiation was confirmed also by the single sphere assay. Activation of A1 receptor with the specific agonist N^6-Cyclopentyladenosine (CPA, 100 μM) had a more pronounced effect compared to adenosine in inhibiting neuronal differentiation (88% vs 60% of inhibition), whereas blockage of A1 by the specific antagonist PSB36 reverted the effect of adenosine (Fig. 28).

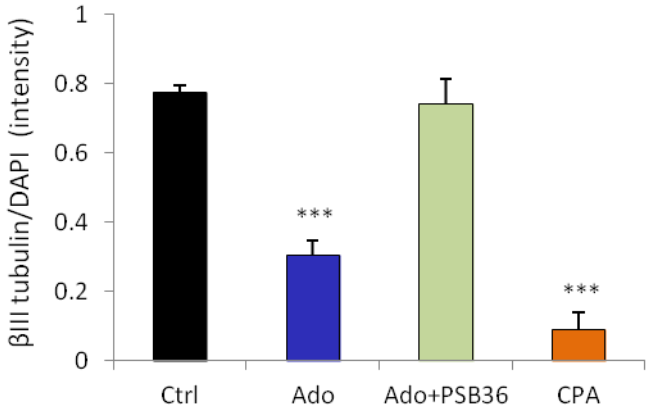

Figure 28. Adenosine receptor A1 modulates neuronal differentiation: single sphere assay. Neurospheres were differentiated for 7 days to assess neuronal differentiation in the presence of 100 μM adenosine (Ado), Ado plus 1 μM PSB36 or the specific A1 agonist CPA (100 μM). Neuronal differentiation was calculated after immunofluorescence by densitometry as the ratio between βIII tubulin expression and total cells counterstained with DAPI. Counts represent means ± SEM (n = 6 independent experiments); 3 single spheres in each experimental condition were counted every experiment. *** $p < 0.001$ vs. Ctrl. One-way ANOVA.

Finally, we corroborated the involvement of A1 receptor in neuronal differentiation inhibition by means of silencing assay. This experiment consisted in transfecting shRNA targeted to A1 receptor, which silences its expression. In a first approach, we determined the protein inhibition level using neurospheres after 6 days of differentiation (maximum silencing peak). Cells were also transfected as a control with a scrambled and GFP plasmids (Fig. 29). Silencing with shRNA produced a 60% of inhibition of A1 receptor expression respect to the cells transfected with GFP plasmid.

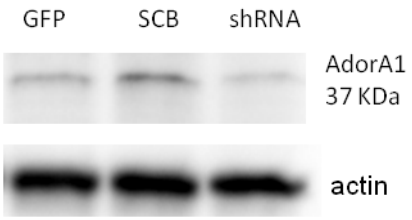

Figure 29. A1 receptor silencing. Neurospheres were transfected with EGFP, scrambled (SCB) or A1 shRNA plasmids and after 6 days of differentiation the A1 receptor expression was assessed by Western blot. Analysis was performed with anti-A1 and normalized with anti-actin as described in the text.

Once we confirmed that silencing decreased the A1 receptor expression, we analyzed by immunofluorescence the effect of CPA on A1^{-} neurospheres after 10-12 days of differentiation. Control cells were transfected with scrambled plasmid and differentiated with CPA (SCB/CPA); both SCB/CPA and untransfected cells treated with CPA decreased neuronal differentiation by 40%. Silencing of Adora1 abolished the effect of CPA, restoring the level of neuronal differentiation to the control level (Fig. 30).

Thus, this set of experiments demonstrated that activation of the A1 receptor in SVZ inhibits neuronal differentiation.

A

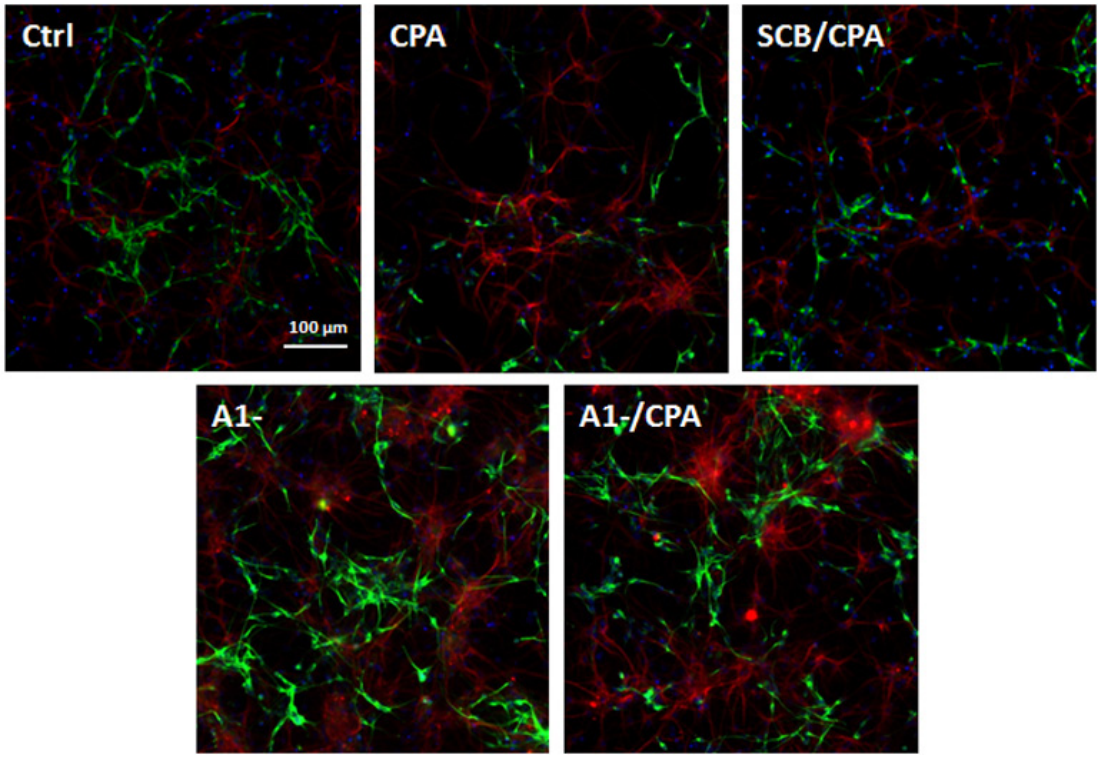

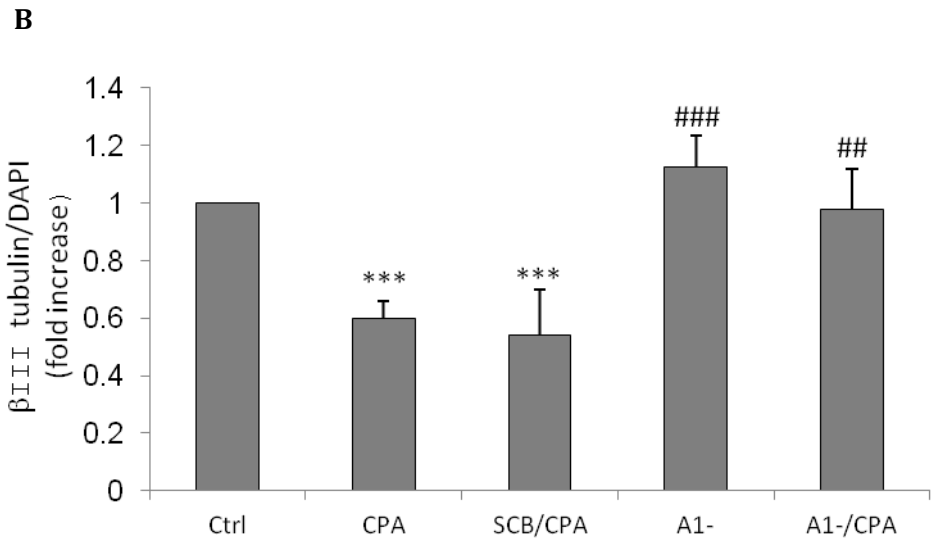

Figure 30. Silencing of adenosine A1 receptor reverted the effect of CPA. A) Untransfected cells (Ctrl and CPA) or transfected cells, $A1^-$ and scramble (SCB), were differentiated during 10-12 days in the absence (Ctrl) or presence of 100 μM CPA. Cells were stained with βIII tubulin (green), GFAP (red) and DAPI (blue). Neuronal differentiation was calculated in B after immunofluorescence by densitometry as the ratio between βIII tubulin expression and total cells counterstained with DAPI. Counts represent means ± SEM (n = 6 independent experiments). *** $p < 0.001$ vs. Ctrl whereas ### $p < 0.001$ or ## $p < 0.01$ vs. CPA. One-way ANOVA. Scale bar = 100 μm.

5. A1 RECEPTORS INHIBIT DIFFERENTIATION FROM TRANSIT AMPLIFYING PRECURSORS TO NEUROBLASTS

Once we identified A1 receptor activation inhibits neuronal differentiation, we investigated the cellular target of adenosine.

Early progenitor cells (B cells) differ from neuroblasts (A cells) by their expression of EGF receptors in the former and of neuronal filaments in the latter. Expression of these two markers overlaps in transit amplifying cells (C cells) (Fig. 31). In order to identify the cellular target of adenosine and CPA we labeled differentiating neurospheres with a fluorescent EGF receptor agonist (A640EGF) and overexpressed the neurofilament M fused with GFP (pEGFP-NFM). After treatment with the A1 agonists, adenosine or CPA and the antagonist PSB36, cells were analyzed by cytofluorimetry assay (Fig. 32). We found that adenosine treatment reduced the number of C cells (co-expressing EGF receptor and EGFP-NFM) and neuroblasts (expressing only EGFP-NFM), both to 56% respect to the control, whereas specific A1 activation by CPA decreased especially the number of A cells by 90% (and C cells by 37%, Fig. 32). PSB36 reverted the effects of adenosine in both C

and A cells, indicating that specific activation of receptor A1 inhibits the differentiation from transit amplifying cells to neuroblasts.

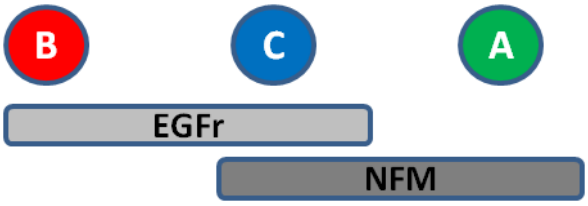

Figure 31. Markers used to analyze the presence of cell type B, C or A. EGF receptor (EGFr); medium neurofilaments (NFM).

A

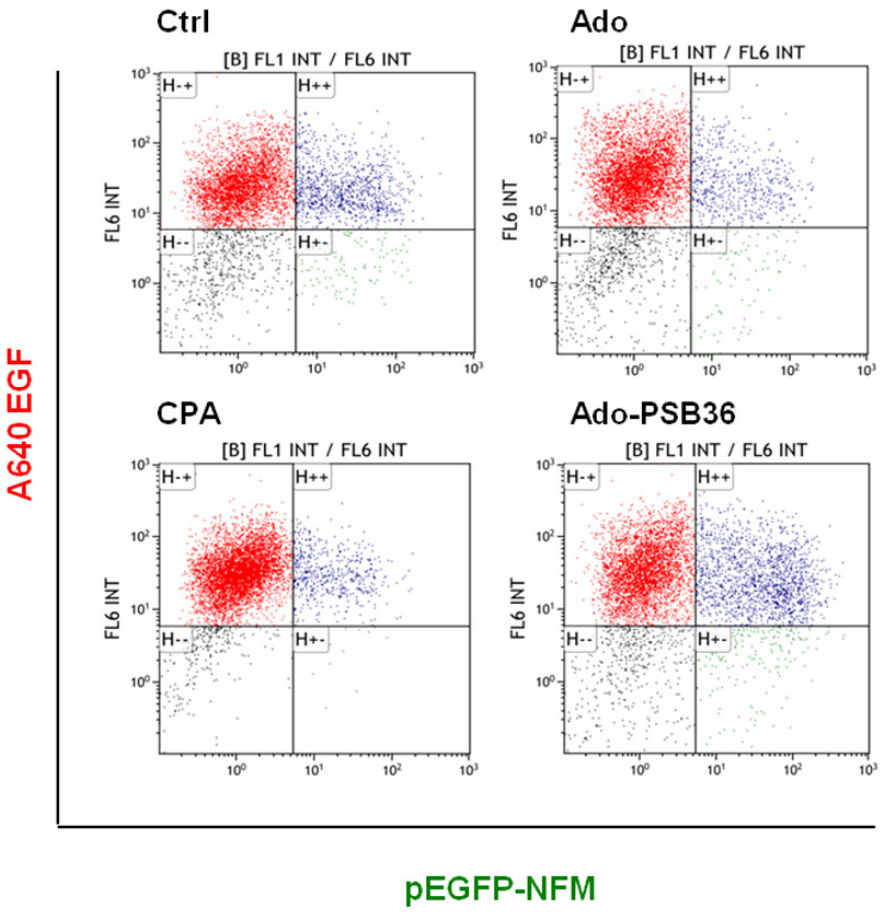

B

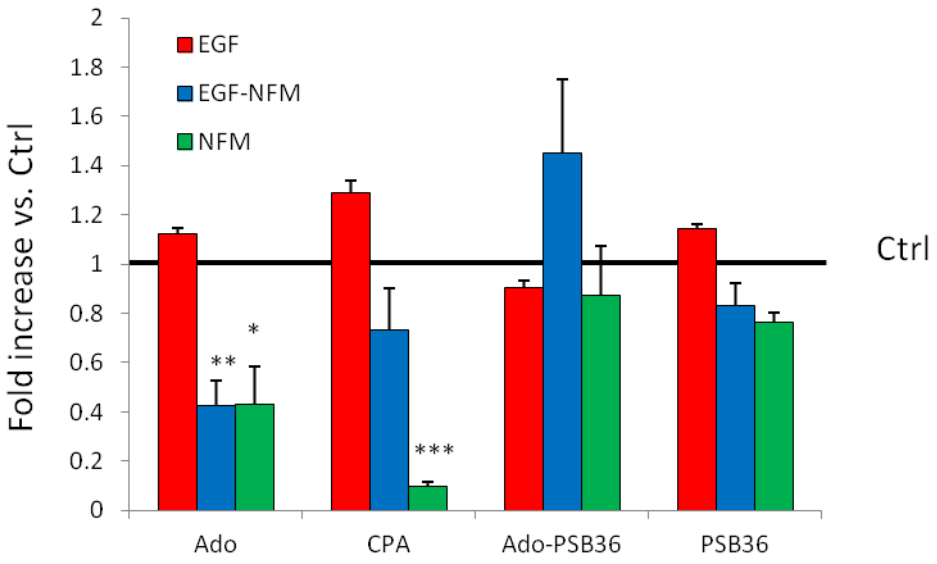

Figure 32. Activation of A1 receptor inhibits the differentiation from type C cells to neuroblasts (A cells). A) Neurosphere cultures were transfected with EGFP-NFM plasmid to label neuroblasts, then differentiated for 7 days in the presence of the agonists adenosine (100 μM; Ado) and CPA (100 μM) or the antagonist PSB36 (1 μM). 2 hours before the cytometry analysis type B progenitor cells were labeled with A640EGF. Type B cells are shown in red (upper-left quadrant), A cells in green (down-right) and type C cells in blue (upper-right). B) Cytometry analysis was quantified as a fold increase respect to the control (Ctrl). Counts represent means ± SEM (n = 4 independent experiments). * $p < 0.05$, ** $p < 0.01$ and *** $p < 0.001$ vs. Ctrl. One-way ANOVA.

6. A1 RECEPTORS-MEDIATED MECHANISMS OF NEURONAL DIFFERENTIATION INHIBITION

6.1. ACTIVATION OF A1 RECEPTOR MODULATES IL-10 RELEASE

As we stated in the introduction, one of the factor that modulates adult neurogenesis, especially in pathological conditions, is the inflammation (Ekdahl et al. 2009). Moreover, cytokine release can be modulated in turn by small heat shock proteins (Ramírez-Rodríguez et al. 2013). Among these, crystallin alpha-B (CRYAB) is a potent negative regulator of the secretion of various interleukins (IL6, IL10, IL17 and TNF-α; refs. (Ousman et al. 2007; Shao et al. 2013). In order to link A1 receptor signaling with inflammation, we measured the levels of CRYAB transcript in A1 activated cultures. We differentiated neurosphere cultures for 1, 5 and 7 days in the presence of CPA and compared Adora1 transcript with untreated cultures by semi-quantitative PCR. We found

a transient decrease of CRYAB mRNA shortly after CPA treatment (30% after 1 and 5 days) with transcript levels similar to the control after 7 days (Fig. 33).

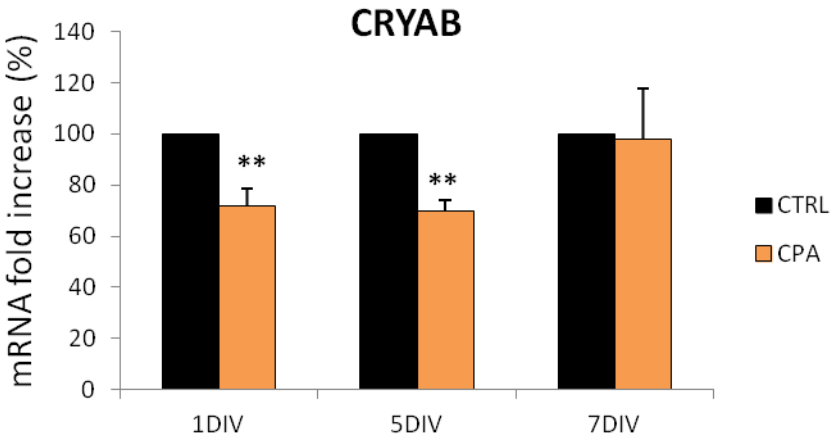

Figure 33. Stimulation of A1 receptor decreases CRYAB transcription. Neurospheres were differentiated for 1, 5 and 7 days *in vitro* (DIV) in the presence of 100 µM CPA. Expression of CRYAB transcripts was quantified by qRT-PCR and calculated as a percentage of ΔΔCt vs control conditions (CTRL). Counts represent means ± SEM (n = 6 independent experiments). ** $p < 0.01$ vs. CTRL. Two-way ANOVA followed by Bonferroni post-hoc tests.

We then monitored if activation of A1 receptor induced the secretion of different pro- and anti-inflammatory cytokines (IL1, IL6, IL10 and TNF-α). To that end, we harvested media conditioned by neurosphere cultures differentiated for 5 days in the absence or presence of CPA, and measured the presence of released cytokines. Among the cytokines tested, only IL10 and TNF-α were detected at high levels and only IL10 was modulated by CPA treatment (Fig. 34). Accordingly, IL10 mRNA was also up-regulated by CPA, as shown by quantitative RT-PCR (Fig. 35). Finally, to confirm that inhibition of neuronal differentiation induced by A1 activation was mediated by IL10 release we measured neuronal differentiation in the presence of CPA and a blocking antibody against IL10. This antibody inhibited significantly the effect of CPA, as measured after 7 days of differentiation (Fig. 36). Moreover, no significant changes were observed between control cultures and those treated with CPA together with anti-IL10 antibodies. In turn, we observed that both neuroblasts (DCX) and progenitor cells (GFAP) can be sensitive to the action of IL10 as all expressed its receptor (Fig. 37A). Nevertheless, activation of A1 receptor significantly increased only the number of progenitor cells (Fig. 37B, C) as shown by cytofluorimetry assay after gating IL-10R cell population, suggesting a possible effect of adenosine on progenitor cells.

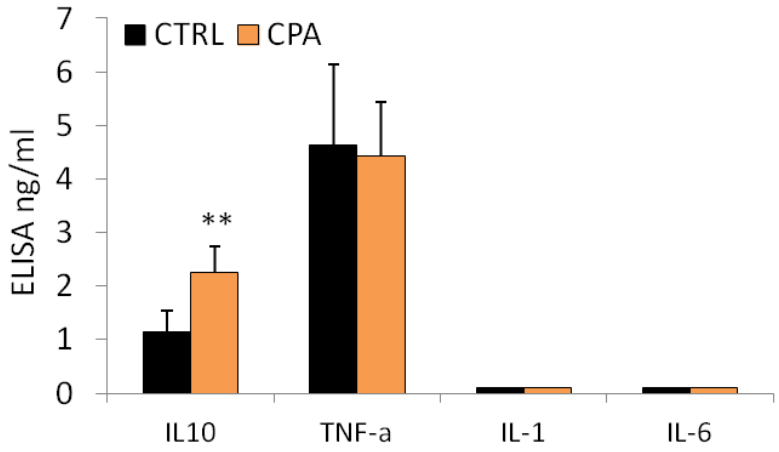

Figure 34. Activation of A1 receptor stimulates the release of IL-10. Supernatants of neurospheres differentiated for 5 days in the presence of CPA were analyzed by ELISA for the release of soluble IL10, TNF-α, IL1 and IL6. Counts represent means ± SEM (n = 4 independent experiments). ** $p < 0.01$ vs. CTRL. T test.

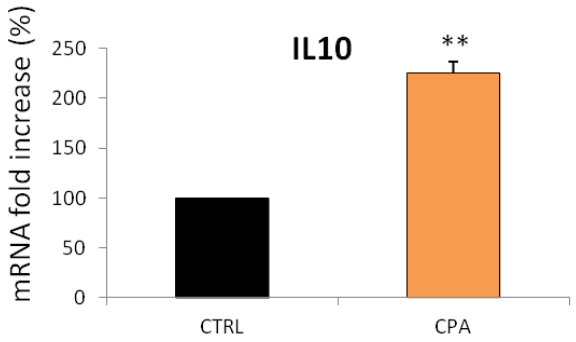

Figure 35. Activation of A1 receptor induces IL10 transcription. IL10 mRNA transcripts of cells differentiated for 5 days in the presence of CPA were analyzed by qRT-PCR and calculated as a percentage of ΔΔCt vs control conditions (CTRL). Counts represent means ± SEM (n = 6 independent experiments). ** $p < 0.01$ vs. CTRL. T test.

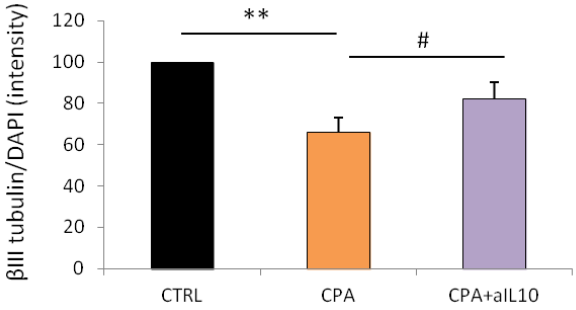

Figure 36. Inactivation of IL10 re-established neuronal differentiation. Neurosphere cultures were differentiated for 7 days in the presence of 100 μM CPA. Blocking antibody against IL10 (aIL10; 2 μg/ ml) was added 30 minutes before the CPA treatment. Differentiation was quantified after immunofluorescence by densitometry as a percentage of the ratio between βIII tubulin vs total cells stained with DAPI. Counts represent means ± SEM (n = 3 independent experiments). ** $p < 0.01$ vs. CTRL and # $p < 0.05$ vs. CPA. One-way ANOVA.

A

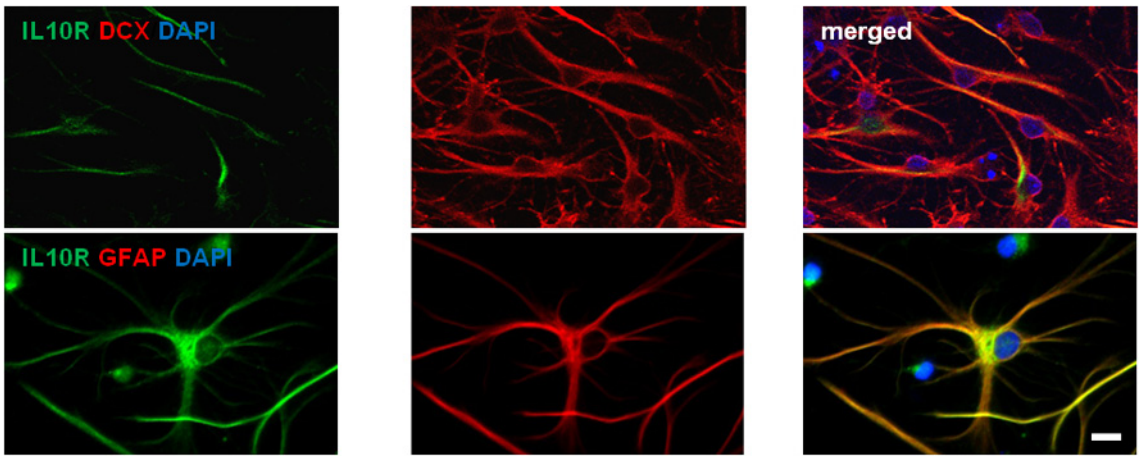

B

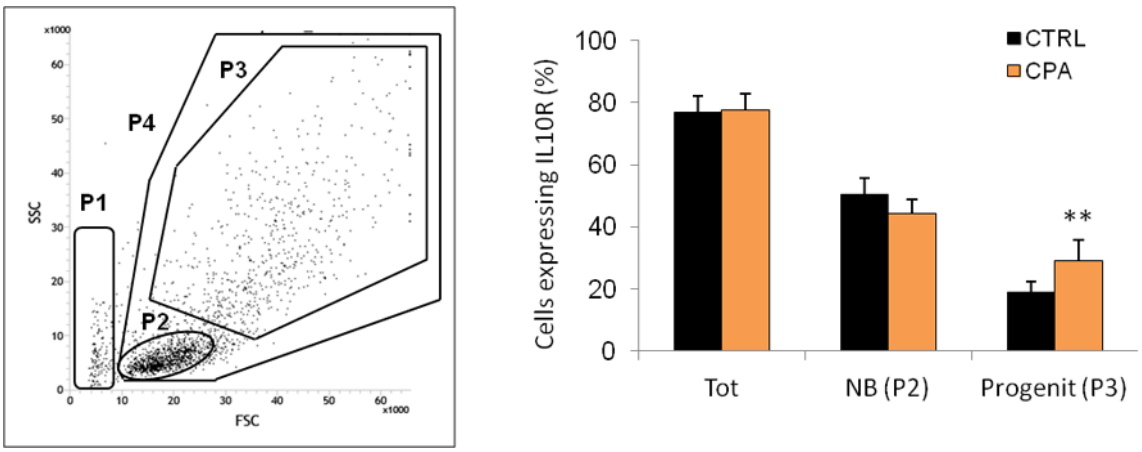

Figure 37. IL10 receptor localization. A) Neurospheres were differentiated for 7 days and double stained with IL10 receptor (IL10R in green) and the neuroblast marker DCX or the marker for multipotentiality GFAP (both in red). Nuclei were counterstained with DAPI (blue). B) After 5 days of differentiation in the presence of 100 µM CPA, cells expressing IL10R were analyzed by cytofluorimetry assay under morphological parameters (FSC vs SSC). As described previously (Azari et al. 2011) living cells positive for IL10R were gated in P4, neuroblasts (NB) in P2 and progenitor cells (Progenit.) in P3. Death cells gated in P1 were excluded from the counts. Counts are expressed as a percentage of total living cells in P4 and represent means ± SEM (n = 5 independent experiments). ** $p < 0.01$ vs. CTRL. T test. Scale bar = 20 µm

6.2. A1 STIMULATION ACTIVATES THE BMP2/SMAD PATHWAY

Previous studies demonstrated that stimulation of IL10R induces STAT3 phosphorylation that in turn stimulates Bmp2 transcription. This in turn triggers the phosphorylation of cytosolic SMAD and both, Bmp2 and SMAD, initiate the route to astrogliogenesis (Nakashima et al. 1999; Fukuda et al. 2007). To test this hypothesis first we measured the activity of STAT3 by luciferin/luciferase assay. We used the plasmid 4xBwt-pGL3 (Fukuda et al. 2007) that possesses two STAT3 binding sites in the Bmp2 promoter fused with the luciferase gene (Fig. 38).

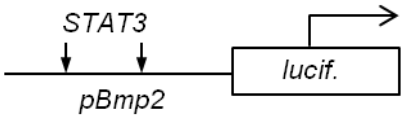

Figure 38. Plasmid 4xBwt-pGL3 used for neurosphere transfection. Plasmid 4xB2wt-pGL3 contains the luciferase reporter gene under the control of the Bmp2 promoter with two STAT3 consensus sequences.

After 3 days of differentiation cells were stimulated for 12 hours (time course of luciferase activity not shown) with CPA and luciferase activity was measured. We found that CPA treatment induces a two-fold increase in the STAT3 activity on the Bmp2 promoter (Fig. 39). Simultaneous treatment with the A1 antagonist PSB36 or the blocking IL10 antibody reduced the luciferase activity to control levels (Fig. 39) suggesting that the Bmp2 promoter is activated by A1 receptor and IL10 receptor through the phosphorylation of STAT3.

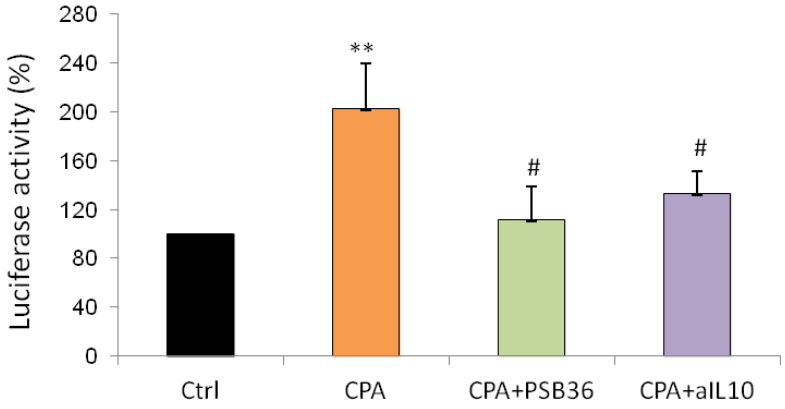

Figure 39. Activation of A1 receptor stimulates STAT3/Bmp2 pathway. Transfected cells were differentiated for three days and then stimulated for 12 hours with CPA (100 μM) and in the presence of the antagonist PSB36 (1 μM) or the blocking antibody against IL10 (2 μg/ml). STAT3-dependent Bmp2 activation was measured as luciferase activity expressed as a percentage respect to control (Ctrl). Counts represent means ± SEM (n = 3 independent experiments). ** $p < 0.01$ vs. CTRL and # $p < 0.05$ vs CPA. One-way ANOVA.

In parallel, we analyzed the Bmp2 mRNA after 3 days of differentiation and we noted an increase of Bmp2 transcripts after CPA treatment (Fig. 40).

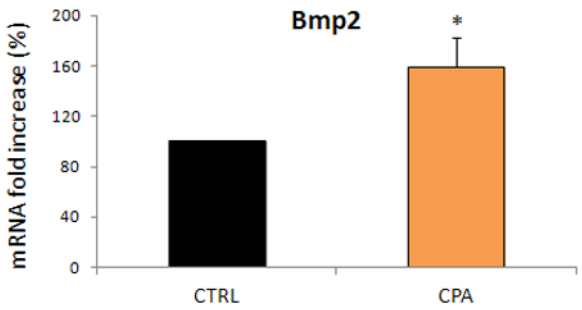

Figure 40. Stimulation of A1 receptor increases Bmp2 transcription. Bmp2 transcripts were quantified by qRT-PCR after 5 days of differentiation in the presence or absence (CTRL) of CPA and calculated as a percentage of ΔΔCt vs CTRL conditions. Counts represent means ± SEM (n = 6 independent experiments). * $p < 0.05$ vs. CTRL. T test.

In order to demonstrate that activated Bmp2 triggered the activation of SMAD, we stimulated the cells with 100 µM CPA for 12 hours at 3 days of differentiation. Then we labeled the phospho-SMAD (pSMAD1/5) protein and analyzed the number of cells expressing pSMAD by cytofluorimetry (Fig. 41). We found a significant increase of cells expressing pSMAD (from 58% to 68%) after A1 receptor stimulation with CPA.

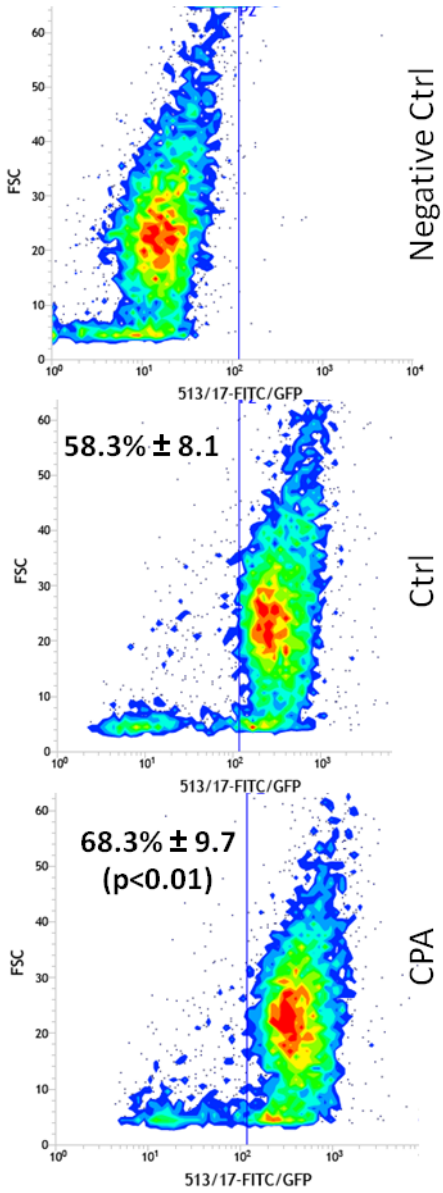

Figure 41. Activation of A1 receptor increase the number of cells expressing phosphorylated SMAD (pSMAD). Cells were differentiated for three days and stimulated with CPA for 12 hours before cytofluorimetry analysis. Percentage represents number of cells expressing pSMAD after specific immunostaining. Figure represents the mean of 4 independent experiments.

7. *IN VIVO* INHIBITION OF NEUROGENESIS BY SELECTIVE ACTIVATION OF A1 RECEPTOR

We next examined *in vivo* the role of A1 receptors in neuronal differentiation in the olfactory bulb. Expression of adenosine receptors in adult SVZ was assessed using the "expression" layer of Allen brain Atlas (McCarthy 2006) (Fig. 42A, B) and by immunofluorescence in adult neurosphere cultures from P42 rats (Fig. 42C).

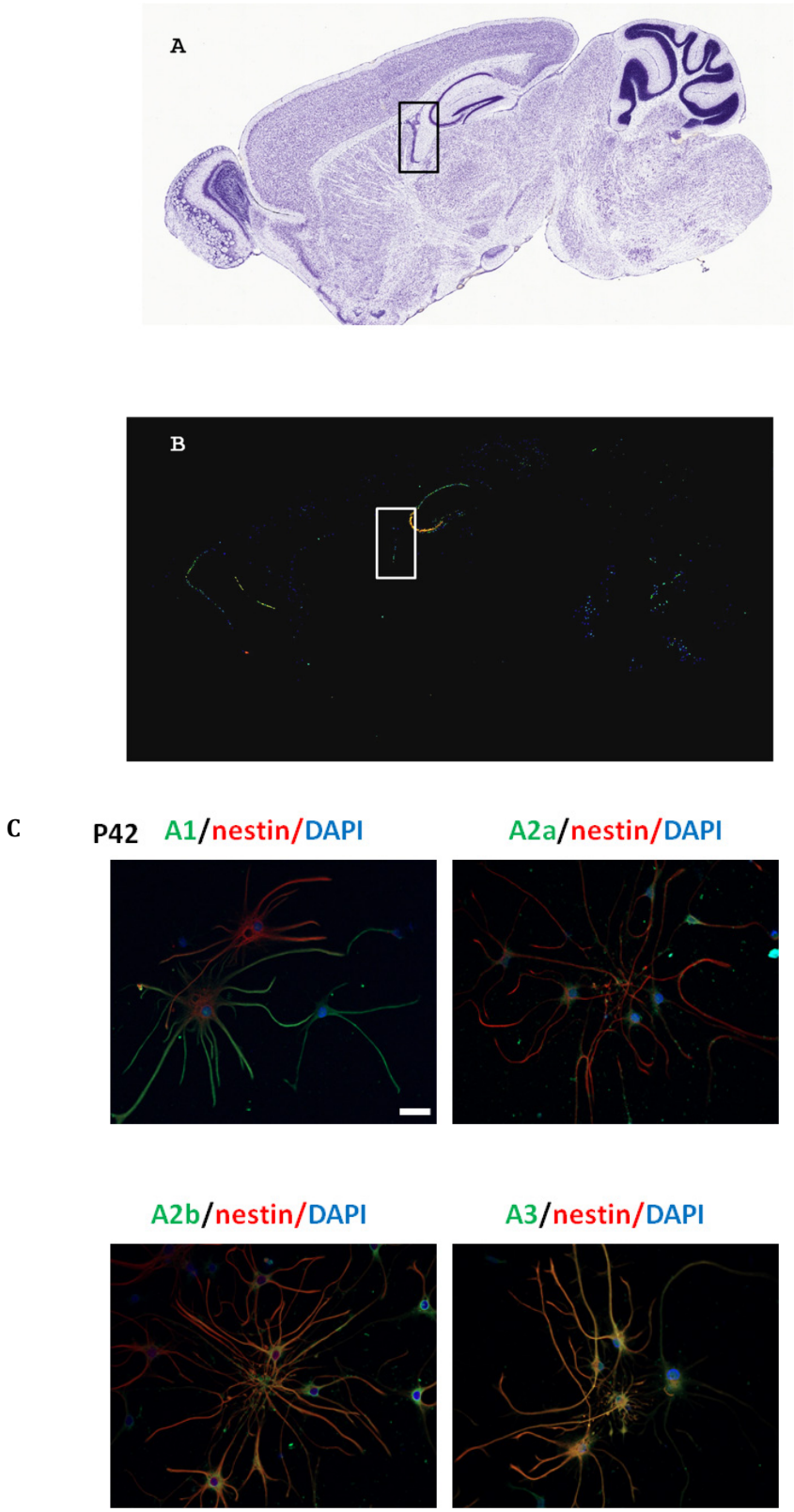

Figure 42. A1 receptor expression in the SVZ of adult rodent. Expression of A1 receptor was confirmed in the SVZ after analysis in the "Allen Brain Atlas" by Nissl staining (A) or mRNA expression (B). Adenosine receptors expression was evaluated after 7 days of proliferation in adult (P42) neurosphere cultures by double immunofluorescence with A1, A2a, A2b, A3 (all in green) and nestin (red). Nuclei were counterstained with DAPI. Scale bar = 20 µm.

To study the modulation of A1 receptor in neurogenesis, we infused on adult rats (6-8 -weeks-old) vehicle (PBS) or CPA (0.5 mM) intracerebroventricularly with osmotic pumps (delivery rate 250 nl/h, 14 days). This method allows CPA delivery into the SVZ and therefore the activation of A1 receptor of NSCs. Proliferating cells were labeled with three injections of BrdU (100 mg/Kg body weight, i.p.) one day before inserting osmotic pumps. After 14 days we checked the expression of different markers of neurogenesis and BrdU incorporation in the olfactory bulb that is the natural site of neurogenesis originating in the SVZ. CPA treatment drastically decreased the number of neuroblasts (DCX/BrdU) by 40% less (Fig. 43A-B). The same rate of inhibition was measured for the newborn neurons, labeled with NeuN/BrdU whereas we noted a significant increase of newborn astrocytes labeled with S100β/BrdU. The total number of proliferating cells (BrdU) did not change, demonstrating that neuroblasts decrease was neither due to neuronal death nor to the inhibition of neuroblast migration.

A

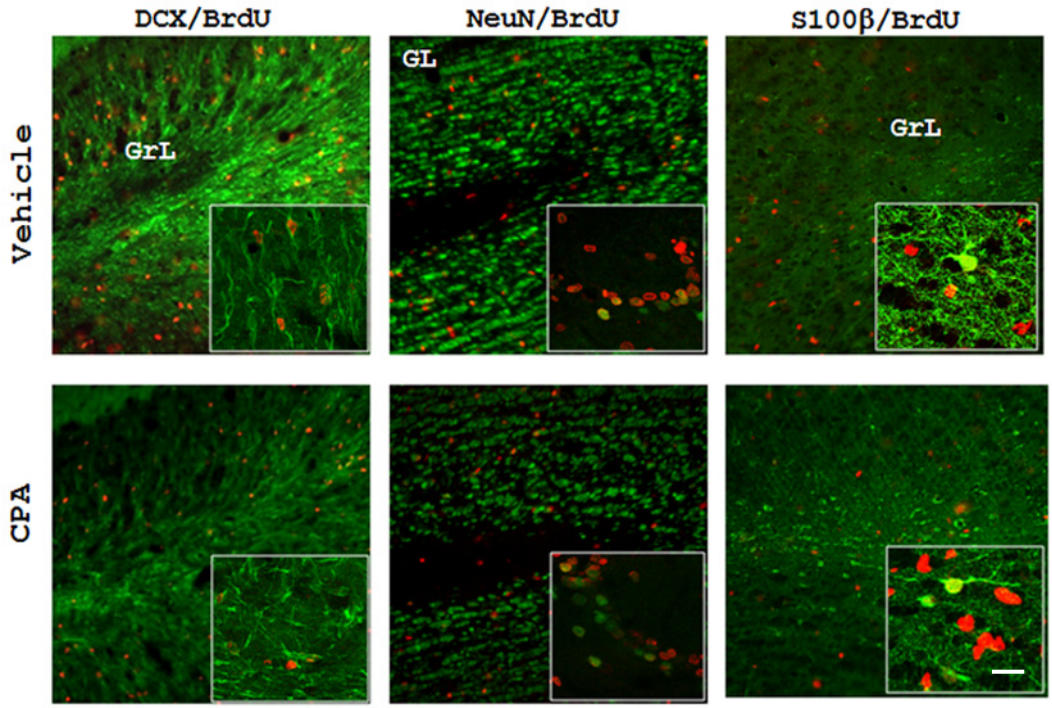

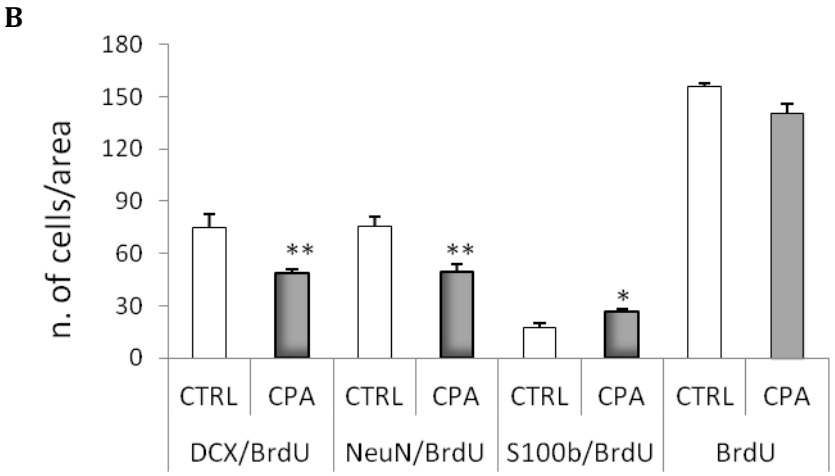

Figure 43. Activation of A1 receptor in the SVZ inhibits neurogenesis in the olfactory bulb and sustains astrogliogenesis. A and B) 0.5 mM CPA or PBS (Vehicle) were infused with osmotic pumps into the lateral ventricle of adult rats for 14 days. The total pool of proliferating cells primed by A1 activation was labeled with three injections of 100 mg/Kg BrdU before infusion. Neurogenesis was assessed in the granular layer of olfactory bulb (GrL) by double immunofluorescence with doublecortin (DCX, green) and BrdU (red) or in the glomerular layer (GL) by double immunofluorescence with NeuN (green) and BrdU. Astrogliogenesis was assessed in the GL by double immunofluorescence with S100β (green) and BrdU (A). Quantification of newly generated neurons, newly generated astrocytes or total proliferating cells (BrdU) is shown in B. Counts represent means ± SEM (n = 6 independent animals). ** $p < 0.01$ and * $p < 0.05$ vs. CTRL. T test. Scale bar = 25 µm.

Astrogliogenesis dependent by A1 receptor was tested also in *in vitro* neurosphere cultures. After proliferation labelling with BrdU we treated the neurosphere cultures with the agonist CPA in the presence or absence of the antagonist PSB36. We measured the number of newly generated astrocytes with double immunofluorescence for S100β and BrdU (Fig. 44). The results showed an increase of astrocytes (2.6 folds) after CPA treatment, which was reverted to control levels with the A1 antagonist PSB36.

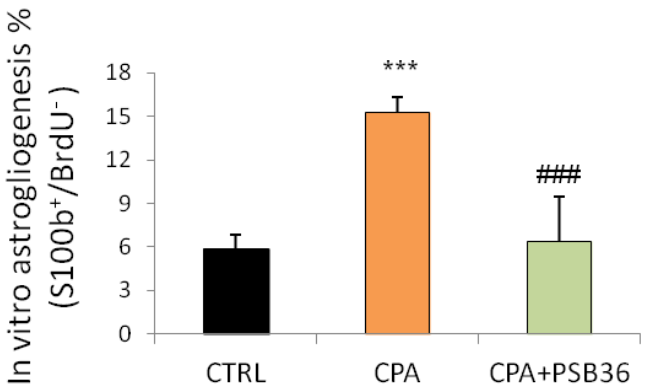

Figure 44. Activation of A1 receptor *in vitro* sustains astrogliogenesis. Neurospheres were differentiated for 7 days in the presence of 10 µM BrdU and double stained with anti S100β and anti BrdU. Double positive cells were counted and quantified vs the total cells counterstained with DAPI. Counts represent means ± SEM (n = 4 independent experiments). *** $p < 0.001$ vs. CTRL and ### $p < 0.001$ vs CPA. One-way ANOVA followed by Tukey post-hoc tests.

8. ACTIVATION OF A1 RECEPTOR DURING BRAIN ISCHEMIA ACTIVATES ASTROGLIOGENESIS TO THE DETRIMENT OF NEUROGENESIS

Given that adenosine is massively released during brain ischemia (Schubert & Kreutzberg 1993) we wanted to test if the block of A1 receptor in ischemic conditions can sustain adult neurogenesis. We induced mice brain ischemia by transit middle cerebral artery occlusion (tMCAO), which mimics accurately enough the human stroke. tMCAO generates focal ischemia with irreversible injury in a core region and partially reversible damage in the surrounding penumbra core, which is sensible to regeneration. We occluded the middle cerebral artery for 50 minutes then we evaluated different parameters in animals treated with the A1 antagonist DPCPX (0.1 mg/Kg) vs vehicle (PBS) at 7, 15 and 30 days after ischemia (DAI). Before studying neurogenesis modulation we analyzed neurological score, body weight, survival, infarct size and functional recovery with the pole test.

8.1. Body weight, neurological score, and survival after DPCPX treatment in tMCAO

The **body weight, neurological score and survival** of ischemic animals, vehicle and treated, were recorded after one hour and every day after ischemia. With **body weight** we observed a significant drastic decrease after the first three days in vehicle and treated animals then, they recovered their body mass until similar values of initial body weight. Nevertheless, the A1 antagonist DPCPX did not modify significantly the body weight respect to control animals (PBS) (Fig. 45).

After stroke, animals suffer motor deficits which were assessed by **neurological score**. We used a five-point scale, being grade 0 = no observable deficit and grade 5 = dead animal (see Material and Methods for a detailed description). In general, animals treated with DPCPX showed a lower neurological score that is reflected in a better ability of movement. Already after 3-5 days, ischemic animals treated with DPCPX recover a large proportion of the lost locomotion with less variability respect with vehicle animals (Fig. 46).

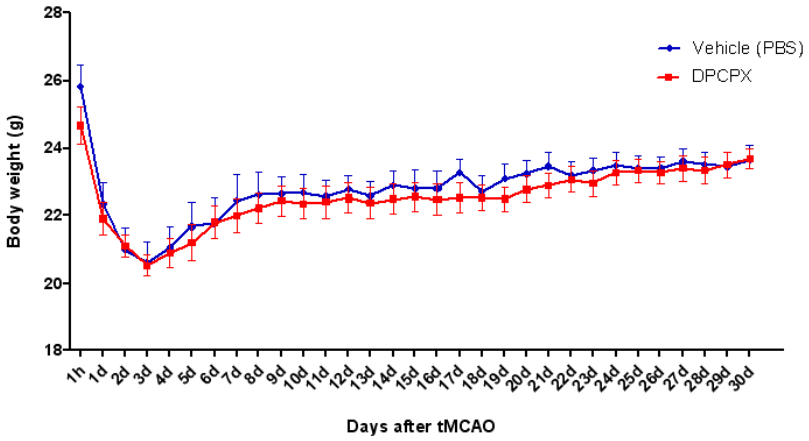

Figure 45. Blocking A1 receptor during brain ischemia in mice did not change their body weight. tMCAO was conducted for 50 minutes in vehicle (PBS treated) and 0.1 mg/Kg DPCPX treated mice. The body weight was measured 1 hour after tMCAO and every day during 30 days. Counts represent means ± SEM (n = 7 for vehicle animals and n = 11 for DPCPX treatment). Two-way ANOVA followed by Bonferroni post-hoc tests.

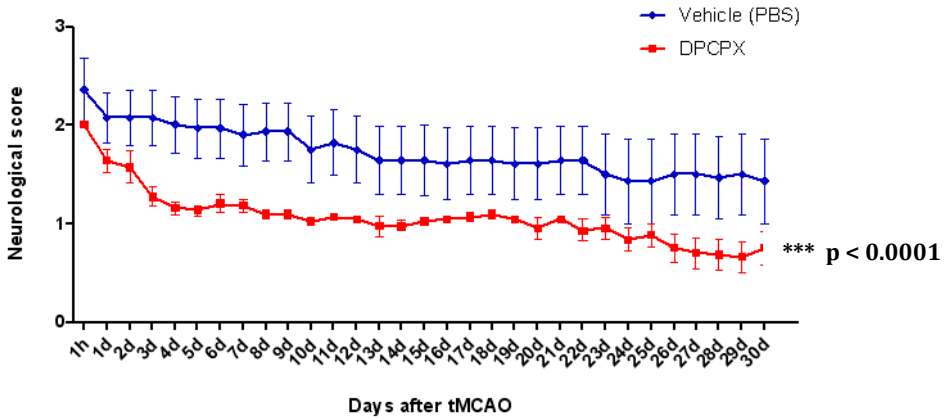

Figure 46. Blocking A1 receptor during brain ischemia in mice improves neurological score. tMCAO was conducted for 50 minutes in vehicle (PBS treated) and 0.1 mg/Kg DPCPX treated mice. The neurological score was measured 1 hour after tMCAO and every day during 30 days. Counts represent means ± SEM (n = 7 for vehicle animals and n = 11 for DPCPX treatment). *** p < 0.0001. Two-way ANOVA followed by Bonferroni post-hoc tests.

Better neurological score in DPCPX treated animals was reflected also in the analysis of **survival** (78.5% vs 34.8% in vehicle animals 30 days after ischemia; figure 47).

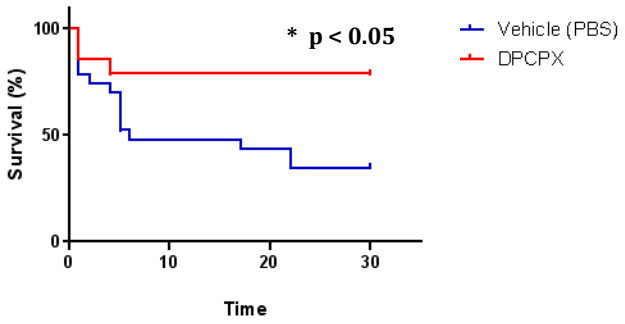

Figure 47. Blocking A1 receptor during brain ischemia in mice improves animal survival. tMCAO was conducted for 50 minutes in vehicle (PBS treated) and 0.1 mg/Kg DPCPX treated mice. Animal survival was verified every day during 30 days. Counts represents percentage of survival (n = 23 in vehicle animals and n = 14 in DPCPX animals). * p< 0.05. Log-rank test and Behand-Breslow-Wilcoxon test.

In table 4 is resumed the effect of A1 receptor blocking on neurological score, body weight and survival 7, 15 and 30 days after tMCAO.

Time after tMCAO	Neurological score	Body weight	Survival
7d	✓	✗	✗
15d	✓	✗	✓
30d	✓	✗	✓

Table 4. The effect of A1 receptor blocking in ischemic animals on neurological score, body weight and survival. Green V, treatment modifies significantly the studied parameter; red cross, administration of DPCPX is not significantly efficient.

8.2. Infarct size and brain volume

The infarct size was measured by cresyl violet staining (see materials and methods). Histological examination of ischemic sections revealed no significant changes in the damaged area of DPCPX treated respect to the vehicle animals (Fig. 48B). The ischemic area showed a pale intensity or higher blue in case of the arrival of inflammatory cells. As control we used sham animals, which did not suffer occlusion of middle cerebral artery. For this reason, the tissue of those sections is completely viable (Fig. 48A). The infarct size volume varies from 16% to 30%, focusing the affected area mainly in SVZ, although in some cases hippocampus is seriously damaged (data not shown).

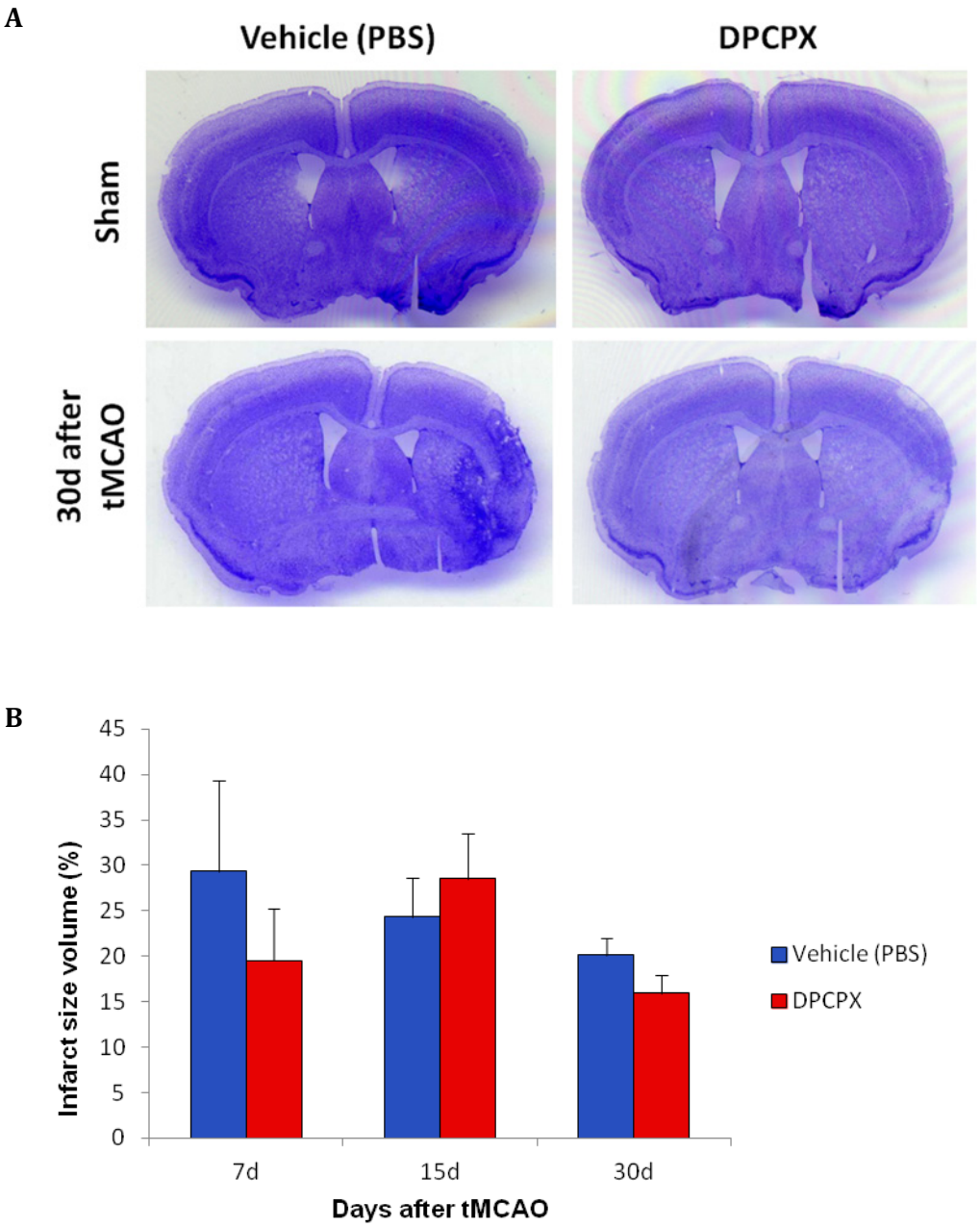

Figure 48. Infarct size evolution after tMCAO. tMCAO was conducted for 50 minutes in vehicle (PBS treated) and 0.1 mg/Kg DPCPX treated mice. A) Representative images from animals subjected to tMCAO (30 days after ischemia) and sham animals. The ischemic area appears in pale or deep blue in case of astrogliogenesis. B) Quantification of infarct size volume (6-7 sections were measured per brain) according to (Storini et al. 2006) in ischemic animals treated with DPCPX (in red) or PBS (in blue). Counts represent means of the infarct size volume percentage ± SEM (n = 6 for vehicle animals and n = 5-9 for DPCPX treatment). Two-way ANOVA followed by Bonferroni post-hoc tests.

As a result of ischemic insult, brain suffers volume changes due to edema. During the first days, we observed an increase in volume (data not shown); however at longer times a significant progressive reduction ($p < 0.0001$) of brain volume is observed in both DPCPX treated and untreated mice (Fig. 49). Volume reduction is achieved by the progressive

clearance of dead cells by immune system which generates a volume decrease especially in the ipsilateral hemisphere. We observed the maximal volume reduction 30 days after tMCAO (49% of reduction) and 4% and 35% after 7 and 15 days respectively. Treatment with DPCPX did not affect brain volume respect to vehicle animals.

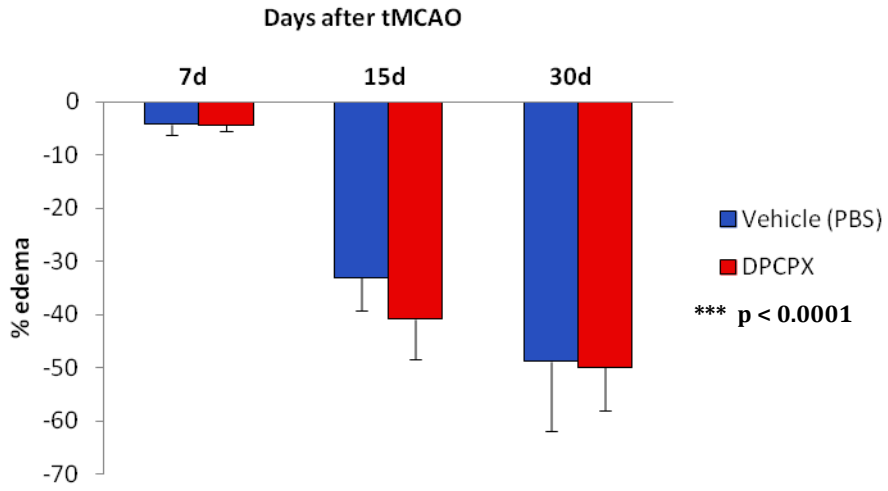

Figure 49. Blocking A1 receptor does not alter the brain volume after tMCAO. tMCAO was conducted for 50 minutes in vehicle (PBS treated) and 0.1 mg/Kg DPCPX treated mice. Mice were sacrificed 7, 15 and 30 days after ischemia. Quantification of volume edema was measured in the two groups according to (Storini et al. 2006). Measurement was calculated in correlation with areas of contralateral and ipsilateral hemispheres. Counts represent means of volume edema percentage ± SEM (n = 6 for vehicle animals and n = 5-9 for DPCPX treatment). Two-way ANOVA followed by Bonferroni post-hoc tests.

8.3. Blocking A1 receptor during tMCAO improves mobility shortly after ischemia.

After stroke, animals lose the most of their mobility due to the damage in cortical regions responsible for movement. In order to check functional recovery after ischemia we performed the pole test in vehicle and DPCPX treated animals. This test is a useful method for evaluating the mouse movement disorder caused by brain damage after stroke.

The day before tMCAO, mice were trained to descend a 50 cm pole; the time the mouse needs to turn and to reach the floor after being placed head up is taken in the two groups of animals, vehicle and DPCPX treated, and test was repeated every two days up to 30 DAI. One day after tMCAO in vehicle animals, the latency to complete the test is maximal (18s)

but the values turned to the baseline already 5 DAI (Fig. 50). Surprisingly, the treatment with the DPCPX improved significantly the movement 1 DAI (9s vs. 18s in vehicle animals), suggesting the effect of the drug is not related with increased neurogenesis.

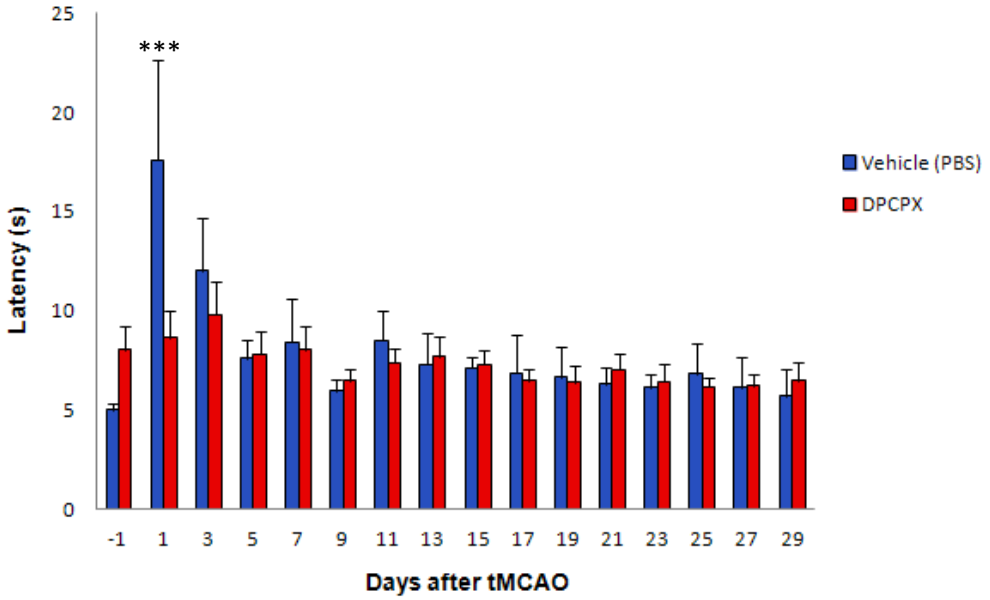

Figure 50. DPCPX treatment improves legs movement in the pole test. Animals subjected to ischemic insult were treated with DPCPX (0.1 mg/Kg) or PBS (vehicle) every day and forced to descend down a horizontal pole every other day measuring the time to reach the surface of the cage. Each animal was subjected to 3 trials every day and the average of 3 trials was used as final score. Counts represent means of the time ± SEM (n = 4 for vehicle animals and n = 8 for DPCPX treatment). *** $p < 0.001$. Two-way ANOVA followed by Bonferroni post-hoc tests.

8.4. Positron tomography emission (PET) analysis of cell proliferation

This experiment reports that endogenous NSCs can be visualized in the living animal with positron emission tomography (PET) using the radiotracer 3'-deoxy-3'-[^{18}F]-fluorothymidine ([^{18}F] FLT) that enables imagining and measuring of cell proliferation. Our objective was to determine the effect of the antagonist of A1 receptor in ischemic animals at different time points using PET technology. Adult rats subjected to tMCAO were injected with the radiolabeled thymidine [^{18}F] FLT to visualize proliferating cells in the brain *in vivo.* We analyzed proliferation level in several regions of the brain (olfactory bulb, amygdala, striatum, hypothalamus, midbrain, cortex, cerebellum and hippocampus). But only striatum showed elevated level of the tracer in ischemic animals treated with DPCPX respect to saline solution at 8 days after tMCAO. However, this increase is not significant; therefore proliferation is not affected by DPCPX treatment (Fig. 51).

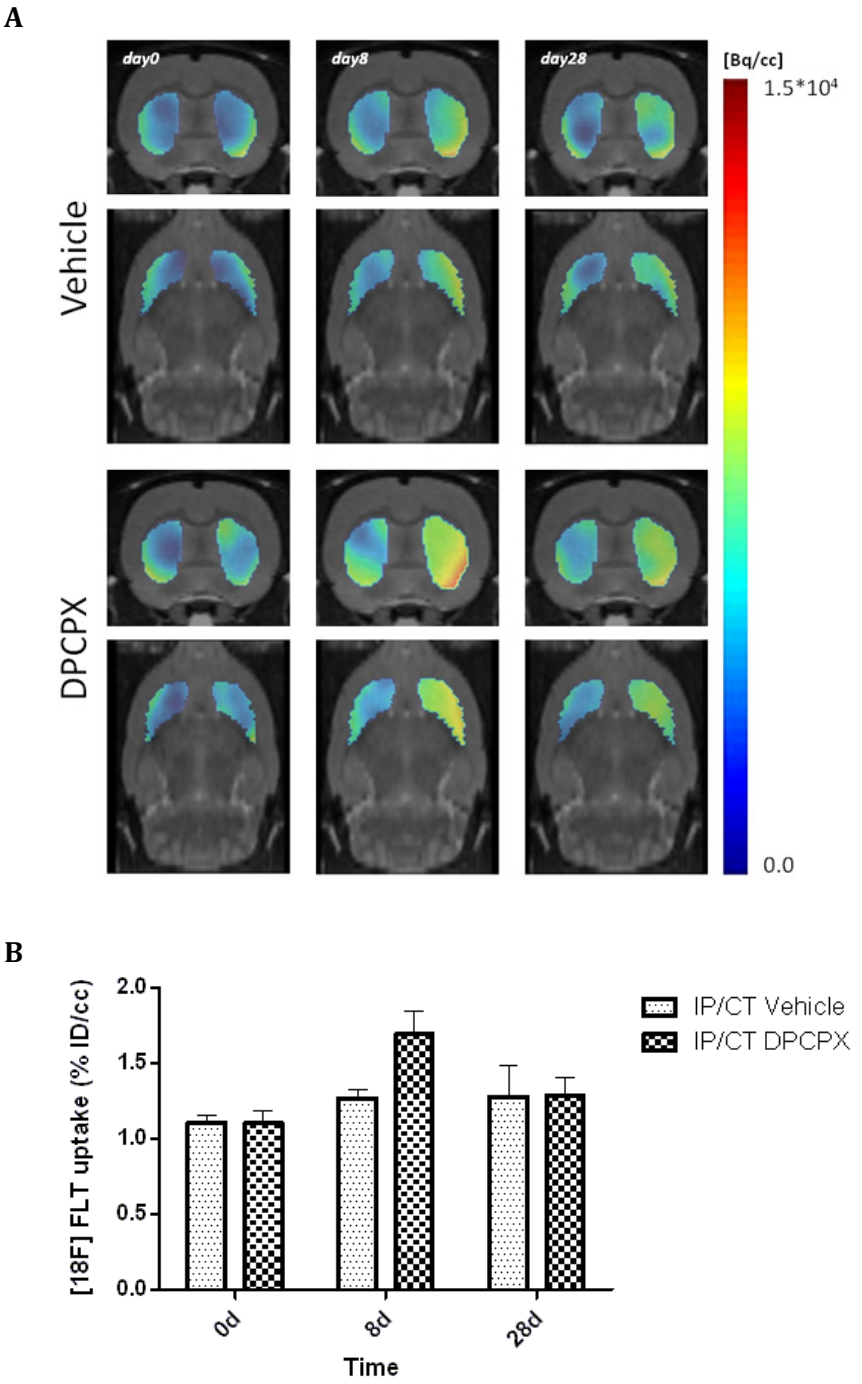

Figure 51. Cell proliferation analysis in the striatum of ischemic animals using the radioligand [^{18}F] FLT in PET. A) Normalized coronal (upper quadrants) and sagittal (down quadrants) PET images of ischemic brains in DPCPX (0.1 mg/Kg) or PBS (vehicle) treated rats. 0, 8, and 28 days after tMCAO brains are co-registered with a MRI (T2W) rat brain template to localize anatomically the PET signal in the contralateral and ipsilateral hemisphere. Increased [^{18}F] FLT signal level corresponds to colored scale (from blue to dark red) B) The percentage of injected dose per cubic centimeter (%ID/cc; mean ± SEM) of [^{18}F] FLT was measured in the ipsilateral (IP) and contralateral (CT) hemisphere and the quantification corresponds to the ratio between ipsilateral and contralateral hemisphere. n = 8 (vehicle animals) and n = 7 (DPCPX-treated animals). Two-way ANOVA followed by Bonferroni post-hoc tests.

8.5. Activation of A1 receptor modulates neurogenesis and astrogliogenesis during brain ischemia

To test the effect of A1 receptor blocking on tMCAO-induced neurogenesis and to confirm its modulation on astrogliogenesis we performed a time course study after tMCAO. Two animal groups, vehicle (treated with PBS) and DPCPX (0.1 mg/Kg) were subjected to tMCAO and sacrifices after 7, 15 or 30 days. Proliferating cells were labeled before ischemia and thereafter with a daily dose of 100 mg/Kg of BrdU and treatment, PBS or DPCPX, were given i.p every days. Neurogenesis was evaluated at every time point after immunofluorescence by direct count of induced neuroblasts (DCX/BrdU$^+$) and newborn neurons (NeuN/BrdU$^+$). As shown in figure 52, tMCAO induced a progressive, not significant increase of newborn neuroblasts and newborn neurons whereas DPCPX treatment significantly increased the neurogenesis already 15 days after ischemia (1.96 fold for neuroblasts and 2.27 for newborn neurons). Block of A1 receptor by DPCPX increased the number of newborn neuroblasts but not newborn neurons also 30 days after tMCAO (1.41 fold).

In order to confirm our data *in vitro* we compared the effect of blocking A1 receptor on neurogenesis vs astrogliogenesis 15 days after ischemia (Fig. 53). We selected newborn astrocytes as positive for Thbs4/GFAP/BrdU. Thbs4 is expressed in several cells types but in CNS only in the astrocytes generated from the SVZ (Benner et al. 2013). We observed by immunofluorescence analysis that tMCAO generated new polarized astrocytes located mainly in the penumbra (Fig. 53A). Moreover, we confirmed that block of the A1 receptor by DPCPX treatment sustained the generation of newborn neuroblasts (DCX/BrdU$^+$ cells) but reduced the formation of new astrocytes with the same rate of neuroblasts increase (rate = 1.8) (Fig. 53B), suggesting that activation of A1 receptor during ischemia can be the modulator of neurogenesis and astrogliogenesis.

A

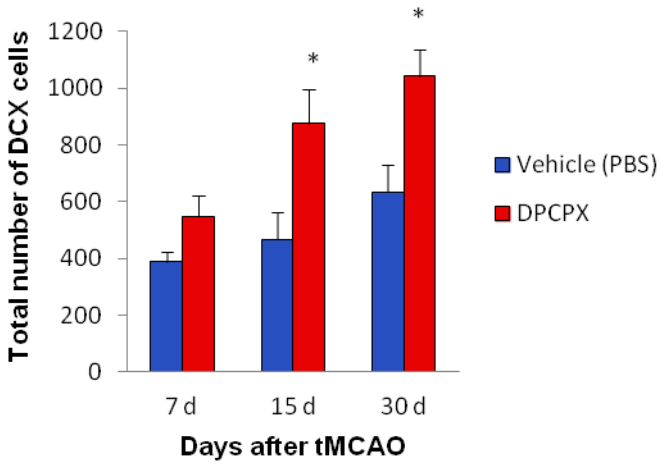

B

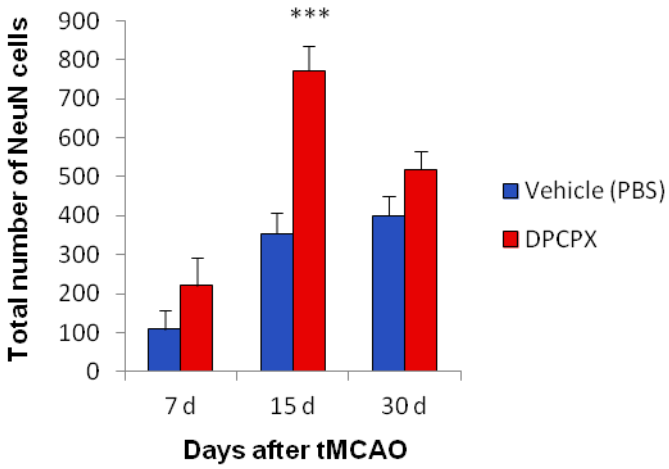

Figure 52. Block of A1 receptor by DPCPX during brain ischemia stimulates neurogenesis. Proliferating cells were labeled before tMCAO with three injections of 100 mg/Kg BrdU. DPCPX (0.1 mg/kg) or PBS were injected i.p. every day together with BrdU. Mice were sacrificed 7, 15 and 30 days after tMCAO and neurogenesis was quantified after double immunofluorescence with doublecortin (DCX) and BrdU (A; neuroblasts) or NeuN and BrdU (B; newborn neurons) by direct count of double positive cells in the striatum and cortex. Stereological methods were used for quantification [6 slices per animal were analyzed and 6 regions (3 striatum and 3 cortex) in each slice]. Counts represent means of total cells ± SEM (n = 4-6 for vehicle animals and n = 6-8 for treated animals). * $p < 0.05$ and *** $p < 0.001$. Two-way ANOVA followed by Bonferroni post-hoc tests.

A

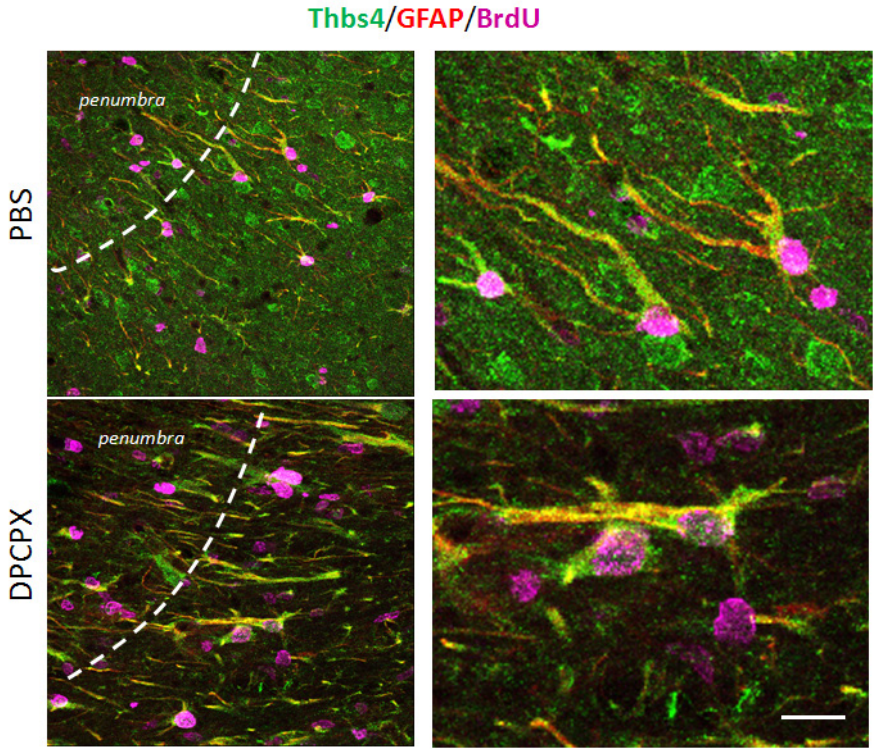

B

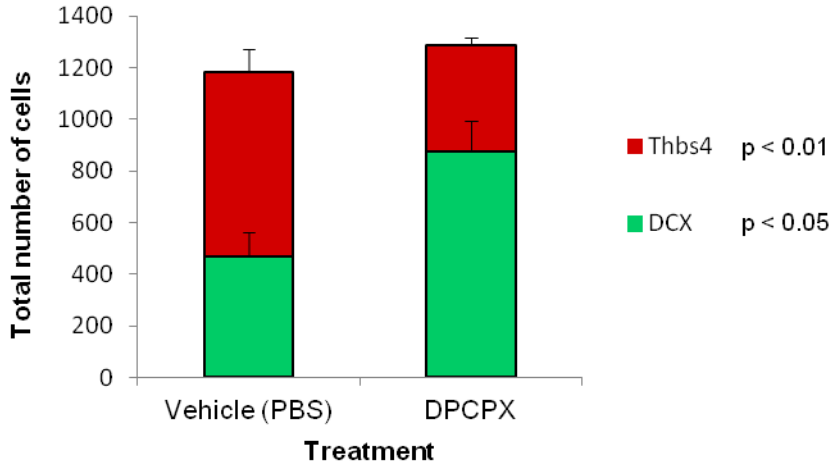

Figure 53. Block of A1 receptor during ischemia stimulates neurogenesis and inhibits astrogliogenesis. Ischemic mice were treated as in figure 52. 15 days after brain ischemia, astrogliogenesis in vehicle (PBS) and DPCPX mice was visualized in A by immunofluorescence with Thbs4 (green)/GFAP (red)/BrdU (pink-purple). Astrogliogenesis (red bars in B) and neurogenesis (green bars in B) were quantified by immunofluorescence as a direct count of Thbs4/GFAP/BrdU or DCX/BrdU positive cells respectively, in the striatum and cortex. Stereological methods were used for quantification [6 slices per animal were analyzed and 6 regions (3 striatum and 3 cortex) in each slice]. Counts represent means of total cells ± SEM (n = 6 for vehicle animals and n = 6 for treated animals). * $p < 0.05$ and ** $p < 0.01$. T-test. Scale bar = 25 µm.

Discussion

1. ADENOSINE AND NEUROGENESIS

The modulation of adult neurogenesis by purinergic system has been addressed in recent years and it is a matter of intense debate (e.g. (Zimmermann 2011). Depending on the concentration threshold, time of receptor stimulation and development stage, extracellular ATP can sustain or inhibit the different steps of adult neurogenesis. In particular, in our laboratory we demonstrated that ATP released after oxygen and glucose deprivation is among the repellent factors that inhibits neuroblasts migration and neuronal differentiation (Vergni et al. 2009). In addition, data from several groups support the idea of a trophic role of ATP and its derivatives in neurogenesis (Delic & Zimmermann 2010; Cao et al. 2013). Surprisingly, few papers have been published on the role of adenosine in adult neurogenesis (for example (Stafford et al. 2007)).

What is clear is the different role of the different adenosine receptors in sustaining or inhibiting neuronal differentiation. As mentioned in the introduction adenosine can inhibit or activate the adenylate cyclase depending if the inhibitory A1/A3 or excitatory A2a/A2b receptors are stimulated. It is suggested that an increment of adenylate cyclase activity stimulates neurite outgrowth in PC12 cells and that A2a receptor is involved in neuritogenesis (Sun et al. 2010; Yung et al. 2010). In parallel A1 receptor activation was described early in the 1998 to be involved in the inhibition of neuritogenesis (Shaban et al. 1998). Starting from these hypotheses we decided to investigate the role of adenosine and its receptors in modulating neuronal differentiation of adult multipotent cells and *in vivo* neurogenesis.

In this study we, first, used the neurospheres assay to measure the effect of different adenosine concentration in neuronal differentiation. We found that adenosine had a linear effect in inhibiting neuronal differentiation already at 10 μM and 100 μM. We decided to use the 100 μM concentration for all experiments because the results were more statistically significant and because this concentration is closer to the adenosine concentration found in brains of several neurodegenerative diseases (Hagberg et al. 1987; Pedata et al. 2001). The idea of adenosine acting as a repressor of neurogenesis is in line with previous results (Gampe et al. 2015) showing that an increase of ATP and consequent decrease of adenosine induced by nucleotidase inhibition, sustained neurogenesis.

The decrease of immature and mature neurons, given by βIII tubulin staining, was directly linked to the reduction of neuronal differentiation and not to the death of neuronal progenitors. Indeed, the block of the apoptotic pathway by the caspase inhibitor

ZVAD-FMK did not change the rate of βIII tubulin labeled neurons in the neurosphere assay. Moreover, also in the *in vivo* experiments, after CPA treatment we did not observe a reduction of total Brdu$^+$ cells in the olfactory bulb. Nevertheless, adenosine stimulation induced a small percentage (15% vs 60-70% of differentiation inhibition) of apoptotic-independent cell death. This can be linked to the activation of A2a/A2b receptors which are expressed at low levels as compared to the A1 receptors in SVZ-derived neurospheres. On the other hand we cannot exclude a role of nucleoside transporters in modulating neuronal differentiation.

The expression of all P1 adenosine receptors in neural progenitor cells from SVZ was demonstrated by PCR, Western blot and immunocytochemistry, corroborating partially the results obtained by (Stafford et al. 2007), who found primary neurosphere expressing P2X, P2Y and P1 (A1, A2A and A2B) receptors. In general, A1 and A2A receptors are the most expressed in the brain, unlike our results showing a higher expression of A1 and A2B receptors and the expression of A3. The expression of adenosine receptors is modified throughout life as an example the expression and density of A1 receptors in cortical and hippocampal regions decreases in aged animals (Cunha 2005). Thus, we deduce that the role of adenosine receptor and its efficacy in neurogenesis are modulated with age of animal.

2. A1 RECEPTOR-MEDIATED MECHANISMS OF NEUROGENESIS INHIBITION

In neurosphere model the A1 receptor is predominantly expressed and stimulation with adenosine gave the highest rate of A1 mRNA modulation, for this we hypothesized that A1 activation is involved in the inhibition of neurogenesis. This hypothesis was confirmed by the effect of specific agonist and antagonist of A1 receptors [i.e., CPA and PSB36 (Williams et al. 1986; Müller & Jacobson 2011) which efficiently mimic or block, respectively, the effects of adenosine (inhibiting or recovering neuronal differentiation). In particular, our results displayed a higher protein expression of A1 receptor under adenosine conditions. However, an agonist does not necessarily increase the level of its own receptor, as it can modulate the signaling pathway without modifying receptor expression. In addition, specific gene silencing of A1 receptors prevented adenosine from modulating neurogenesis, corroborating our previous results.

We suggest that adenosine can exert its negative action on neuronal differentiation by acting at transcriptional and synaptic level. We found a pool of genes involved in the generation of new neurons that are downregulated when cells are differentiated in the presence of adenosine and a little pool of genes (only six) that are upregulated. Among

these, the adenosine receptors Adora1 and Adora2a, and two of the gene family of Bmp (Bmp2 and Bmp15). As already mentioned in the introduction, Bmp proteins inhibit neuronal differentiation by a mechanism involving degradation of the pro-neuronal transcription factors Ascl1 (Shou et al. 1999) which is in turn downregulated by adenosine treatment. The upregulation of Adora1 was another evidence to trigger the essential role in neuronal differentiation on this receptor.

Latest studies suggest that the inhibition of neuronal differentiation is mainly produced at transcriptional level (Telley et al. 2016). Terminal differentiation occurred in the olfactory bulb from neuronal precursors to interneurons is controlled by several factors, among them the transcription factor NeuroD1 (Boutin et al. 2010), which is down-regulated in our neurogenesis array corroborating the role of adenosine in neuronal differentiation inhibition.

In addition, after adenosine treatment, we found an increment of synaptophysin and the glutamate transporter VGLUT2 in the cytoplasm respect to the synaptic terminals, as demonstrated by immunofluorescence and synaptosomes analysis. This situation would trigger to the absence of the vesicular transport to the axon and consequently inhibition of synaptic function (Duane E. Haines 2013). These results corroborated the previously published data describing the modulatory effect of A1 receptor in synaptogenesis and fine tune of synaptic activity (Ribeiro & Sebastião 2010; Sebastião & Ribeiro 2009). The effect of adenosine on synaptic activity was also confirmed in our genetic array where we found a downregulation of genes involved in synaptogenesis (Ache, acetyl cholinesterase and Dlg4, discs large homolog 4) (Sperling et al. 2012) and synaptic activity (Gpi, glucose-6-phosphate-isomerase and Ptn, pleiotrophin)(Jung et al. 2004), suggesting the inhibition of neuropoietic factors release and an autocrine control of differentiation mediated by adenosine. This blockage in vesicular transport could participate on neuronal differentiation inhibiting the release of differentiation factors like, for example BDNF or other neurotrophic factors. Nevertheless, more appropriated studies must be conducted to understand whether these events are causal or effect of adenosine modulation.

3. CHARACTERIZATION OF A1 RECEPTOR MECHANISMS

After identifying which receptor is involved in the negative modulation of adult neurogenesis, we wanted to characterize the cellular target of adenosine. Cytofluorimetry assay performed with the specific agonist CPA demonstrated that activation of A1 receptor induced a drastic decrease of newborn neurons, labeled with medial neurofilaments but

not of transient amplifying C cells, suggesting that activation of A1 receptor inhibits the differentiation from C- to A cells. *In vivo* experiments confirmed this hypothesis since intracerebroventricular infusion of CPA decreased the number of neuroblasts and newly generated neurons (DCX/BrdU$^+$ and NeuN/BrdU$^+$) in the olfactory bulb but not the number of total BrdU$^+$ cells. The decrease of DCX/BrdU$^+$ and NeuN/BrdU$^+$ cells in the olfactory bulb was quantified at granular and glomerular layer, respectively. Additional studies of the specific regionalization of these cells inside the olfactory bulb can contribute to new information on cellular type from SVZ (Fiorelli et al. 2015).

As stated previously a high concentration of extracellular adenosine is a hallmark of neurodegenerative diseases and brain damage which are usually accompanied by a neuroinflammatory response (Glaser et al. 2012). Here we investigated if over-activation of A1 receptors triggers to the release of inflammatory cytokines (Fig. 54). Surprisingly, we did not find A1-dependent release of pro-inflammatory cytokines (IL-1 and IL-6) but release of the anti-inflammatory IL-10 that is also modulated by CPA at transcriptional level. Consistent with previous findings (Perez-Asensio et al. 2013) IL-10 receptor is expressed in progenitor cells and in neuroblasts, and blocking its function (in our case by a blocking antibody) can sustains neurogenesis through the down-regulation of pro-neuronal genes. Moreover, increased neurogenesis was also observed in the olfactory bulb of IL-10 knockout mice (Perez-Asensio et al. 2013). The control of the expression and release of cytokines by adenosine has also been studied in other cellular types such as glial cells (Schwaninger et al. 2000). On the other hand, IL-10 is also expressed by B lymphocytes and is increased by the presence of CPA in ischemic models (Winerdal et al. 2016), which open new hypothesis on the exact role of IL-10 in pathological conditions, which can act as a second messenger more than an anti-inflammatory cytokine. In fact, the release of IL10 leads to the activation of Bmp2/STAT3/SMAD pathway that is finally involved in the transcription of genes related with astrocyte genesis (Fig. 54). In this view, A1 receptor represents the input for IL10 release which in turn acts as a mediator of astrocyte vs neuronal differentiation. Nevertheless, other pro-inflammatory cytokines, such as IL-1β and TNF-α, can contribute to astrocyte differentiation from NSC activating STAT3 pathway (Chen et al. 2013).

In the *in vitro* and *in vivo* paradigms used in our study, the decrease of neurogenesis is accompanied by the stimulation of astrogliogenesis. This is supported by recent evidences that SVZ can give rise to reactive astrocytes following brain ischemia (Faiz et al. 2015; Grégoire et al. 2015), which is a phenomenon characterized by high release of adenosine. They conclude that this unusual behavior of NSCs is modulated by the loss of function of

Ascl1, a transcription factor that we see downregulated *in vitro* after adenosine treatment. Furthermore, the latest findings attribute the cellular fate decision to epigenetic mechanism, in particular the ablation of the histone acetyltransferase Hdac3 leads to an increase of astrocytes (Zhang et al. 2016). Our results showed a downregulation of several members of histone acetyltransferase family (Hdac4 and Hdac7) under adenosine conditions, which opens promising pathways of research.

We suggest that astrocytes can regulate their genesis in an autocrine manner, a possibility that requires further experiments. In line with our hypothesis, the ATP released from the astrocytes can stimulate progenitor cells in the hippocampus (Cao et al. 2013) stimulating astrogliogenesis. Other experiments support this hypothesis. Activation of A2b receptor of the astrocytes stimulates their differentiation and, in parallel, reduced proliferation , demonstrating the relationship of purinergic system, and astrocytes differentiation (Michel et al. 1999).

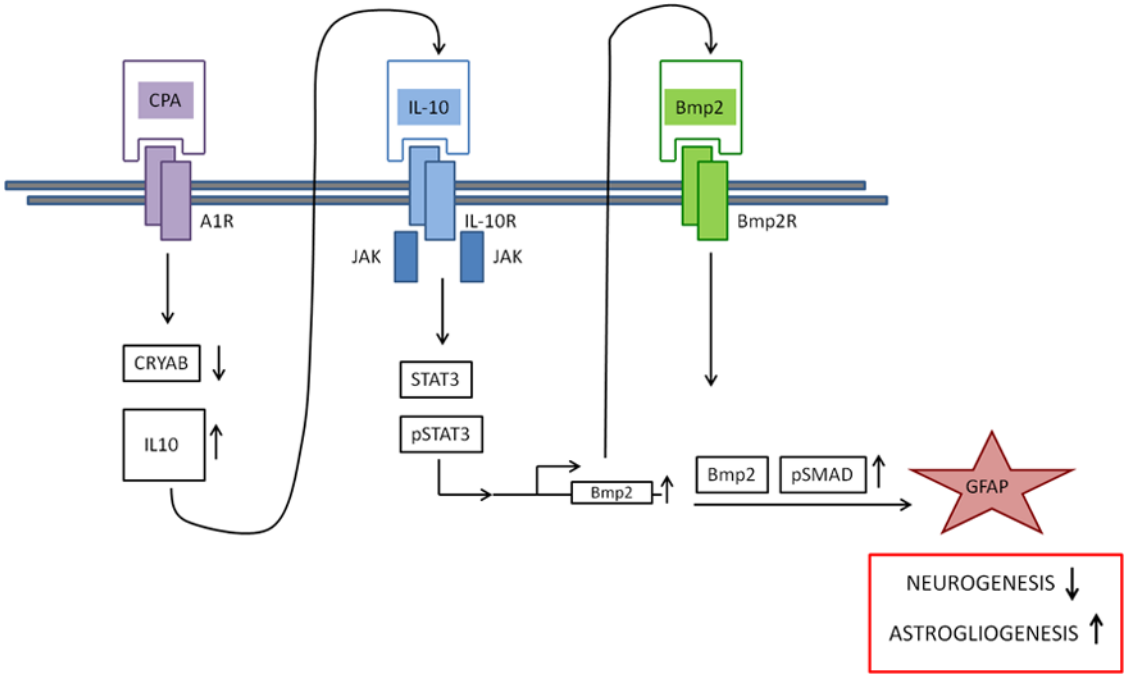

Figure 54. Model of astrogliogenesis activation through A1 and IL-10 receptors. The activation of both receptors leads to the induction of signaling pathway STAT3-Bmp2-SMAD and as a consequence promoting astrogliogenesis and hence neurogenesis reduction. Modified from (Fukuda et al. 2007).

4. A1 RECEPTOR-MEDIATED STIMULATION OF NEUROGENESIS IN ISCHEMIC MICE

Extracellular adenosine levels in brain are generally low, but can increase up to 100-fold during hypoxia or ischemic events (Phillis et al. 1996; Fredholm et al. 2005). These elevated concentrations of adenosine produce the inhibition of neuronal differentiation through A1 receptor according to our *in vitro* and *in vivo* results. Thus, we wanted to test if the antagonism of A1 receptor in an ischemic model (tMCAO) sustained neurogenesis from the SVZ.

Unlike the antagonist PSB36 used for *in vitro* studies, in this set of experiments we decide to use the specific DPCPX antagonist instead of PSB36. The main reason was from one hand, the absence of bibliography about PSB36 in *in vivo* experiments, and on the other hand the effectiveness of DPCPX in ischemic models (Nakamura et al. 2002; Cipriani et al. 2011; Phillis 1995) at low concentrations (0.1-1 mg/Kg). Moreover, DPCPX can reach efficiently the brain parenchyma inhibiting A1 receptor activity in the brain (Phillis 1995). Nevertheless, not only A1 receptor antagonists have positive effects after brain injury. Different A1 receptor agonists are related with an increase of the anti-apoptotic protein Bcl-2 expression with a reduction of apoptotic cell death in the penumbra of ischemic mice (Dai et al. 2012).

Our results showed that the administration of the A1 receptor antagonist DPCPX improved survival of ischemic animals. Our data are in line with those obtained by Von Lubitz (Von Lubitz et al. 1994) but in contrast with others showing worsened survival and increase of neuronal loss, a phenomenon thought to depend on A1 receptor desensitization (Jacobson et al. 1996).

Apart from survival, ischemic mice treated with DPCPX showed a better neurological score and concrete effect on motor activity. The restoration of motor activity was corroborated by the pole test. In particular, shortly after tMCAO, A1 receptor antagonist improved significantly animal mobility. However, at longer times (30 days) we did not observe any difference attributed to the treatment. It is worth to note that the motor improvement observed is a time frame too short (1 day post ischemia) to assign this effect to an increase of neurogenesis.

Our analysis did not show any significant effect of DPCPX related with infarct size, although the trend is a light reduction at 7 and 30 days after tMCAO and an increase at 15 days. Neither other groups (Nakamura et al. 2002; Yoshida et al. 2004) observed any kind

of effect of DPCPX, although they used different paradigms of DPCPX treatment. On the contrary, the absence of A1 receptor is associated with a larger brain damage and worse neuromotor score after hypoxic ischemia in neonatal mice (Winerdal et al. 2016), which agree with the trend observed in infarct size at 15 days after tMCAO. The limited bibliography corroborating the results could be attributed to different variables used in protocols. Factors modulating infarct size are the time of drug administration (before or after ischemia), duration of treatment, animal species, ischemic model type, occlusion time, temperature...

Analysis of neurogenesis in ischemic animals did not show a significant modulation of proliferation, observed by PET studies. Likely, the activation of A1 receptor in the SVZ by osmotic pumps neither showed changes in the number of $BrdU^+$ cells, suggesting that A1 receptor does not modulate cell proliferation. Indeed, neuronal differentiation was increased by the antagonism of A1 receptor. After a time course analysis we found the highest and more significant increase of neuroblasts and newborn neurons, 15 days after tMCAO. In parallel with the neurogenesis increase, we observed the same ratio of astrogliogenesis reduction by DPCPX treatment. In ischemic conditions where massive ATP and adenosine are released the activation of A1 receptor in NSCs increase the number of astrocytes, which are triggered to scar formation (Benner et al. 2013). For this reason, the astrocyte decrease observed by us could lead to defective glial scar formation. Furthermore, recent findings note that a population of dormant neural stem cells become activated after ischemia (Llorens-Bobadilla et al. 2015). We do not exclude that A1 receptor antagonist also affects to this population as essential molecules (Bmp and Ascl1 (Genander et al. 2014; Andersen et al. 2014)) involved in quiescent process are also affected in our experiments.

The role of A1 receptor in neurogenesis after ischemia depends on which cellular type express this receptor. In the case of endothelial cells, A1 receptor regulates cell migration and extravasation of leukocytes (Fredholm 2007), which has important consequences to control ischemic injury. In our case, we identified transient amplifying C cells expressing this receptor, which modulates differentiation of NSCs after ischemia, regenerating partially the area of penumbra. Apart from this receptor, other candidates have been proposed as effective target in stroke such as the neuronal adenosine transporters (ENT1). In this case the way of improving ischemia was by means of controlling adenosine levels (Zhang et al. 2011). Anyway, the importance of purinergic system in pathologies like stroke is provided with these studies and opens a wide range of future experiments. Some of the immediate assays would be to check the role of A1 receptor in older animals since

ischemic brain insults typically occur at advanced age and the endogenous NSC response is likely less robust than observed in our young adult animal models.

In conclusion, A1 receptor plays an important role in neurogenesis modulation. Thus, it would be a proper candidate to subsequent studies and it maybe become into a useful tool in therapeutical approaches.

Conclusions

1. All adenosine receptors (A1, A2A, A2B and A3) are expressed in neurosphere cultures from rat SVZ. Neurospheres cultures exposed to adenosine showed an inhibition in synaptic vesicular transport.

2. Adenosine reduces neurogenesis but sustains astrogliogenesis *in vivo* and *in vitro* models (using neurospheres cultures from rat SVZ).

3. A1 receptor is involved in adult neurogenesis modulation.

4. Transit amplifying cells are the cellular target of adenosine.

5. Activation of A1 receptor triggers the release of IL10 and activation of STAT3/Bmp2/Smad pathway. This cascade of events leads to the activation of astrogliogenesis.

6. Blocking of A1 receptor improve neurological score and survival of ischemic mice, without affecting infarct size.

7. Antagonism of A1 receptor increases the number of new born neurons and a reduction of new astrocytes in the penumbra area of ischemic mice. However, the blocking of A1 receptor does not modulate neural stem cells proliferation.

These results indicate that A1 receptor is a target for neurogenesis modulation, whose inhibition promotes an increment in neuronal differentiation after ischemic injury. However, more studies are necessary to test if these new cells establish connections into preexisting neuronal network. The A1 receptor modulation is suggested as a potential therapy regenerating damaged area in brain ischemia.

Bibliography

Adinolfi, E. et al., 2010. Trophic activity of a naturally occurring truncated isoform of the P2X7 receptor. *FASEB journal*, 24(9), pp.3393–404.

Ahmed, S., Reynolds, B.A. & Weiss, S., 1995. BDNF enhances the differentiation but not the survival of CNS stem cell-derived neuronal precursors. *The Journal of neuroscience*, 15(8), pp.5765–78.

Aimone, J.B., Deng, W. & Gage, F.H., 2011. Resolving new memories: a critical look at the dentate gyrus, adult neurogenesis, and pattern separation. *Neuron*, 70(4), pp.589–96.

Altman, J. & Das, G.D., 1965. Autoradiographic and histological evidence of postnatal hippocampal neurogenesis in rats. *The Journal of comparative neurology*, 124(3), pp.319–35.

Alvarez-Buylla, A. & Garcia-Verdugo, J.M., 2002. Neurogenesis in adult subventricular zone. *The Journal of neuroscience*, 22(3), pp.629–34.

Amankulor, N.M. et al., 2009. Sonic hedgehog pathway activation is induced by acute brain injury and regulated by injury-related inflammation. *The Journal of neuroscience*, 29(33), pp.10299–308.

Andersen, J. et al., 2014. A transcriptional mechanism integrating inputs from extracellular signals to activate hippocampal stem cells. *Neuron*, 83(5), pp.1085–97.

Araldi, D., Ferrari, L.F. & Levine, J.D., 2016. Adenosine-A1 receptor agonist induced hyperalgesic priming type II. *Pain*, 157(3), pp.698–709.

Arvidsson, A. et al., 2002. Neuronal replacement from endogenous precursors in the adult brain after stroke. *Nature medicine*, 8(9), pp.963–70.

Astic, L. et al., 2002. Expression of netrin-1 and netrin-1 receptor, DCC, in the rat olfactory nerve pathway during development and axonal regeneration. *Neuroscience*, 109(4), pp.643–56.

Azari, H. et al., 2011. Purification of Immature Neuronal Cells from Neural Stem Cell Progeny. *PLoS ONE*, 6(6), p.e20941.

Bajetto, A. et al., 2002. Characterization of chemokines and their receptors in the central nervous system: physiopathological implications. *Journal of neurochemistry*, 82(6), pp.1311–29.

Bambakidis, N.C. et al., 2012. Improvement of neurological recovery and stimulation of neural progenitor cell proliferation by intrathecal administration of Sonic hedgehog. *Journal of neurosurgery*, 116(5), pp.1114–20.

Bederson, J.B. et al., 1986. Rat middle cerebral artery occlusion: evaluation of the model and development of a neurologic examination. *Stroke*, 17(3), pp.472–6.

Benedetti, A. et al., 1995. Brefeldin A inhibits the transcytotic vesicular transport of horseradish peroxidase in intrahepatic bile ductules isolated from rat liver. *Hepatology*, 22(1), pp.194–201.

Benner, E.J. et al., 2013. Protective astrogenesis from the SVZ niche after injury is controlled by Notch modulator Thbs4. *Nature*, 497(7449), pp.369–73.

Berninger, B. et al., 2007. Functional properties of neurons derived from in vitro reprogrammed postnatal astroglia. *The Journal of neuroscience*, 27(32), pp.8654–64.

Boccazzi, M. et al., 2014. Purines regulate adult brain subventricular zone cell functions: contribution of reactive astrocytes. *Glia*, 62(3), pp.428–39.

Bolteus, A.J. & Bordey, A., 2004. GABA release and uptake regulate neuronal precursor migration in the postnatal subventricular zone. *The Journal of neuroscience*, 24(35), pp.7623–31.

Boutin, C. et al., 2010. NeuroD1 induces terminal neuronal differentiation in olfactory neurogenesis. *Proceedings of the National Academy of Sciences of the United States of America*, 107(3), pp.1201–6.

Bramlett, H.M. & Dietrich, W.D., 2004. Pathophysiology of cerebral ischemia and brain trauma: Similarities and differences. *Journal of Cerebral Blood Flow & Metabolism*, 24(2), pp.133–150.

Braun, N. et al., 1998. Upregulation of the enzyme chain hydrolyzing extracellular ATP after transient forebrain ischemia in the rat. *The Journal of neuroscience*, 18(13), pp.4891–900.

Brezun, J.M. & Daszuta, A., 1999. Depletion in serotonin decreases neurogenesis in the dentate gyrus and the subventricular zone of adult rats. *Neuroscience*, 89(4), pp.999–1002.

Burnstock, G., 2004. Introduction: P2 receptors. *Current topics in medicinal chemistry*, 4(8), pp.793–803.

Burnstock, G., 2007. Purine and pyrimidine receptors. *Cellular and molecular life sciences*, 64(12), pp.1471–83.

Burnstock, G., 2009. Purinergic cotransmission. *Experimental physiology*, 94(1), pp.20–4.

Burnstock, G. & Ulrich, H., 2011. Purinergic signaling in embryonic and stem cell development. *Cellular and molecular life sciences*, 68(8), pp.1369–94.

Burnstock, G. & Verkhratsky, A., 2010. Long-term (trophic) purinergic signalling: purinoceptors control cell proliferation, differentiation and death. *Cell death & disease*, 1, p.e9.

Cacci, E. et al., 2008. In vitro neuronal and glial differentiation from embryonic or adult neural precursor cells are differently affected by chronic or acute activation of microglia. *Glia*, 56(4), pp.412–25.

Cameron, H.A. & Gould, E., 1994. Adult neurogenesis is regulated by adrenal steroids in the dentate gyrus. *Neuroscience*, 61(2), pp.203–9.

Cao, X. et al., 2013. Astrocytic adenosine 5'-triphosphate release regulates the proliferation of neural stem cells in the adult hippocampus. *Stem cells*, 31(8), pp.1633–43.

Carden, D.L. & Granger, D.N., 2000. Pathophysiology of ischaemia-reperfusion injury. *The Journal of pathology*, 190(3), pp.255–66.

Cate, H.S. et al., 2010. Modulation of bone morphogenic protein signalling alters numbers of astrocytes and oligodendroglia in the subventricular zone during cuprizone-induced demyelination. *Journal of neurochemistry*, 115(1), pp.11–22.

Cavaliere, F. et al., 2001. Glucose deprivation and chemical hypoxia: neuroprotection by P2 receptor antagonists. *Neurochemistry international*, 38(3), pp.189–97.

Cavaliere, F. et al., 2013. NMDA modulates oligodendrocyte differentiation of subventricular zone cells through PKC activation. *Frontiers in cellular neuroscience*, 7, p.261.

Cavaliere, F. et al., 2012. Oligodendrocyte differentiation from adult multipotent stem cells is modulated by glutamate. *Cell death & disease*, 3, p.e268.

Cavaliere, F. et al., 2007. P2 receptor antagonist trinitrophenyl-adenosine-triphosphate protects hippocampus from oxygen and glucose deprivation cell death. *J Pharmacol Exp Ther*, 323(1), pp.70–77.

Cavaliere, F. et al., 2005. The metabotropic P2Y4 receptor participates in the commitment to differentiation and cell death of human neuroblastoma SH-SY5Y cells. *Neurobiology of disease*, 18(1), pp.100–9.

Cavaliere, F., Dinkel, K. & Reymann, K., 2006. The subventricular zone releases factors which can be protective in oxygen/glucose deprivation-induced cortical damage: an organotypic study. *Experimental neurology*, 201(1), pp.66–74.

Cavaliere, F., Donno, C. & D'Ambrosi, N., 2015. Purinergic signaling: a common pathway for neural and mesenchymal stem cell maintenance and differentiation. *Frontiers in cellular neuroscience*, 9, p.211.

Chen, E. et al., 2013. A novel role of the STAT3 pathway in brain inflammation-induced human neural progenitor cell differentiation. *Current molecular medicine*, 13(9), pp.1474–84.

Cheung, K.-K., Ryten, M. & Burnstock, G., 2003. Abundant and dynamic expression of G protein-coupled P2Y receptors in mammalian development. *Developmental dynamics*, 228(2), pp.254–66.

De Chevigny, A. et al., 2012. miR-7a regulation of Pax6 controls spatial origin of forebrain dopaminergic neurons. *Nature neuroscience*, 15(8), pp.1120–6.

Duane E. Haines, 2013 in Fundamental Neuroscience for Basic and Clinical Applications, Ed. Elsevier Science, ISBN-13: 978-1437702941.

Christie, K.J. & Turnley, A.M., 2012. Regulation of endogenous neural stem/progenitor cells for neural repair-factors that promote neurogenesis and gliogenesis in the normal and damaged brain. *Frontiers in cellular neuroscience*, 6, p.70.

Cipriani, R. et al., 2011. CX3CL1 is neuroprotective in permanent focal cerebral ischemia in rodents. *The Journal of neuroscience*, 31(45), pp.16327–35.

Codega, P. et al., 2014. Prospective identification and purification of quiescent adult neural stem cells from their in vivo niche. *Neuron*, 82(3), pp.545–59.

Cunha, R.A., 2005. Neuroprotection by adenosine in the brain: From A(1) receptor activation to A (2A) receptor blockade. *Purinergic signalling*, 1(2), pp.111–34.

Czyz, J. et al., 2003. Potential of embryonic and adult stem cells in vitro. *Biological chemistry*, 384(10-11), pp.1391–409.

Dai, Q.-X., Wang, L.-L. & Chao, J., 2012. Effects of injecting adenosine A1 receptor agonist into baihui (GV20) on the cerebral cortex in ischemia/reperfusion injury model rats. *Chinese journal of integrated traditional and Western medicine*, 32(3), pp.390–3.

Delic, J. & Zimmermann, H., 2010. Nucleotides affect neurogenesis and dopaminergic differentiation of mouse fetal midbrain-derived neural precursor cells. *Purinergic signalling*, 6(4), pp.417–28.

Díez-Tejedor, E. et al., 2001. Classification of the cerebrovascular diseases. Iberoamerican Cerebrovascular diseases Society. *Revista de neurologia*, 33(5), pp.455–64.

Dirnagl, U., Iadecola, C. & Moskowitz, M.A., 1999. Pathobiology of ischaemic stroke: an integrated view. *Trends in neurosciences*, 22(9), pp.391–7.

Doetsch, F. et al., 2002. EGF converts transit-amplifying neurogenic precursors in the adult brain into multipotent stem cells. *Neuron*, 36(6), pp.1021–34.

Domercq, M. et al., 2010. P2X7 receptors mediate ischemic damage to oligodendrocytes. *Glia*, 58(6), pp.730–40.

Donnan, G.A. et al., 2008. Stroke. *Lancet*, 371(9624), pp.1612–23.

Doyle, K.P., Simon, R.P. & Stenzel-Poore, M.P., 2008. Mechanisms of ischemic brain damage. *Neuropharmacology*, 55(3), pp.310–8.

Du, C. et al., 1996. Very delayed infarction after mild focal cerebral ischemia: a role for apoptosis? *Journal of cerebral blood flow and metabolism*, 16(2), pp.195–201.

Eddleston, M. & Mucke, L., 1993. Molecular profile of reactive astrocytes—Implications for their role in neurologic disease. *Neuroscience*, 54(1), pp.15–36.

Ekdahl, C.T., Kokaia, Z. & Lindvall, O., 2009. Brain inflammation and adult neurogenesis: the dual role of microglia. *Neuroscience*, 158(3), pp.1021–9.

Ernst, A. et al., 2014. Neurogenesis in the striatum of the adult human brain. *Cell*, 156(5), pp.1072–83.

Faiz, M. et al., 2015. Adult Neural Stem Cells from the Subventricular Zone Give Rise to Reactive Astrocytes in the Cortex after Stroke. *Cell stem cell*, 17(5), pp.624-34.

Fiorelli, R. et al., 2015. Adding a spatial dimension to postnatal ventricular-subventricular zone neurogenesis. *Development (Cambridge, England)*, 142(12), pp.2109–20.

Fredholm, B.B. et al., 2005. Adenosine and brain function. *International review of neurobiology*, 63, pp.191–270.

Fredholm, B.B., 2010. Adenosine receptors as drug targets. *Experimental cell research*, 316(8), pp.1284–8.

Fredholm, B.B., 2007. Adenosine, an endogenous distress signal, modulates tissue damage and repair. *Cell death and differentiation*, 14(7), pp.1315–23.

Fredholm, B.B. et al., 2001. International Union of Pharmacology. XXV. Nomenclature and classification of adenosine receptors. *Pharmacological reviews*, 53(4), pp.527–52.

Fukuda, S. et al., 2007. Potentiation of astrogliogenesis by STAT3-mediated activation of bone morphogenetic protein-Smad signaling in neural stem cells. *Molecular and cellular biology*, 27(13), pp.4931–7.

Gabel, S. et al., 2015. Inflammation Promotes a Conversion of Astrocytes into Neural Progenitor Cells via NF-κB Activation. *Molecular neurobiology*, pp.1-15.

Gampe, K. et al., 2015. NTPDase2 and purinergic signaling control progenitor cell proliferation in neurogenic niches of the adult mouse brain. *Stem cells*, 33(1), pp.253–64.

Garcia, A.D.R. et al., 2004. GFAP-expressing progenitors are the principal source of constitutive neurogenesis in adult mouse forebrain. *Nature neuroscience*, 7(11), pp.1233–41.

Gehrmann, J. et al., 1995. Reactive microglia in cerebral ischaemia: an early mediator of tissue damage? *Neuropathology and applied neurobiology*, 21(4), pp.277–89.

Genander, M. et al., 2014. BMP signaling and its pSMAD1/5 target genes differentially regulate hair follicle stem cell lineages. *Cell stem cell*, 15(5), pp.619–33.

Gil-Perotín, S. et al., 2013. Adult neural stem cells from the subventricular zone: a review of the neurosphere assay. *Anatomical record (Hoboken)*, 296(9), pp.1435–52.

Glaser, T. et al., 2012. Perspectives of purinergic signaling in stem cell differentiation and tissue regeneration. *Purinergic Signalling*, 8(3), pp.523–537.

Gómez-Gaviro, M.V. et al., 2012. Betacellulin promotes cell proliferation in the neural stem cell niche and stimulates neurogenesis. *Proceedings of the National Academy of Sciences of the United States of America*, 109(4), pp.1317–22.

Gould, E. et al., 1992. Adrenal hormones suppress cell division in the adult rat dentate gyrus. *The Journal of neuroscience*, 12(9), pp.3642–50.

Grégoire, C.-A. et al., 2015. Endogenous neural stem cell responses to stroke and spinal cord injury. *Glia*, 63(8), pp.1469–82.

Griffith, D.A. & Jarvis, S.M., 1996. Nucleoside and nucleobase transport systems of mammalian cells. *Biochimica et biophysica acta*, 1286(3), pp.153–81.

Hack, I. et al., 2002. Reelin is a detachment signal in tangential chain-migration during postnatal neurogenesis. *Nature neuroscience*, 5(10), pp.939–45.

Hack, M.A. et al., 2005. Neuronal fate determinants of adult olfactory bulb neurogenesis. *Nature neuroscience*, 8(7), pp.865–72.

Hagberg, H. et al., 1987. Extracellular adenosine, inosine, hypoxanthine, and xanthine in relation to tissue nucleotides and purines in rat striatum during transient ischemia. *Journal of neurochemistry*, 49(1), pp.227–31.

Hakanen, J., Duprat, S. & Salminen, M., 2011. Netrin1 is required for neural and glial precursor migrations into the olfactory bulb. *Developmental biology*, 355(1), pp.101–14.

Headrick, J.P. et al., 2013. Cardiovascular adenosine receptors: expression, actions and interactions. *Pharmacology & therapeutics*, 140(1), pp.92–111.

Heiss, W.-D., 2012. The ischemic penumbra: how does tissue injury evolve? *Annals of the New York Academy of Sciences*, 1268, pp.26–34.

Heldmann, U. et al., 2005. TNF-alpha antibody infusion impairs survival of stroke-generated neuroblasts in adult rat brain. *Experimental neurology*, 196(1), pp.204–8.

Hoehn, B.D., Palmer, T.D. & Steinberg, G.K., 2005. Neurogenesis in rats after focal cerebral ischemia is enhanced by indomethacin. *Stroke*, 36(12), pp.2718–24.

Höglinger, G.U. et al., 2004. Dopamine depletion impairs precursor cell proliferation in Parkinson disease. *Nature neuroscience*, 7(7), pp.726–35.

Honda, S. et al., 2007. Migration and differentiation of neural cell lines transplanted into mouse brains. *Neuroscience research*, 59(2), pp.124–35.

Hossmann, K.-A., 2008. Cerebral ischemia: models, methods and outcomes. *Neuropharmacology*, 55(3), pp.257–70.

Hu, H., 1999. Chemorepulsion of neuronal migration by Slit2 in the developing mammalian forebrain. *Neuron*, 23(4), pp.703–11.

Hu, H. et al., 1996. The role of polysialic acid in migration of olfactory bulb interneuron precursors in the subventricular zone. *Neuron*, 16(4), pp.735–43.

Im, S.H. et al., 2010. Induction of striatal neurogenesis enhances functional recovery in an adult animal model of neonatal hypoxic-ischemic brain injury. *Neuroscience*, 169(1), pp.259–268.

Imitola, J. et al., 2004. Directed migration of neural stem cells to sites of CNS injury by the stromal cell-derived factor 1alpha/CXC chemokine receptor 4 pathway. *Proceedings of the National Academy of Sciences of the United States of America*, 101(52), pp.18117–22.

Iosif, R.E. et al., 2006. Tumor necrosis factor receptor 1 is a negative regulator of progenitor proliferation in adult hippocampal neurogenesis. *The Journal of neuroscience*, 26(38), pp.9703–12.

Iyú, D. et al., 2011. Adenosine derived from ADP can contribute to inhibition of platelet aggregation in the presence of a P2Y12 antagonist. *Arteriosclerosis, thrombosis, and vascular biology*, 31(2), pp.416–22.

Jacob, F. et al., 2013. Purinergic signaling in inflammatory cells: P2 receptor expression, functional effects, and modulation of inflammatory responses. *Purinergic signalling*, 9(3), pp.285–306.

Jacobson, K.A. et al., 1996. Adenosine receptor ligands: differences with acute versus chronic treatment. *Trends in pharmacological sciences*, 17(3), pp.108–13.

Jessberger, S. et al., 2005. Seizures induce proliferation and dispersion of doublecortin-positive hippocampal progenitor cells. *Experimental Neurology*, 196(2), pp.342–351.

Jin, K. et al., 2002. Stem cell factor stimulates neurogenesis in vitro and in vivo. *The Journal of clinical investigation*, 110(3), pp.311–9.

Jung, C.-G. et al., 2004. Pleiotrophin mRNA is highly expressed in neural stem (progenitor) cells of mouse ventral mesencephalon and the product promotes production of dopaminergic neurons from embryonic stem cell-derived nestin-positive cells. *FASEB journal*, 18(11), pp.1237–9.

Kamphuis, W. et al., 2012. GFAP isoforms in adult mouse brain with a focus on neurogenic astrocytes and reactive astrogliosis in mouse models of Alzheimer disease. *PloS one*, 7(8), p.e42823.

Kempermann, G., Wiskott, L. & Gage, F.H., 2004. Functional significance of adult neurogenesis. *Current opinion in neurobiology*, 14(2), pp.186–91.

Kim, E.J. et al., 2007. In vivo analysis of Ascl1 defined progenitors reveals distinct developmental dynamics during adult neurogenesis and gliogenesis. *The Journal of neuroscience*, 27(47), pp.12764–74.

Kobayashi, T. et al., 2006. Intracerebral infusion of glial cell line-derived neurotrophic factor promotes striatal neurogenesis after stroke in adult rats. *Stroke*, 37(9), pp.2361–7.

Kokaia, Z. et al., 2006. Regulation of stroke-induced neurogenesis in adult brain--recent scientific progress. *Cerebral cortex*, 16 Suppl 1, pp.i162–7.

Kolb, B. et al., 2007. Growth factor-stimulated generation of new cortical tissue and functional recovery after stroke damage to the motor cortex of rats. *Journal of cerebral blood flow and metabolism*, 27(5), pp.983–97.

Laptook, A., 2014. The importance of temperature on the neurovascular unit. *Early human development*, 90(10), pp.713–7.

Lee, J.M., Zipfel, G.J. & Choi, D.W., 1999. The changing landscape of ischaemic brain injury mechanisms. *Nature*, 399(6738 Suppl), pp.A7–14.

Lehtinen, M.K. et al., 2011. The cerebrospinal fluid provides a proliferative niche for neural progenitor cells. *Neuron*, 69(5), pp.893–905.

Leker, R.R. et al., 2007. Long-lasting regeneration after ischemia in the cerebral cortex. *Stroke*, 38(1), pp.153–61.

Li, X. et al., 2010. Relationship between single nucleotide polymorphism of the equilibrative nucleoside transporter ENT3 and susceptibility to lung cancer. *Chinese journal of lung cancer*, 13(5), pp.458–63.

Lim, D.A. et al., 2000. Noggin antagonizes BMP signaling to create a niche for adult neurogenesis. *Neuron*, 28(3), pp.713–26.

Lim, D.A. & Alvarez-Buylla, A., 2014. Adult neural stem cells stake their ground. *Trends in neurosciences*, 37(10), pp.563–71.

Lin, J.H.-C. et al., 2007. Purinergic signaling regulates neural progenitor cell expansion and neurogenesis. *Developmental biology*, 302(1), pp.356–366.

Lindberg, O.R. et al., 2012. Characterization of epidermal growth factor-induced dysplasia in the adult rat subventricular zone. *Stem cells and development*, 21(8), pp.1356–66.

Liu, X. et al., 2005. Nonsynaptic GABA signaling in postnatal subventricular zone controls proliferation of GFAP-expressing progenitors. *Nature Neuroscience*, 8(9), pp.1179–1187.

Liu, X. et al., 2008. The role of ATP signaling in the migration of intermediate neuronal progenitors to the neocortical subventricular zone. *Proceedings of the National Academy of Sciences of the United States of America*, 105(33), pp.11802–7.

Llorens-Bobadilla, E. et al., 2015. Single-Cell Transcriptomics Reveals a Population of Dormant Neural Stem Cells that Become Activated upon Brain Injury. *Cell Stem Cell*, 17(3), pp.329–40.

Lovelace, M.D. et al., 2015. P2X7 receptors mediate innate phagocytosis by human neural precursor cells and neuroblasts. *Stem cells*, 33(2), pp.526–41.

Von Lubitz, D.K., 1999. Adenosine and cerebral ischemia: therapeutic future or death of a brave concept? *European journal of pharmacology*, 371(1), pp.85–102.

Von Lubitz, D.K. et al., 1994. Chronic administration of selective adenosine A1 receptor agonist or antagonist in cerebral ischemia. *European journal of pharmacology*, 256(2), pp.161–7.

Macrae, I.M., 2011. Preclinical stroke research--advantages and disadvantages of the most common rodent models of focal ischaemia. *British journal of pharmacology*, 164(4), pp.1062–78.

Malaterre, J. et al., 2008. c-Myb is required for neural progenitor cell proliferation and maintenance of the neural stem cell niche in adult brain. *Stem cells*, 26(1), pp.173–81.

Mao, Y. et al., 2009. Disrupted in schizophrenia 1 regulates neuronal progenitor proliferation via modulation of GSK3beta/beta-catenin signaling. *Cell*, 136(6), pp.1017–31.

Matute, C. & Cavaliere, F., 2011. Neuroglial interactions mediated by purinergic signalling in the pathophysiology of CNS disorders. *Semin Cell Dev Biol*, 22(2), pp.252–259.

McCarthy, M., 2006. Allen Brain Atlas maps 21,000 genes of the mouse brain. *The Lancet. Neurology*, 5(11), pp.907–8.

McCool, B.A. & Farroni, J.S., 2001. A1 adenosine receptors inhibit multiple voltage-gated Ca^{2+} channel subtypes in acutely isolated rat basolateral amygdala neurons. *British journal of pharmacology*, 132(4), pp.879–88.

Merkle, F.T. et al., 2014. Adult neural stem cells in distinct microdomains generate previously unknown interneuron types. *Nature neuroscience*, 17(2), pp.207–14.

Michel, P.P. et al., 1999. Adenosine prevents the death of mesencephalic dopaminergic neurons by a mechanism that involves astrocytes. *Journal of neurochemistry*, 72(5), pp.2074–82.

Mirzadeh, Z. et al., 2008. Neural stem cells confer unique pinwheel architecture to the ventricular surface in neurogenic regions of the adult brain. *Cell stem cell*, 3(3), pp.265–78.

Mishra, S.K. et al., 2006. Extracellular nucleotide signaling in adult neural stem cells: synergism with growth factor-mediated cellular proliferation. *Development*, 133(4), pp.675–84.

Müller, C.E. & Jacobson, K.A., 2011. Xanthines as adenosine receptor antagonists. *Handbook of experimental pharmacology*, (200), pp.151–99.

Nakamura, M. et al., 2002. Rapid tolerance to focal cerebral ischemia in rats is attenuated by adenosine A1 receptor antagonist. *Journal of cerebral blood flow and metabolism*, 22(2), pp.161–70.

Nakanishi, M. et al., 2007. Microglia-derived interleukin-6 and leukaemia inhibitory factor promote astrocytic differentiation of neural stem/progenitor cells. *The European journal of neuroscience*, 25(3), pp.649–58.

Nakashima, K. et al., 1999. Astrocyte differentiation mediated by LIF in cooperation with BMP2. *FEBS letters*, 457(1), pp.43–6.

Ng, K.L. et al., 2005. Dependence of olfactory bulb neurogenesis on prokineticin 2 signaling. *Science*, 308(5730), pp.1923–7.

Ohab, J.J. et al., 2006. A neurovascular niche for neurogenesis after stroke. *The Journal of neuroscience*, 26(50), pp.13007–16.

Ousman, S.S. et al., 2007. Protective and therapeutic role for alphaB-crystallin in autoimmune demyelination. *Nature*, 448(7152), pp.474–9.

Pardal, R. et al., 2007. Glia-like stem cells sustain physiologic neurogenesis in the adult mammalian carotid body. *Cell*, 131(2), pp.364–77.

Parish, C. & Thompson, L., 2013. Developing stem cell-based therapies for neural repair. *Frontiers in cellular neuroscience,*7, p.198.

Pedata, F. et al., 2001. Adenosine extracellular brain concentrations and role of A2A receptors in ischemia. *Annals of the New York Academy of Sciences*, 939, pp.74–84.

Perez-Asensio, F.J. et al., 2013. Interleukin-10 regulates progenitor differentiation and modulates neurogenesis in adult brain. *Journal of cell science*, 126(Pt 18), pp.4208–19.

Phillis, J.W., 1995. The effects of selective A1 and A2a adenosine receptor antagonists on cerebral ischemic injury in the gerbil. *Brain research*, 705(1-2), pp.79–84.

Phillis, J.W., Smith-Barbour, M. & O'Regan, M.H., 1996. Changes in extracellular amino acid neurotransmitters and purines during and following ischemias of different durations in the rat cerebral cortex. *Neurochemistry international*, 29(2), pp.115–20.

Piccin, D. & Morshead, C.M., 2011. Wnt signaling regulates symmetry of division of neural stem cells in the adult brain and in response to injury. *Stem cells*, 29(3), pp.528–38.

Platel, J.-C. et al., 2010. NMDA receptors activated by subventricular zone astrocytic glutamate are critical for neuroblast survival prior to entering a synaptic network. *Neuron*, 65(6), pp.859–72.

Plenz, D. & Kitai, S.T., 1996. Organotypic cortex-striatum-mesencephalon cultures: the nigrostriatal pathway. *Neuroscience letters*, 209(3), pp.177–80.

Rahpeymai, Y. et al., 2006. Complement: a novel factor in basal and ischemia-induced neurogenesis. *The EMBO journal*, 25(6), pp.1364–74.

Ramírez-Castillejo, C. et al., 2006. Pigment epithelium-derived factor is a niche signal for neural stem cell renewal. *Nature neuroscience*, 9(3), pp.331–9.

Ramírez-Rodríguez, G. et al., 2013. The α crystallin domain of small heat shock protein b8 (Hspb8) acts as survival and differentiation factor in adult hippocampal neurogenesis. *The Journal of neuroscience*, 33(13), pp.5785–96.

Ramos, A.D. et al., 2013. Integration of genome-wide approaches identifies lncRNAs of adult neural stem cells and their progeny in vivo. *Cell stem cell*, 12(5), pp.616–28.

Reif, A. et al., 2004. Differential effect of endothelial nitric oxide synthase (NOS-III) on the regulation of adult neurogenesis and behaviour. *European Journal of Neuroscience*, 20(4), pp.885–895.

Ribeiro, J.A. & Sebastião, A.M., 2010. Modulation and metamodulation of synapses by adenosine. *Acta physiologica*, 199(2), pp.161–9.

Ribeiro, J.A., Sebastião, A.M. & de Mendonça, A., 2002. Adenosine receptors in the nervous system: pathophysiological implications. *Progress in neurobiology*, 68(6), pp.377–92.

Robin, A.M. et al., 2006. Stromal cell-derived factor 1alpha mediates neural progenitor cell motility after focal cerebral ischemia. *Journal of cerebral blood flow and metabolism*, 26(1), pp.125–34.

Rock, R.B. et al., 2004. Role of microglia in central nervous system infections. *Clinical microbiology reviews*, 17(4), pp.942–64, table of contents.

Sabo, J.K. et al., 2011. Remyelination is altered by bone morphogenic protein signaling in demyelinated lesions. *The Journal of neuroscience*, 31(12), pp.4504–10.

Sanai, N. et al., 2011. Corridors of migrating neurons in the human brain and their decline during infancy. *Nature*, 478(7369), pp.382–6.

Schubert, P. & Kreutzberg, G.W., 1993. Cerebral protection by adenosine. *Acta neurochirurgica. Supplementum*, 57, pp.80–8.

Schwaninger, M. et al., 2000. Adenosine-induced expression of interleukin-6 in astrocytes through protein kinase A and NF-IL-6. *Glia*, 31(1), pp.51–8.

Sebastião, A.M. & Ribeiro, J.A., 2009. Tuning and fine-tuning of synapses with adenosine. *Current neuropharmacology*, 7(3), pp.180–94.

Shaban, M., Smith, R.A. & Stone, T.W., 1998. Adenosine receptor-mediated inhibition of neurite outgrowth from cultured sensory neurons is via an A1 receptor and is reduced by nerve growth factor. *Brain research. Developmental brain research*, 105(2), pp.167–73.

Shao, W. et al., 2013. Suppression of neuroinflammation by astrocytic dopamine D2 receptors via αB-crystallin. *Nature*, 494(7435), pp.90–4.

Shimozaki, K., Clemenson, G.D. & Gage, F.H., 2013. Paired related homeobox protein 1 is a regulator of stemness in adult neural stem/progenitor cells. *The Journal of neuroscience*, 33(9), pp.4066–75.

Shou, J., Rim, P.C. & Calof, A.L., 1999. BMPs inhibit neurogenesis by a mechanism involving degradation of a transcription factor. *Nature neuroscience*, 2(4), pp.339–45.

Sierra, A. et al., 2015. Neuronal hyperactivity accelerates depletion of neural stem cells and impairs hippocampal neurogenesis. *Cell stem cell*, 16(5), pp.488–503.

Sims, J.R. et al., 2009. Sonic hedgehog regulates ischemia/hypoxia-induced neural progenitor proliferation. *Stroke*, 40(11), pp.3618–26.

Sperlágh, B. et al., 2006. P2X7 receptors in the nervous system. *Progress in neurobiology*, 78(6), pp.327–46.

Sperling, L.E. et al., 2012. Mouse acetylcholinesterase enhances neurite outgrowth of rat R28 cells through interaction with laminin-1. *PloS one*, 7(5), p.e36683.

Stafford, M.R., Bartlett, P.F. & Adams, D.J., 2007. Purinergic receptor activation inhibits mitogen-stimulated proliferation in primary neurospheres from the adult mouse subventricular zone. *Molecular and cellular neurosciences*, 35(4), pp.535–48.

Storini, C. et al., 2006. Selective inhibition of plasma kallikrein protects brain from reperfusion injury. *The Journal of pharmacology and experimental therapeutics*, 318(2), pp.849–54.

Suh, H., Deng, W. & Gage, F.H., 2009. Signaling in adult neurogenesis. *Annual review of cell and developmental biology*, 25, pp.253–75.

Sun, C.-N. et al., 2010. The A2A adenosine receptor rescues neuritogenesis impaired by p53 blockage via KIF2A, a kinesin family member. *Developmental neurobiology*, 70(8), pp.604–21.

Suyama, S. et al., 2012. Purinergic signaling promotes proliferation of adult mouse subventricular zone cells. *The Journal of neuroscience*, 32(27), pp.9238–47.

Tajbakhsh, S., Rocheteau, P. & Le Roux, I., 2009. Asymmetric cell divisions and asymmetric cell fates. *Annual review of cell and developmental biology*, 25, pp.671–99.

Tajiri, N. et al., 2013. In vivo animal stroke models: a rationale for rodent and non-human primate models. *Translational stroke research*, 4(3), pp.308–21.

Telley, L. et al., 2016. Sequential transcriptional waves direct the differentiation of newborn neurons in the mouse neocortex. *Science*, 351(6280), pp.1443-6.

Teramoto, T. et al., 2003. EGF amplifies the replacement of parvalbumin-expressing striatal interneurons after ischemia. *The Journal of clinical investigation*, 111(8), pp.1125–32.

Thored, P. et al., 2006. Persistent production of neurons from adult brain stem cells during recovery after stroke. *Stem cells*, 24(3), pp.739–47.

La Torre, B.P. et al., 1991. Ischemic cerebral pathologies and K opioid receptors in rabbits. *Italian journal of neurological sciences*, 12(3 Suppl 11), pp.7–10.

Tsao, H.-K., Chiu, P.-H. & Sun, S.H., 2013. PKC-dependent ERK phosphorylation is essential for P2X7 receptor-mediated neuronal differentiation of neural progenitor cells. *Cell death & disease*, 4, p.e751.

Turbic, A., Leong, S.Y. & Turnley, A.M., 2011. Chemokines and inflammatory mediators interact to regulate adult murine neural precursor cell proliferation, survival and differentiation. *PloS one*, 6(9), p.e25406.

Ueki, T. et al., 2003. A novel secretory factor, Neurogenesin-1, provides neurogenic environmental cues for neural stem cells in the adult hippocampus. *The Journal of neuroscience*, 23(37), pp.11732–40.

Vergni, D. et al., 2009. A model of ischemia-induced neuroblast activation in the adult subventricular zone. *PLoS One*, 4(4), p.e5278.

Vukovic, J. et al., 2011. Activation of neural precursors in the adult neurogenic niches. *Neurochemistry international*, 59(3), pp.341–6.

Wang, H. et al., 2006. Secretion of brain-derived neurotrophic factor from brain microvascular endothelial cells. *The European journal of neuroscience*, 23(6), pp.1665–70.

Watson, B.D. et al., 1985. Induction of reproducible brain infarction by photochemically initiated thrombosis. *Annals of neurology*, 17(5), pp.497–504.

WIDERA, D., 2004. MCP-1 induces migration of adult neural stem cells. *European Journal of Cell Biology*, 83(8), pp.381–387.

Widera, D. et al., 2006. Tumor necrosis factor alpha triggers proliferation of adult neural stem cells via IKK/NF-kappaB signaling. *BMC neuroscience*, 7, p.64.

Williams, M., Braunwalder, A. & Erickson, T.J., 1986. Evaluation of the binding of the A-1 selective adenosine radioligand, cyclopentyladenosine (CPA), to rat brain tissue. *Naunyn-Schmiedeberg's archives of pharmacology*, 332(2), pp.179–83.

Winerdal, M. et al., 2016. Adenosine A1 receptors contribute to immune regulation after neonatal hypoxic ischemic brain injury. *Purinergic signalling*, 12(1), pp.89–101.

Wu, H. et al., 2010. Dnmt3a-dependent nonpromoter DNA methylation facilitates transcription of neurogenic genes. *Science*, 329(5990), pp.444–8.

Yamashita, T. et al., 2006. Subventricular Zone-Derived Neuroblasts Migrate and Differentiate into Mature Neurons in the Post-Stroke Adult Striatum. *Journal of Neuroscience*, 26(24), pp.6627–6636.

Yoshida, M. et al., 2004. Adenosine A(1) receptor antagonist and mitochondrial ATP-sensitive potassium channel blocker attenuate the tolerance to focal cerebral ischemia in rats. *Journal of cerebral blood flow and metabolism*, 24(7), pp.771–9.

Yung, H.S. et al., 2010. Nerve growth factor-induced differentiation of PC12 cells is accompanied by elevated adenylyl cyclase activity. *Neuro-Signals*, 18(1), pp.32–42.

Zhang, D. et al., 2011. Expression of human equilibrative nucleoside transporter 1 in mouse neurons regulates adenosine levels in physiological and hypoxic-ischemic conditions. *Journal of neurochemistry*, 118(1), pp.4–11.

Zhang, L. et al., 2016. Hdac3 Interaction with p300 Histone Acetyltransferase Regulates the Oligodendrocyte and Astrocyte Lineage Fate Switch. *Developmental cell*, 36(3), pp.316–330.

Zhang, N. et al., 2006. Adenosine A2a receptors induce heterologous desensitization of chemokine receptors. *Blood*, 108(1), pp.38–44.

Zhang, R. et al., 2001. A nitric oxide donor induces neurogenesis and reduces functional deficits after stroke in rats. *Annals of neurology*, 50(5), pp.602–11.

Zhang, R.L. et al., 2006. Reduction of the cell cycle length by decreasing G1 phase and cell cycle reentry expand neuronal progenitor cells in the subventricular zone of adult rat after stroke. *Journal of cerebral blood flow and metabolism*, 26(6), pp.857–63.

Zhang, Z. et al., 1997. A new rat model of thrombotic focal cerebral ischemia. *Journal of cerebral blood flow and metabolism*, 17(2), pp.123–35.

Zhao, C., Deng, W. & Gage, F.H., 2008. Mechanisms and functional implications of adult neurogenesis. *Cell*, 132(4), pp.645–60.

Zhu, D.Y. et al., 2003. Expression of inducible nitric oxide synthase after focal cerebral ischemia stimulates neurogenesis in the adult rodent dentate gyrus. *The Journal of neuroscience*, 23(1), pp.223–9.

Zhu, W. et al., 2008. Insulin growth factor-1 gene transfer enhances neurovascular remodeling and improves long-term stroke outcome in mice. *Stroke*, 39(4), pp.1254–61.

Zhu, W. et al., 2015. Intranasal nerve growth factor enhances striatal neurogenesis in adult rats with focal cerebral ischemia. *Drug Delivery*, 18(5), pp.338–343.

Zimmermann, H., 2006. Nucleotide signaling in nervous system development. *Pflügers Archiv: European journal of physiology*, 452(5), pp.573–88.

Zimmermann, H., 2011. Purinergic signaling in neural development. *Seminars in Cell and Developmental Biology*, 22(2), pp.194–204.